ADDIS ABABA UNIVERSITY

COLLEGE OF NATURAL AND COMPUTATIONAL SCIENCES

SCHOOL OF EARTH SCIENCES

REMOTE SENSING AND GIS APPROACH FOR ESTIMATION OF LAND SURFACE TEMPERATURE TO EXAMINE URBAN HEAT ISLAND EFFECT ON A CITY SCALE; THE CASE OF HAWASSA CITY, ETHIOPIA

A Thesis submitted to

The School of Graduate Studies of Addis Ababa University in partial fulfillment of the requirements for the Degree of Master of Science in Remote Sensing and Geo-informatics

By:

DAGNACHEW SISAY

ID: GSR/3422/09

Advisor:

DR. TESFAYE KORME

Addis Ababa, Ethiopia

May, 2018

ADDIS ABABA UNIVERSITY

COLLEGE OF NATURAL AND COMPUTATIONAL SCIENCES

SCHOOL OF EARTH SCIENCES

REMOTE SENSING AND GIS APPROACH FOR ESTIMATION OF LAND SURFACE TEMPERATURE TO EXAMINE URBAN HEAT ISLAND EFFECT ON A CITY SCALE; THE CASE OF HAWASSA CITY, ETHIOPIA.

A THESIS SUBMITTED TO

THE SCHOOL OF GRADUATE STUDIES OFADDIS ABABA UNIVERSITY IN PARTIAL FULFILLMENT OF THE REQUIREMENTS FOR THE DEGREE OF MASTERS OF SCIENCE IN REMOTE SENSING AND GEO-INFORMATICS

BY

DAGNACHEW SISAY CHAKA

ID.No: GSR/34/22/09

Addis Ababa University

MAY, 2018

Addis Ababa University

School of Graduate Studies

This is to certify the thesis prepared by Dagnachew Sisay Chaka entitled as "**Remote sensing and GIS approach for estimation of land surface temperature to examine urban heat island effect on a city scale; The Case of Hawassa city, Ethiopia**" is submitted in partial fulfillment of the requirements for the Degree of Master of Science in Remote Sensing and Geo-informatics compiles with the regulations of the University and meets the accepted standards with respect to originality and quality.

Approved by Board of Examiner:

Dr. K.V.SURYABHAGAVAN	_____	_____/_____/_____
Examiner	Signature	Date
Prof. M.BALAKRISHNAN	_____	_____/_____/_____
Examiner	Signature	Date
Dr. K.V.SURYABHAGAVAN	_____	_____/_____/_____
Chairman	Signature	Date
Dr. TESFAYE KORME	_____	_____/_____/_____
Advisor	Signature	Date

Acknowledgments

I would like to express my heartful gratitude to my advisor Dr. Tesfaye Korme for his generous guidance and careful supervision at every stage of this study. This research would not be in its current shape without his continuous exertion and support. I would also like to thank Hawassa University for awarding this opportunity to continue my MSc in Remote sensing and Geo-informatics, and for financial support for the entire study period. I thank Dr. Ameha Atnafu for his commitment and positive response in time of need.

I would like to extend my gratitude to all my friends for their willingness and patience to help whenever I need assistance. They made my graduate life more fun and meaningful.

I have a great gratitude to acknowledge all my instructors, school of earth science, different governmental organizations such as, Ethiopian Meteorological Agency and Hawassa City Administration who have helped me, from time to time complete the study by providing necessary data and information and important equipment to carry out this research.

My deepest gratitude goes to my mom, W/ro Merkeb Demo for always being supportive and understanding.

Last but not least, All Praise and Glory goes to **Almighty God**!

Dagnachew Sisay

Addis Ababa University,

May, 2018

Table of contents

List of Tables

List of Figures

Acronyms

UHI	Urban Heat Island
LST	Land Surface Temperature
LU/LC	Land-use/land-cover
NUPI	National Urban Planning Institute
SNNPRS	Southern Nation Nationality and Peoples Regional State
UGC	Urban Green Cover
NDVI	Normalized Difference Vegetation Index
IDP	Integrated Development Plan
USGS	United States Geological Survey
MODIS	Moderate resolution Imaging Spectroradiometer
GPS	Geographic Positioning System
GIS	Geographic Information System
ERDAS	Earth Resource Data Analysis System
W.W.D.S. E	Water Work Design Service Enterprise

Abstract

Estimation of Land Surface Temperature (LST) in a city scale is essential for various applications, especially for examining the Urban Heat Island (UHI) effect caused by different factors and identify the relationship of LU/LC types with LST. The integration of interpreted results obtained from Landsat 8 TIRS and MODIS night time data are helpful to identify the major causes for the spatial variation of LST. This helps to examine the heat island effect caused by the geological setting of an area located within the rift zones. Landsat 8 TIRS band 10 data was used to estimate LST of the area. An algorithm that was prepared for Landsat 8 band 10 were used by taking the NDVI method for the estimation of emissivity. The LU/LC maps of the area were prepared with better accuracy using on screen classification technique by identifying 18 different classes that have strong relation with the spatial variation of LST. The UGC types were identified and mapped by integrating computer aided and on-screen classification method using sentinel-2A data. The derived LST showed that the surface temperature of the city ranges from 20.6 to 41.3^{0}C and the minimum temperature of the area was observed within the lake and the surrounding areas such as the wetland. The maximum temperature was registered on the scattered and small hills (Tabor Ridge) and areas that are used for mining and some parts of bare lands including industrial park of the city. The spatial variation of LST in the city is the result of four (4) major factors namely: 1) geological setting (volcanic lava domes) and mining areas, 2) human induced activities, 3) the LU/LC type, 4) the nature of the rock (volcanic ash), for their immediate response as a result of absorbance of incident energy from the sun. The mapping of UGC for Hawassa city in detail was found to be good, though mapping and validation of smaller and scattered tree covers were difficult. Increasing of evergreen tree cover and rehabilitation of existing mining areas are among the recommended strategy to mitigate the UHI effects in the city. For future studies in areas that are susceptible to natural heat sources, the satellite data should have high spatial resolution and derived from multiple sensors and satellites that can provide better tools to understand the UHI effect considering the geological setting of the area.

Key words: Hawassa, LST, TIRS, Remote sensing, Rift, UHIs

CHAPTER ONE

1 INTRODUCTION

1.1 Background to the study

Following the urbanization process, humans play a considerable role in the large-scale modification of global environment. As a result, rapid urbanization or sprawl have severely altered the quality of the environment. A number of previous studies tell that most of the earth's surface is already modified, except those areas that are peripheral in location or are fairly inaccessible. Therefore, for cities that grow at alarming rate, sustainable urban planning and development play key roles in mitigating urban heat island effects and ensure the quality of urban environment (Meyer and Turner, 1992; Sundara *et al.*, 2012 and Tongliga et al., 2015). Urbanization has always been accompanied by the process of replacing natural vegetation with man-made non-transpiring and non-evaporating impervious structures or surfaces (Odindi *et al.,* 2015) and this phenomenal change brought significant differences in mean surface temperatures in between land cover types (Dewan and Corner, 2012). Impervious surfaces in urban areas will not only absorb and accumulate more solar radiation and heat but also impede long-wave sky radiation loss (Oke, 1988; Rizwan *et al.,* 2008), which will cause the phenomenon defined as the Urban Heat Island (UHI) effect, where atmospheric and land surface temperatures (LST) in urban areas are higher than in surrounding rural areas (Oke, 1988; Kuang *et al.,* 2015). Different urban structures such as, buildings, concrete, asphalt and industrial activity of urban areas causes the urban heat island (Dousset and Gourmelon, 2003 and Liu and Zhang, 2011). In general, from the above scholars' study, one can understand when the natural land cover is replaced by pavement that takes away the natural cooling effect, the surrounding land surface temperature and the airflow could be affected. This is due to building materials thermal properties, urban design geometry, road width and directions, existence of canyons, anthropogenic factors, existing land-use/land-cover and altitudes are some of the factors that contribute to UHI phenomenon. Building materials reflectance is low so they reflect less and absorb more energy, which lead to temperature increase at surface level. Building materials have high remittance values, so they release heat quickly and stay cooler (Odindi *et al.,* 2015).

According to Kuang *et al.* (2015) heat from vehicles, factories and air conditioners adds warmth to the surroundings, further exacerbating the heat island effect. In general, urban heat island mainly

appeared in the spatial distribution of Land Surface Temperature (LST), which is governed by surface heat fluxes and obviously affected by urbanization.

In the present time, remote sensing has become vital in the field of urban studies, including the study of urban climate and the urban heat island. The improved availability of satellite data having high temporal and spatial resolutions offers many opportunities. Thermal infrared images correlated with real-time ground temperature measurements allow the spatial distribution of LST to be modelled and estimated for an area of interest. (Osman et al., 2014).

Thermal infrared (TIR) sensors is used to study or obtain quantitative information of surface temperature across different LU/LC categories. There are many available thermal infrared sensors to study LST. The Geostationary Operational Environmental Satellite (GOES) has a 4-km resolution in the thermal infrared, while the NOAA-Advanced Very High-Resolution Radiometer (AVHRR), Terra and Aqua- (MODIS) have 1-km spatial resolution. High resolution data from the Terra-Advanced Space borne Thermal Emission and Reflection Radiometer (ASTER) has a 90-m resolution and Landsat-7 Enhanced Thematic Mapper (ETM+) has a 60-m resolution, were as Landsat 8 has two thermal bands (band 10 &11) with a resolution of 100m in thermal region. However, band 11 has calibration uncertainty caused by stray light (http://landsat.usgs.gov/documents /Landsat8 DataUsersHandbook.pdf).

1.2 Statement of the problem

Hawassa city is growing at a fairly rate. This growth and expansion are considered to be radical, particularly since the 1980s. Different factors like climate, accessibility and other social factors including defense, administration, economy and the political system are considered as a factor for growth and development of Hawassa city (Teshale Refera, 2015). The distribution and abundance of different land-use/land-cover as a strong correlation with the LST of urban areas (Falahatkar *et al.,* 2011; Lo CP *et al.,* 1997; Weng, 2001, 2003; Weng *et al.,* 2004). As a result of this, the increasing population density, industries, expansion of impervious surfaces, existence of various land-use/land-cover type are considered as a reason for the surface temperature change of the city, besides, the natural sources caused by the geological set up of the area.

There have been number of studies, conducted using high resolution satellite data like Landsat TM and Landsat ETM+ by taking numerous contributing factors to discover the relationship between LST and each factor, that had limited accuracy due to atmospheric transmission

(Lo CP *et al.*, 1997; Weng, 2001, 2003; Weng *et al.*, 2004; Falahatkar *et al.,* 2011; Sundara *et al.*, 2012). However, this study estimate the land surface temperature of the area, to identify the correlation between land-use/land-cover types and land surface temperature, and see the relationship with land surface temperature and different urban green cover type by using the advantage of the newly launched sentinel-2A data to obtain the urban green cover class and Landsat 8 (band 10 only) for LST estimation, as it has a thermal band of high atmospheric transitivity and no calibration problem caused by stray light to retrieve land surface temperature (http://landsat.usgs.gov/documents/Landsat8 DataUsersHandbook.pdf).

According to Hellman and Ramsey (2004), study the geological process can affect the surrounding surface temperature. Due to the presence of young igneous bodies or hot rocks located deeper in the crust, heat may transfer to the surfaces of the earth. Therefor, areas that are located within or around volcanic activity are highly susceptible to this heat island effect.

Using high resolution data like sentinel-2A for green cover mapping and rectified google earth image for land-use/land-cover mapping reduces the problem caused by pixel level analysis of LST per every land cover classes extracted from comparatively high resolution multi spectral imagery using zonal statistics. Beside this, little has been done with regard to mapping and quantifying Urban Green Cover (UGC) using sentinel 2A to explore the relationship between UGC and LST obtained from Landsat 8 thermal band 10 considering the notice obtained from USGS website in the previous studies.

1.3 Objective

1.3.1 General objective

The aim of this study was to map the current urban green land cover, to analyze the relationship of land-use/land-cover types with land surface temperature and study the UHIs cumulative effect on the specified city.

1.3.2 Specific objectives

In order to achieve the main objective of the research the following sub-objectives were proposed;

1. To map and quantify current urban green land cover in Hawassa.
2. To estimate the land surface temperature of the study area
3. To examine the correlation between land surface temperature and LU/LC, and
4. To prepare a mitigation strategy

1.4 Research Questions

1. Why Urban heat island intensity varies with in urban areas
2. What is the spatial pattern of land surface temperatures (LST) in Hawassa
3. How urban heat island cumulative effect is mitigated

1.5 Scope and limitation of the study

The present research was conducted in the existing settlement areas of Hawassa city, southern part of Ethiopia using the 2017 satellite imagery of the area. In order to examine the urban heat island effect and compute land surface temperature of the area as a function of land-use/land-cover type, the correlation between LST and Land-use/land-cover types was analyzed. As a final point, the study prepared urban heat island mitigation strategy to ensure better air quality of the specified city. To achieve these objectives, this study attempted to see all significant factors that have contributed to the Urban Heat Island (UHIs) effect in the city by integrating all possible efforts in acquiring required inputs in the form of primary and ancillary data collection, analysis and interpretation of the results. However, the study has encountered certain limitations. One of the limitations was lack of high resolution thermal data, which enables to see the impact the geological setting of the area at a different time of the day and small urban structures and the second one was the routine process to get data from different organizations.

1.6 Significance of the study

The present study helps to examine the relationship that exist between land surface temperature and LU/LC classes and provide an insight to urban planner, managers and landscape designer on how to mitigate the urban heat island effect. Because it helps to understand the spatial distribution of LST over various LU/LC classes and prepare mechanism or possible solution in their planning and management practice by incorporating the result in their policies. Finally, it gives an insight to improve the urban ecological environment and the condition of human settlement with in cities from the perspective of urban planning and landscape design by taking in to account the climatic condition.

1.7 Organization of the thesis

This thesis is presented in to Six chapters. The first chapter introduces the proposed topic, estimation of land surface temperature and urban heat island effect. It also includes the problem statements, research questions, objectives, scope, limitation and significances of the study. The second chapter literature review. This section has many relevant topics, such as definition, factors

for change and effect of land surface temperature and urban heat island, thermal remote sensing data types, sources, peculiar characteristics and application areas, merits and demerits of different land surface temperature retrieval algorism and their unique characteristics, land-use/land-cover thermal property, pattern, type, density and their effect on land surface temperature variation, spatial characteristics and impact of urbanization and urban green land cover on land surface temperature, natural source of heat and their impact and finally the chapter presents the role of advanced technologies like remote sensing and GIS for urban heat island studies.

The third chapter illustrates material and methodology used to assess the major problems like detail description of the study area, data used, software packages, techniques applied for image processing, enhancement, classification and accuracy assessment and methods used for urban green land cover extraction, derivation of normalized vegetation index (NDVI) and retrieval of land surface temperature and statistical correlation measures. The fourth chapter presents result of the present study. However, in the first part of this chapter an overview of previous LST of Hawassa and surrounding areas are presented. The fifth chapter has discussion and mitigation strategies based on the finding of the research output. Finally, conclusion and recommendations are presented in the sixth chapter.

CHAPTER TWO

2 LITERATURE REVIEW

2.1 Land Surface Temperature (LST)

Land Surface Temperature (LST) is the radiative skin temperature of the land surface of land surface processes from local through global scales or it can be defined as an average temperature of features of the exact surface of the Earth calculated from measured radiance (Kayet et al., 2016). It is a fundamental property of the Earth's surface that can be determined remotely. Most of the papers uses the term land surface temperature and air temperature interchangeably. However these two terms are not the same or can't be used interchangeably (Denis *et al.,* 2015), as LST is a mixture of bare soil and vegetation temperatures. As a result, due to cloud cover, diurnal variation and aerosol load modifications of illumination both bare soil and vegetation responds to the changes in incoming solar radiation (Norman and Becker, 1995; Denis *et al.,* 2015).

Land surface temperature can be used for ecological study and energy-balance issues at all spatial scales, and it is important for geothermal and volcanic monitoring. Whereas at a reasonable scale, temperature images are used to identify heat sources or hot spots in fighting fires and they are also important for monitoring the seasonal onset of melting and freezing conditions in the Arctic. The importance of LST is being increasingly recognized and displays quick variations. Land surface temperature determines the surface air temperature because it influences the partition of energy between vegetation and ground. The land surface temperature estimation process depends on various factors such as albedo, the vegetation cover and the soil moisture and atmospheric factors can fundamentally influence the derivation of LST including:

- ✓ temperature variations with angles
- ✓ sub-pixel in-homogeneities in temperature and land-cove
- ✓ surface spectral emissivity at the channel wavelengths
- ✓ atmospheric temperature and humidity variations
- ✓ Clouds and large aerosol particles such as dust.

2.2 Urban Heat Island (UHI)

In urban and suburban areas, there were observed heat islands, where air and surface temperatures are hotter than in their rural surroundings or natural surfaces (Abutaleb et al., 2014). This phenomenon of heat island has been found in cities throughout the world. For the purpose of this study, the term urban heat island is defined as the temperature difference between urban areas and

their natural surroundings (Icaza-Echevarria et al., 2016). This temperature difference affect the air temperature and the land surface temperature. Although the two are related, the difference is that while land surface temperature´s peak takes place during the day, the air temperatures differences are largest after the sunset.

Causes of urban heat island

According to Lisa (2008), heat islands exist in urban and suburban areas, because in many urban centers or settlements, common construction materials that can absorb and retain more of the sun's heat than natural materials in less-developed rural areas. Most urban building or pavement materials are impermeable and watertight, so moisture is not readily available to dissipate the sun's heat and the dark materials in concert with canyon like configurations of buildings and pavement collect and trap more of the sun's energy. The temperatures of dark and dry surfaces in direct sun can reach up to 88°C during the day, while vegetated surfaces with moist soil might reach up to 18°C under the same conditions (Shahmohamadi et al., 2011).

Most of the time, human anthropogenic heat, slower wind speeds and air pollution in also considered as a major contributing factor to heat island formation in urban areas. There is also another important reason for heat formation following the geological set up of the location which is dependent on the presence of young igneous bodies or hot rocks located deeper in the crust. As a result of this, elevated geothermal heat is normally transferred to the surface by the convection of ground waters or conduction of rock material to the surface and these phenomena makes the surface hotter and hotter (Hellman and Ramsey, 2004; DiPippio, 2005 and Qin *et al.*, 2011). In general, the causes of UHI are diverse, including natural factors and human factors, whose root cause is the change of land use.

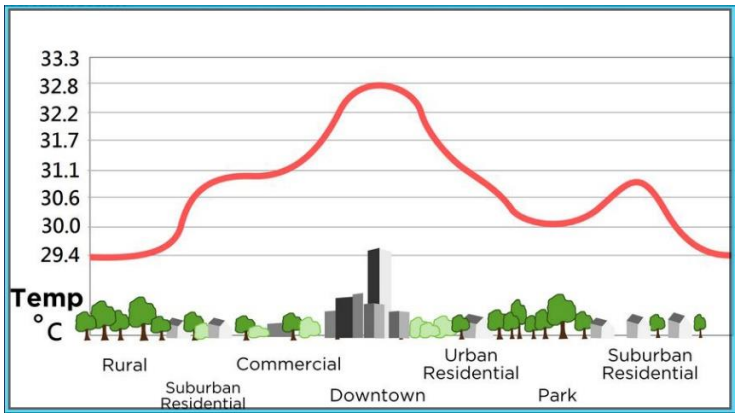

Figure 2.1:urban heat island profile

(Source: http://www.lcs.org.pk/blog/understanding-the-urban-heat-island-effect/ accessed on 2/22/2018, 6:56 PM).

Urban heat islands are characterized by many factors for examples areas with the least vegetation and greatest development tend to be hottest (Fig 2.2). Heat islands tend to become more intense when there are many man-made surfaces that absorb more of the sun's heat than natural vegetation does. Therefore, when compared to under developed rural areas, a heat island is warmer in more developed or settlement areas (Lisa, 2008).

2.3 Thermal Remote Sensing (TIRS)

Before having a concept about thermal remote sensing, it is better to understand about the term thermal data. Thermal data are data which are acquired when a radiant energy is detected by thermal sensors and it is a composite of energy emitted by the land surface that is transmitted through the atmosphere (not absorbed) and energy that is emitted by the atmosphere (Czajkowski *et al.*, 2000). These data can be acquired using different techniques. Ground based measurements using instruments in the field directly, like using thermometer, one can measure the temperature or humidity of the surface and the second source of thermal data is air borne like drone technology with thermal camera and the third one is space-borne thermal remotely sensed data, which the present study used to retrieve LST and examine UHI effect.

Thermal infrared remote sensing (TIRS) is a technique which helps to acquire thermal data by detecting thermal infrared energy emitted from all objects that have a temperature greater than absolute zero, with in a wave length domain of 3.0 _ 14 μm. However, in different papers the TIR domain slightly differently presented, and 80% of the energy thermal sensors receive in the 10.5–12.5μm (Price, 1984 and Becker; Li, 1990).

The main characteristic common to all the above definition is the fact that TIR remote sensing records emitted radiation. From the above definition of TIRS, one can understand that all the

features in the landscape (Sun, vegetation, soil, rocks, water, and even people) on a typical day emit thermal infrared electromagnetic radiation because of that their temperature is above 0^0K.

In different field of studies or researches, thermal remote sensing data are widely used for various application areas such as to assess surface temperature dynamics over various land-use/land-cover, to detect and analyze soil moisture content, map urban heat islands, to map and monitor volcanic eruption, investigations of geothermal areas, mineral mapping, analysis of surface thermal patterns, to detect forest, thermal water pollution, identification of different geologic surfaces (Lillesand and Kiefer,1994; Czajkowski al.,2000; Qin *et al.*,2011).

Characteristics of space born thermal remote sensing data

Some of the common satellites, thermal sensors in particular offer an efficient mode of data collection. For example, those in the Landsat program were collecting data on a world-wide basis since the 1970's. Satellite data from AVHRR, Landsat, MODIS and the Terra satellite have all been used to study land surface temperature. The Landsat Thematic Mapper, Enhanced Thematic Mapper and the Landsat 8 OLI and TIRS series of satellites have collected a particularly extensive archive of images.

Landsat 8 has been in operation since February 2013, providing 100meter spatial resolution images with two thermal bands band 10 and 11 and it has high atmospheric transitivity as compared to the other Landsat series that is sufficient for medium resolution urban temperature studies. However, band 11 has some calibration problem caused by stray light. MODIS and Advanced Very High-Resolution Radiometer (AVHRR) collect data in the thermal band. However, due to their low spatial resolution (1 and 1.1km per pixel), they are not as such suitable for urban studies. Another instrument, Advanced Space borne Thermal Emissions & Reflection Radiometer (ASTER) mounted on the TERRA satellite launched in 1999, was providing higher spatial resolution data, at 90meter per pixel. Both Landsat and TERRA have 16-day ground coverage cycles (Table: 2.1).

Table 2.1 Review of most common satellites with thermal sensors onboard

Platform	Sensor	Designed by (Attribution)	Spatial resolution in (m)	Number of bands	Band type	Spectral range in (μm)	Remark
Landsat 8	TIRS	USA	100	2	10&11	10.4-12.5	Band 11 has calibrati- on uncertainty. Has high atmospheric transitivity
Landsat 7	ETM+	USA	60	1	6	10.4-12.5	Has only one thermal infrared channel. Also, its one thermal channel has lower precision
Landsat 5	TM	USA	120	1	6	10.4-12.5	
Aqua &Terra	ASTER	Japan & USA	30-90	5	10,11, 12,13 & 14	8.125-11.65	show a higher variance of maximum radiance values as compared to AVHRR
Aqua &Terra	MODIS	USA	250 -1000	16		3.66-14.385	Difficult to use it for micro scale analysis of urban phenomena's & has 1000$5600m resolution processed data
NOAA	AVHRR	USA	1100-8000	2	31&32	3.55-3.93 10.3-12.5	Images of the earth are obtained every 30 minutes both day and night and for weather prediction

2.4 Surface temperature retrieval algorism

Considering the development of various thermal sensors, number of thermal bands and sensitivity of the thermal data to the atmospheric conditions, different methods or algorithms were developed in order to process the data (Table 2.2). However, a proper algorithm for retrieving LST from different sensors thermal band still remains unavailable due to many difficulties in the atmospheric correction (Abutaleb *et al.,* 2014; Wang *et al.,* 2015). Therefore, to accurately determine the LST it is better to identify those methods that require to consider the number of thermal bands of a sensor and different atmospheric conditions, which help to estimate those features in the atmosphere to determine the quality of atmospheric transmittance involved in the radiative transfer processes. Following the number of thermal bands and atmospheric sensitivity of the sensors, the following algorithms such as, split window, single Chanel, mono-window, improved split window, improved mono window and radiative transfer equation-based method (Yu *et al.,* 2014) are commonly used.

Table 2.3: Review of most common LST retrieval methods

No.	Algorithm	Unique characteristics	Remark
1	Radiative transfer equation-based method	Requires the atmospheric profile of the image that are acquired during image capturing and also highly dependent on the quality of the atmospheric profile and it is applicable to sensors with only one TIR channel	Sometimes difficult to get the atmospheric condition during the previous image acquisition
2	Mono-window	Applicable to sensors with only one TIR channel like that of radiative transfer equation-based method	Provide more consideration for water vapor content of atmospheric profile
3	Improved mono-window	Developed by considering the notice obtained from USGS web site for Landsat 8, thermal band 10 only	MODTRAN software is required to estimate the atmospheric transmittance.
4	Single channel	Requires the minimum input data and that can be used to different thermal sensors using the same equation and coefficient.	Uses the models of radiative transvers method and unstable at high water vapor concentrations
5	Split window	Applicable to sensors that have two or more thermal channels	Landsat 8 TIR can use it but For single band not recommended
	Improved Split window	Considers the atmospheric radiation effects due to the viewing zenith angle (VZA) variation	Best to retrieve daytime land surface temperature (LST) from the Terra/MODIS data

In general, identifying appropriate methods for the estimation LST is highly dependent on how the sensor's thermal bands are designed, beside the consideration of atmospheric profile. One can classify satellites according to the number of thermal bands to (1) one thermal band such as Landsat ETM+, (2) two thermal bands such as Landsat 8 TIR, NOAA, AVHRR, ATSR (Along-track scanning radiometer) and GOES (Geostationary operational environmental satellite) satellites; and (3) multiple thermal channels such as MODIS and ASTER satellites. For example, split window algorithm is used in various researches to retrieve LST from thermal sensors that have two or more thermal bands, whereas mono window algorithm from single thermal sensors such as Landsat TM,

Landsat ETM+ and so on. However, when there are some calibration uncertainties or any other atmospheric problems, different scholars modify the existing or develop a new method. For example, improved mono-window algorithm (IMO) is developed by modifying the existing mono-window algorithm following the calibration problem of Band 11 thermal data of Landsat 8 TIR caused by stray light (Sobrino et.al.,1994; 2004, Abutaleb *et al.*,2014; Wang *et al.*,2015). There is also an easy method that the present study used, it initially developed by Avdan and Jovanovska (2016) by considering the notice of USGS not use band 11 of TIRS.

2.5 Concept of land-use/land-cover mapping

Mapping of land-use/land-cover help to examine land-use/land-cover distribution pattern, measure the current conditions or quantity and gather information about landscape change and see the correlation with different intra-urban microclimatic conditions (e.g. the urban heat island phenomenon) and natural resource conservation or monitoring of the urban development pattern. Because of the interrelated nature of the elements of the urban environment, the direct effects on one element may cause indirect effects on others. Therefore, it is better to see the relationship among various contributing factors for land surface temperature. The distribution of urban land use and land cover types have environmental impacts at local and regional levels and linked to the global environmental process. As a result, mapping of land-use/land-cover elements helps to examine to what extent that those contributing factors have played significant role in the urban heat island effects and identify the major heat sources and pattern of distribution.

It is obvious that the earth's surface is changing rapidly by different factors among which these human induced are the most dominant. Therefore, it is highly recommended to map and identify the existing situation of the land-use/land-cover phenomena of the surface in order to develop a better monitoring system. However, these two terms (Land-use/land-cover) explain two different parameters and have different meanings. According to Di Gregorio and Jansen, (2000), Land-cover is defined as the observed biophysical cover on the earth's surface, including water bodies, vegetation, soil and hard surfaces. Utilization of the land by human activities for the purpose of settlements, agriculture, forestry, and by pasture altering land surface processes including biogeochemistry, hydrology and biodiversity are considered as Land-use. Considering the spatially heterogeneous nature of the urban land surface, comprised of a mixture of impervious and vegetated land covers the spatial pattern of temperature in urban areas varies from place to place following the variation in land use and land cover. Therefore, in order to understand the correlation

between land surface temperature and land-use/land-cover type mapping is the most important activity, because, it helps to correlate these two phenomena's spatially.

2.6 Urban green land cover

Since urban land surface temperature is highly dependent on the physical or thermal properties of an object or it is a mixture of vegetation and bare soil temperatures, it is important to see the type, density and distribution of green spaces or green land cover in urban areas to see their impact on urban heat island and identify the relation with LST. According to Wu, (1999) urban green space or land cover can be defined as a land use that can be covered by natural or man-made vegetation in the built-up areas and planning areas whereas Jim and Chen (2003) defined the green spaces as a semi-natural areas, managed parks and gardens, scattered vegetated pockets associated with roads and incidental locations in cities that exist mainly for aesthetics.

In balancing of human biophysical interconnections and keeping environmental quality, urban green spaces or vegetation cover plays significant roles. Green space is a basic requirement for better understanding of cities and quality of life in urban areas because they have significant impact on ecosystem functions, local microclimate and air quality (Roza Assaye *et al.,* 2017; Oliveira et al.., 2011). Particularly, urban green land covers are crucial for the mitigation of urban heat island effects that refers to the phenomenon of higher atmospheric and surface temperatures occurring in urban areas. Various researches identify that the distribution pattern, type of vegetation and percentage or density of green land cover can significantly decrease land surface temperatures (Tongliga *et al.,* 2015; Odindi *et al.,* 2015).

According to Voogt and Oke, (2003), there are three application areas of researches on UHI (Urban Heat Island) study using thermal sensor data such as:

1. To examine the spatial structure of urban thermal patterns and their relation to urban surface characteristics,
2. To use thermal remote sensing for urban surface energy balances and
3. To study the relationship between atmospheric heat islands and surface urban heat island,

In different researches vegetation cover were used to indicate UHI effects, and the results showed that vegetation abundance has significant negative correlation with UHI effects. Therefore, urban green spaces directly influence the well-being of urban residents and intra-urban microclimatic conditions or the urban heat island phenomenon.

2.7 Urbanization

Different scholars defined the term urbanization in different ways for example according to Jackson, (1985) urbanization is simply a city's radial expansion into its rural surroundings. Whereas, Tsegaye Tegenu, (2010) defined urbanization as a process of population concentration. It proceeds in two ways: the multiplication of points of concentration and the increase in size of points of concentration. While demographers defined the term urbanization as restricted factors such as population size and density. The economic functional definition refers to the territorial concentration of industries and service rather than population.

Based on the definition of urbanization, there is a change in land-use/land-cover class or modification of the physical characteristics of surface features in to a more impervious structure that can contribute to the change in land surface temperature, because each component of the surface in urban landscapes (e.g., lawn, parking lot, road, building, cemetery, and garden) exhibits a unique radiative, thermal, moisture properties, and relates to their surrounding site (Oke, 1982). In general, urbanization is a disruptive form of land transformation in terms of its ecological impact and the extent of its influence is growing along with increasing population and material requirements (Fu and Qihao, 2016).

According to the United Nations estimate, half of the world's population now resides in urban areas. The same estimate projects that by 2035, the number of urban dwellers will increase to 61%. This dramatic shift in population especially in developing countries from rural to urban areas constitutes a process of global urbanization (Coffyn, 2011).

Major characteristics of urbanization:

As Coffyn (2011) the urbanization processes of the world, especially in developing countries, characterized by different noticeable aspects beside the socio-economic and psychological impacts of this increasing unfriendliness from the natural environment and its processes. Those noticeable aspects described quantitatively are:

1. Construction of roads and other structures, improves impervious surface coverage.
2. Decline in vegetation levels due to deforestation.
3. Increased population density due to migration to the developing area.

Urbanization trend in Ethiopia:

In the last few years, growth rate is very fast in Ethiopia, this can be for two main reasons: first, the fertility rate in Ethiopia still high and secondly, increase in urban growth rapid. According to Lamson *et al.* (2015), four cities (Hawassa, Adama, Mekele and Bahir Dar) are the most rapidly

urbanizing cities in the country due to the rapid increase of economic activities and other political factors. Among these Hawassa is growing very fast and the population is projected to be more than one million by the year 2040.

This phenomena enforces the city to expand in all direction except the northern part, since the city is bounded by Oromia region (Lamson *et al.*,2015). However, this expansion or urbanization trend of the city has a question for different professionals on the consideration of the geological set up of the city and its urban heat island effect (Fig:2.2).

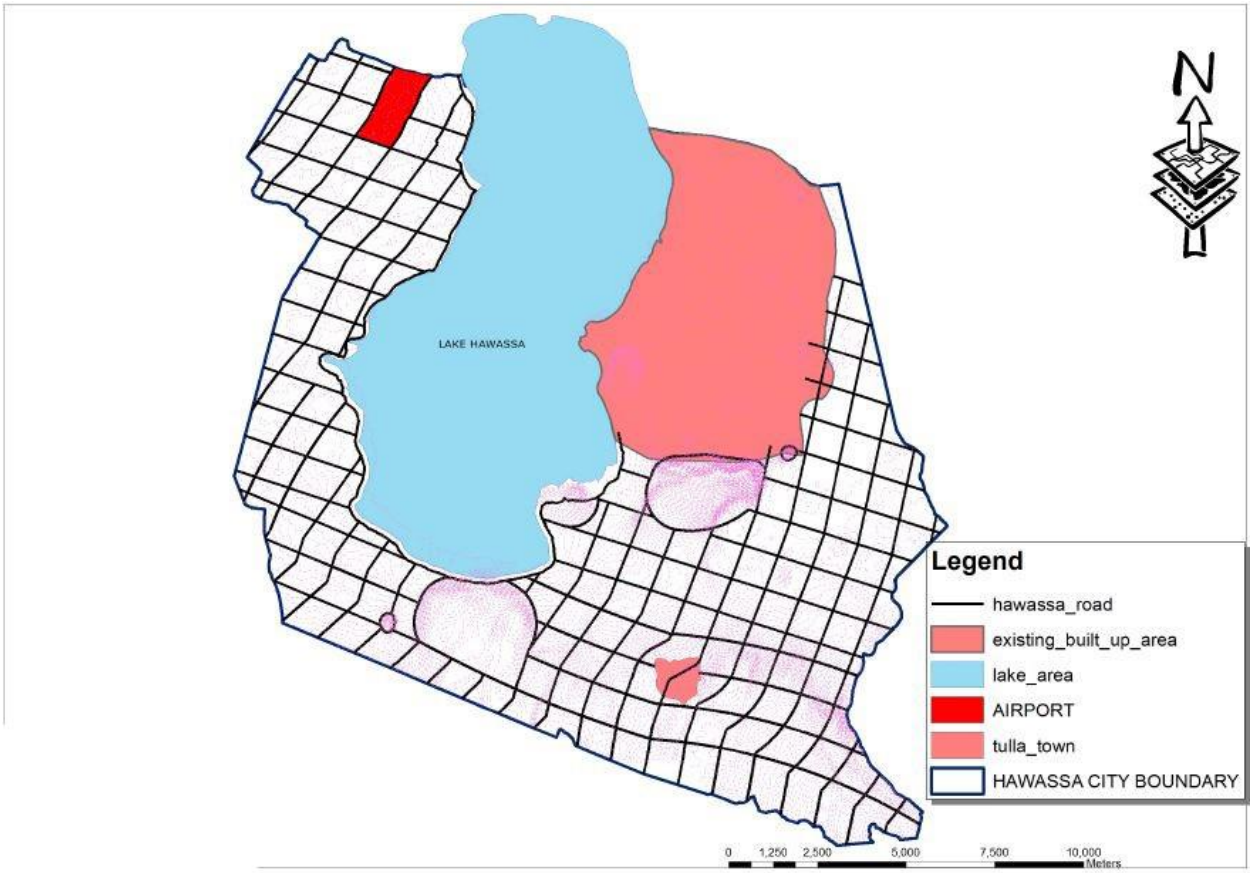

Figure 2.3: Expansion plan of Hawassa.

(Source: Lamson *et al.*, 2015)

2.8 Natural source of heat

Areas that are not susceptible for any human modification and anomalies of high heat island, one can understand that there are still natural or geological process, which generate heat in the surroundings. These geological processes can be the results of the presence of young igneous bodies or hot rocks located deeper in the crust (Hellman and Ramsey, 2004). As a result, heat may transfer to the Earth's surface often via conduction of rocks, water and any other associated

minerals and during volcanic eruption. Following these processes, the surface expressions such as hot springs, fumaroles, heated ground and others show the natural process that takes place inside the earth (Buongiorno *et al.*, 2013; Hellman and Ramsey, 2004).

The diagram (Fig 2.3) represents how heat can be transferred to the surface and contribute the surface temperature change. Hence, from this conceptual representation, one can understand that those urban centers, which are located in rift zones are highly susceptible to urban heat island effect. However, little consideration was provided to this phenomenon for urban heat island study.

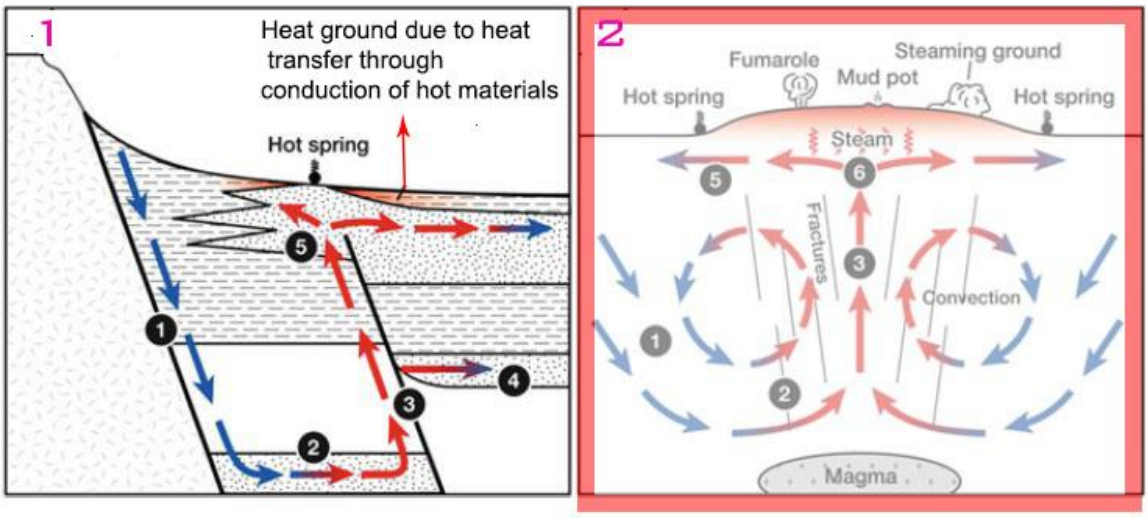

Figure 2.4: Schematic diagram of heat transfer and geo-thermal systems of the surface

Note: In figure 2.3, the geothermal and heat transfer systems formed by deep circulation of materials and magmatic activity. Arrows indicate direction of flow whereas numbers indicate zone of recharge, conductive heating, up flow along fault lateral outflow in deep, outflow in shallow aquifer with associated surface manifestations and boiling of geothermal waters in the subsurface (Source: Claudia and Stefan,2013).

2.9 Role of remote sensing and GIS for UHI study:

For inaccessible areas detection of surface temperature using the conventional meteorological station is sometimes very difficult. This is because, the station coverage is very poor and the collected data may not represent a fair spatial distribution of temperature values. In such cases, the integration of remote sensing and GIS with conventional meteorological data collected is very important because, they are powerful and effective in detecting every phenomenon of land surface. Remote sensing technology helps to acquire relatively higher resolution thermal data by recording the radiance of objects on the earth's surface and enable to extract information, which is valuable for the understanding and monitoring of urban heat island effects in the surrounding area.

According to Schmidt et al. (2006), the use of remote sensing for the monitoring of land surface temperature to study heat island and reflectivity at different spectral regions lies in its ability to spatially integrate over heterogeneous surfaces at a range of resolutions and underpin information systems routinely generating operational areal evaporation products once long time-series data availability issues are overcome. Data entry, analysis and display of those data obtained either from remote sensing technology or field GIS is the most advanced tool. Because, it provides a flexible environment for various spatial representation of activities (e.g. urban feature and hot spot identification, change detection and database development).

CHAPTER THREE

3 MATERIALS AND METHODS

3.1 Description of the study area

3.1.1 Location

Considering the rapid urbanization, industrial development and geological set up, Hawassa has been selected as the study area for this research. The city is geographically bounded by 6°59'N_7°6'N latitude and 38°28'E_38°34'E longitude, and with average elevation of about 1,690m above the mean sea level (Fig 3.1). It is the administrative capital of SNNPRS (Southern Nations, Nationalities and Peoples Regional State) of Ethiopia. It is 275 km south of Addis Ababa via Mojo-Ziway on the main road to Kenya and has an area of 5000 ha. Hawassa is located on the shore of Lake Hawassa (from which the name of the city was driven).

According to Teshale Refera (2015), the city was founded in 1960 G.C by Ras Mangesha Siyoum under the permission of the Emperor Haile Selassie I. The original settlement was initiated at an area called Arab-Sefer. In 1961 G.C, four hundred and four pensioned soldiers and their families were provided with plots to settle in the eastern part of the town, which is now called "404 Sefer".

The city is divided into eight sub-cities (suburbs), these are, Addis Ketema, Hayik-dar, Mehal Ketema, Bahl-Adarash, Misrak, Menharya, Tabor and Tula Sub- City. Each of these has varied number of administrative units known as "Kebele" which collectively adds up to 32 (Hawassa City Municipality Administration).

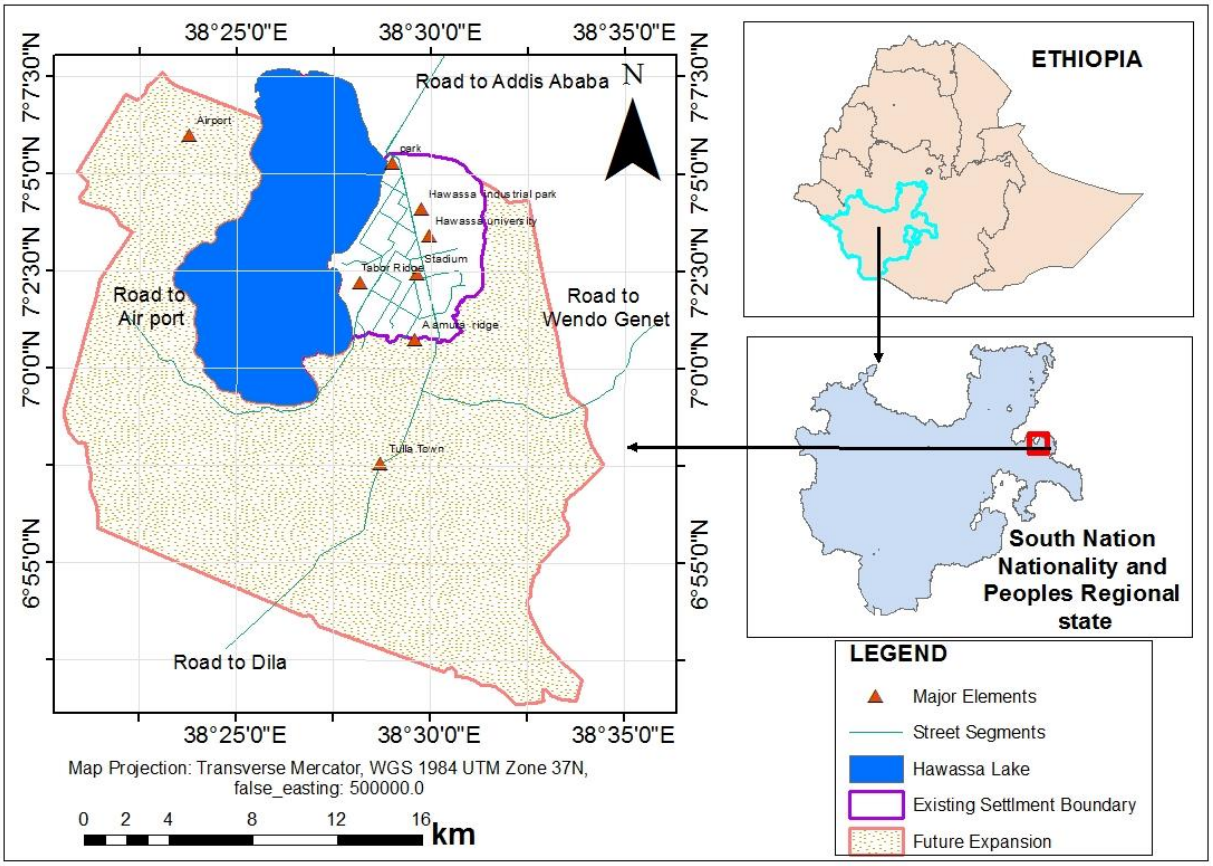

Figure 3.1: Location map of study area.

3.1.2 Population:

The number of residents in the city is increasing very fast (Fig 3.2), according to the CSA (2013) population projection report, the total population of the study area was estimated 335,508. Out of this, 166,009 were male and 169,499 were female population. According to Lamson *et al.* 2015, the population of Hawassa is projected to be more than one million by the year 2040.

The majority of the population livelihood depends on trade, and employment in different governmental and non-governmental organizations and insignificant number of population livelihood depend on farming of local products (Hawassa city administration).

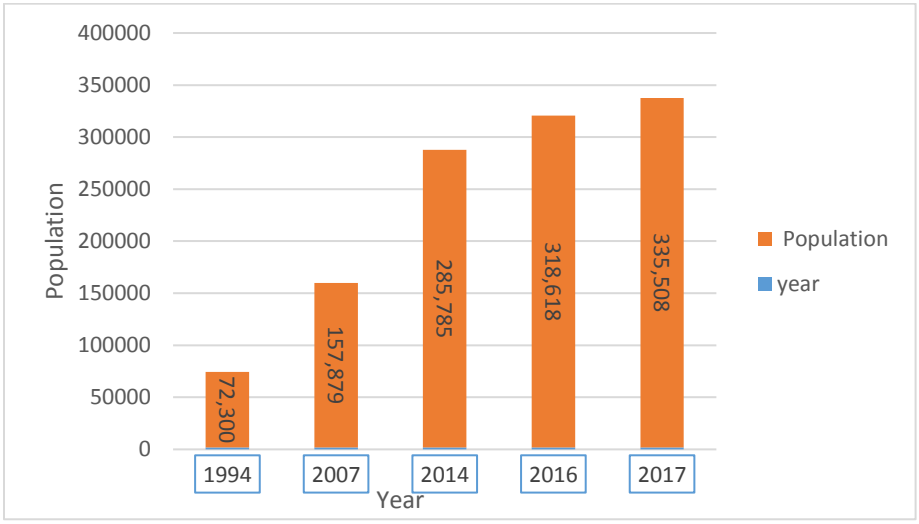

Figure 3.2: Urban population projection of Hawassa city administration.

(Source: Central Statistics Agency (CSA), Population Projection report of 2013 and census 2008 & 1998)

Figure 3.2 shows that the population of the city is increasing very fast from year to year. There are a number of factors that are driving the population increase. Among these, the rapid development of high labor-intensive industries and other economic activities including the political factors that were considered as high pulling factors.

3.1.3 Climate:

Hawassa experiences a temperature that varies between 18°C and 28.9°C with annual mean temperature close to 24°C implying tropical or 'Kola' temperature condition (Fig 3.3).

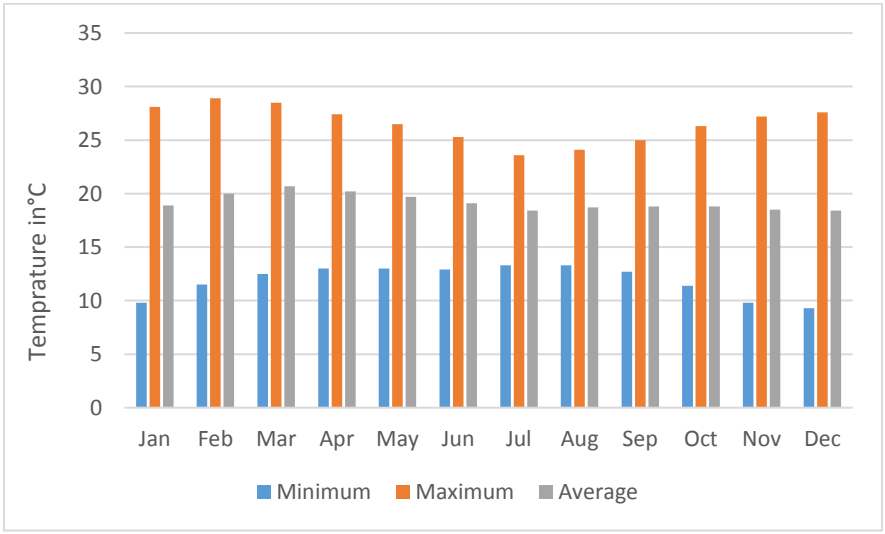

Figure 3.4: Monthly temperature distribution of Hawassa.

(Source: https://en.climate-data.org/location/5992/ accessed on 5/29/2018 10:07 AM)

The monthly temperature of the area in figure 3.3 shows that the maximum temperature is observed in the dry season of the area especially on February and December. Whereas, the minimum temperature is observed on January.

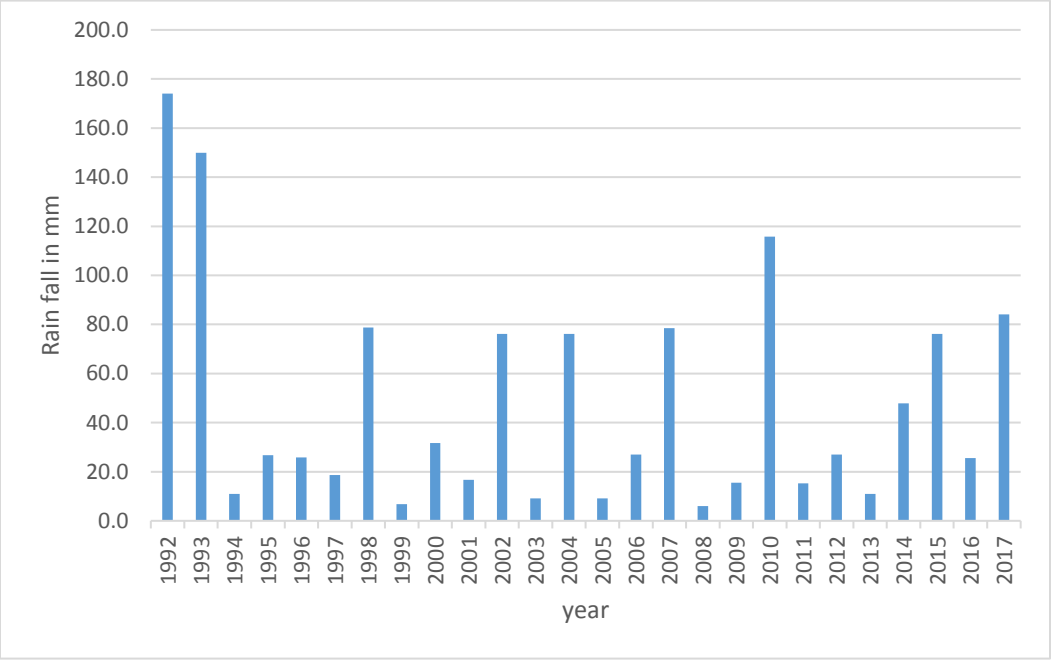

Figure 3.5: Mean precipitation of the month of February for the period 1992-2017

(Source: Ethiopian meteorological agency. 10 station data of 2017)

As shown in the above (Fig 3.3) only the mean rain fall of the month of February were chosen. Because, all the satellite data used for this study is acquired on this month and this help to examine the impact of the existing weather conditions on the thermal remote sensing data. As shown in the fig 3.3 the mean rain fall of the area varies from year to year especially the mean rain fall observed in 1992 was the highest even if the month of February is among the driest season in the area, whereas 1998,2002,2004,2007,2010,2015,2017 had almost similar rainfall, except few years that had rainfall below 20mm, as a result, the existing temperature of the area were affected by the existing weather condition.

3.1.4 Physiography of the study area

The 3D view in, figure 3.5 shows the topographic nature of Hawassa area. The settlement area of Hawassa is characterized by a flat-lying topography with scattered small domes (hills). The elevation of the rift escarpments and ridges in the east and west ranges from 2000 to 2669m. a.m.s.l.

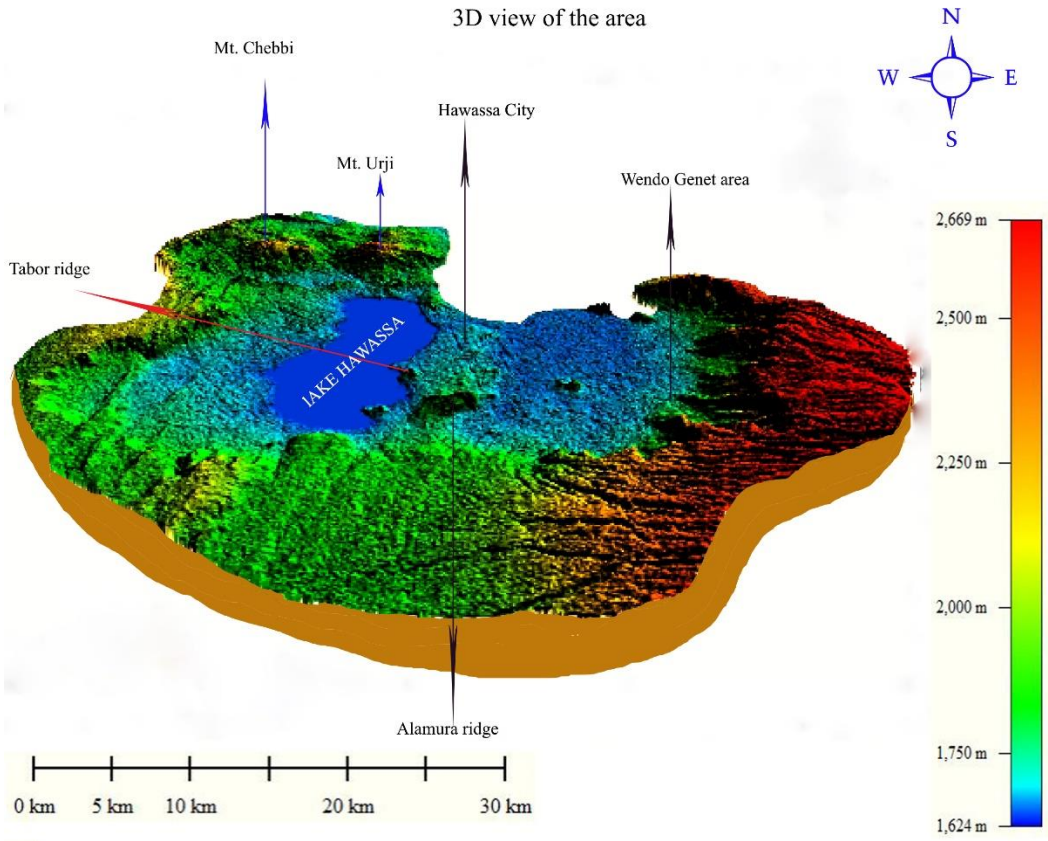

Figure 3.6: *3D view of the Surrounding areas of Hawassa*

3.1.5 Geological setting of Hawassa area

The geological setup of Hawassa and its surroundings shows that the city is located within the central zone of the Main Ethiopian Rift characterized by active volcanism and tectonics. The city itself is located within an old mega caldera that has a number of nested and resurgent volcanos. The active volcanism and tectonics has lots of contributing factors for surface temperature increasing and changes like the hot spring water from the lower part of Wendo Genet (Wesha and Wendo hot springs) and volcanic materials and geysers associated to eruption of the two post-caldera volcanos (Chebi and Urji). The nested Corbetti volcano is located on the northern shore of Lake Hawassa. It can be seen from the Addis Ababa-Wendo road, where it appears with a broad, low, but prominent topographic profile. It lies at the northern end of the Lake Hawassa basin, a

tectonic depression within an uplifted region against the eastern margin of the Rift (Tadesse and Zenaw, 2003).

As of the Basalfew *et al.,* (2012), the Corbetti area is believed to comprise a high water-dominated and gas-rich geothermal system. It lies within a 12km wide caldera that contains widespread thermal activity. Geophysical surveys have identified a low resistivity zone that is believed to represent a channel of geothermal fluid that flows from the caldera northwards.

Since the study area is located within the closed catchment of this nested Hawassa Corbetti caldera complex that has two volcanic centers of Urgi and Chebbi to the north west of Lake Hawassa the area is highly vulnerable to heat island effect. Urgi volcanic center is a source for the formation of pumice in the vicinity, and Chebbi is a center of formation of obsidian, which covers the Chebbi Mountain (Northern part of Lake Hawassa).

Following the sequence of eruptions, different rocks were formed from one volcano to the other. As a result, most of the volcanic products that are mapped in the surrounding area are Rhyolitic Lava flow, Obsidian and Pitch stone, Pumice and Ignimbrites, Basalt flows and Cones, Volcanoclastic lacustrine sedime, Basalts of the plateau trap Seri, Basalts hayaloclastites, Scoria, Alkaline and Peralkaline rock (Fig 3.6) are from the two volcanic centers.

Corbetti is a composite volcano that is characterized by alteration of obsidian lava and pumice-ash flows and beds. The study area (especially the Eastern bottom part of Hawassa Caldera) has highly Alkaline Silicic volcanic Ash (Pantelleritic Obsidian) and youngest Pumicious deposits, several Ignimbrites, scarce scoria, tuff cones and associated basaltic lava flows (Zacek et al., 2015). As a result of these active volcanic activities and other human induced factors the area is highly vulnerable to heat island effects.

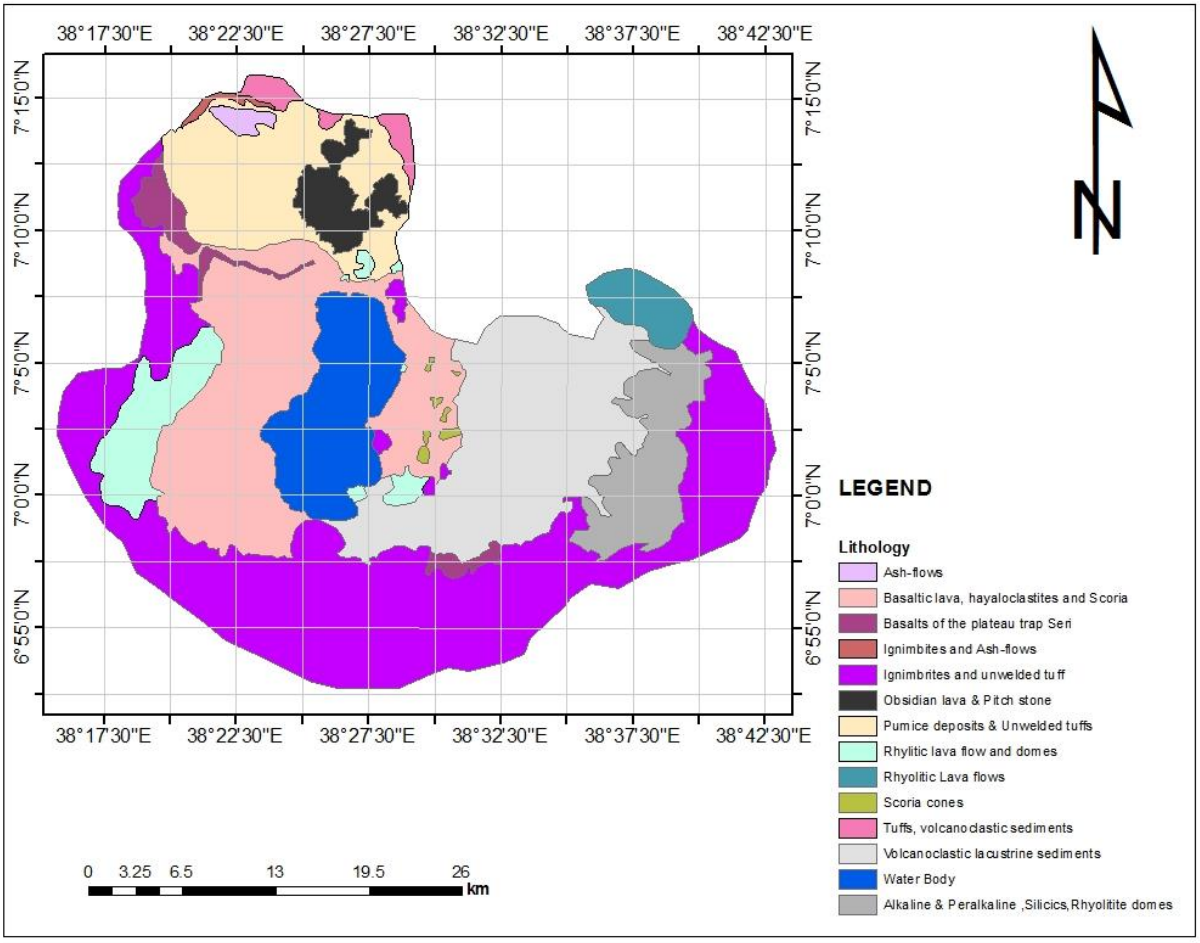

Figure 3.7: Lithology of surrounding of the study area.

(Source: Modified from Water work design service enterprise (W.W.D.S.E), 2001)

3.2 Data used

This research was designed to use the potential of Sentinel-2A cloud free scene, which was acquired on February 19 2017 by downloading from Copernicus scientific data hub for mapping urban green space with native spatial resolutions of 10 m (blue, green, red, and near infrared bands), 20 m (red edge bands), or 60 m (short wave infrared bands) (Sentinel-2 User Handbook, (2015), all bands are resampled to 10 m resolution for further processing. Landsat 8 thermal infrared band (band 10) is featured with spatial resolution of 100m are chosen as the data source to retrieve LST, but, this band and the Landsat 8 OLI are resampled using the nearest neighborhood algorithm with a pixel size 30m x 30m. For classification accuracy assessment field data were used. Finally, MODIS data which was acquired one day before the Landsat-8 OLI/TIRS data was used for the validation of the retrieved LST of the area (Table 3.1.).

Table 3.1: Overview of the data set used for the present study.

Data set	Acquisition date	Source	Data type	Purpose of the data
Landsat 8 OLI /TIRS With a path/row 168/055	2017/02/11	USGS	Landsat 8 OLI	Determination of NDVI,emissivity
Landsat 8 OLI /TIRS With a path/row 168/055	2017/02/11	USGS	TIRS	Estimation of LST
Sentinel-2A	2017/02/19	Copernicus scientific data hub	MSI	For LU/LC and UGC mapping
MOD11A2 .A2017041.h21v08.006	2017/02/10	USGS	Day & Night time temperature data	For validation of LST
Sample data	2018/04/10	Field using GPS	Field data	For supervised classification and validation
Google earth image	2018/01/05	Google satellite image downloader (google earth)	polygon	For LU/LC mapping and Validation

3.3 Software package

For the preparation, processing and mapping of both satellite and field data, the following software packages were used: ERDAS Imagine 15.0, ArcGIS Desktop 10.5, ENVI 5.1, Elshayal smart web online software v 4.11 and IMPACT Toolbox.

3.4 Methodology

Different methods including remote sensing and statistical analysis techniques were used in the analysis of land surface temperature of Hawassa to examine Urban Heat Island (UHIs) effects of the urban climate and identify the correlation of surface temperatures with different land-use/land-cover types and the normalized difference vegetation index (NDVI).

Two different techniques were used to examine the impacts of the geological and urban setting of the area on land surface temperature variation using both qualitative and quantitative analysis methods. These techniques are wider area analysis, this analysis was undertaken by considering the geological setting and vegetation distribution of the surrounding area. To perform this analysis different profile line using cross sections were created using distance-based approach, to get and describe the real value across each location of the thermal channel along the profile line. The

criteria used to create the cross section line in the study area and its surrounding takes in to account the geological setting (the nested Hawassa caldera), urban structure (land use type) and vegetation density. For example, areas on top of the nested Hawassa caldera and its volcanic ash deposit (East of the Lake) are hotter. However, the density and distribution of vegetation has higher impact on the intensity of temperature, as a result, a typical relationship between LST and NDVI was met. Besides, MODIS night time image of the area were used to see the real thermal character of the surface. And also an overview of the previous LST of the area especially the 1992 and 2002 were used to have an insight for the current study of UHIs of the area.

Concerning the variation of LST within the city, detailed urban area heat variation analysis using both descriptive and statistical analysis method was applied by taking zonal statistical data and other descriptive analysis technique. The present study also utilized potentials of unsupervised classification techniques to examine the spectral separabilty of the image and finally supervised classification was applied by integrating it with on screen classification that creates additional class polygons, and that has increased the accuracy of green cover mapping. For the pre-processing of sentinel-2A image IMPACT Toolbox was used. Whereas for the classification and derivation of LST from land surface emissivity and vegetation proportion values ERDAS IMAGINE 2015, ENVI 5.1 and Arc GIS 10.5 software package were used. Finally, the Sentinel-2A urban green cover map, urban land use categorical map and the LST retrieved from Landsat 8 were projected to a common projection system with UTM coordinate system. The detailed description of the methodology is outlined in the flow chart (Fig 3.7).

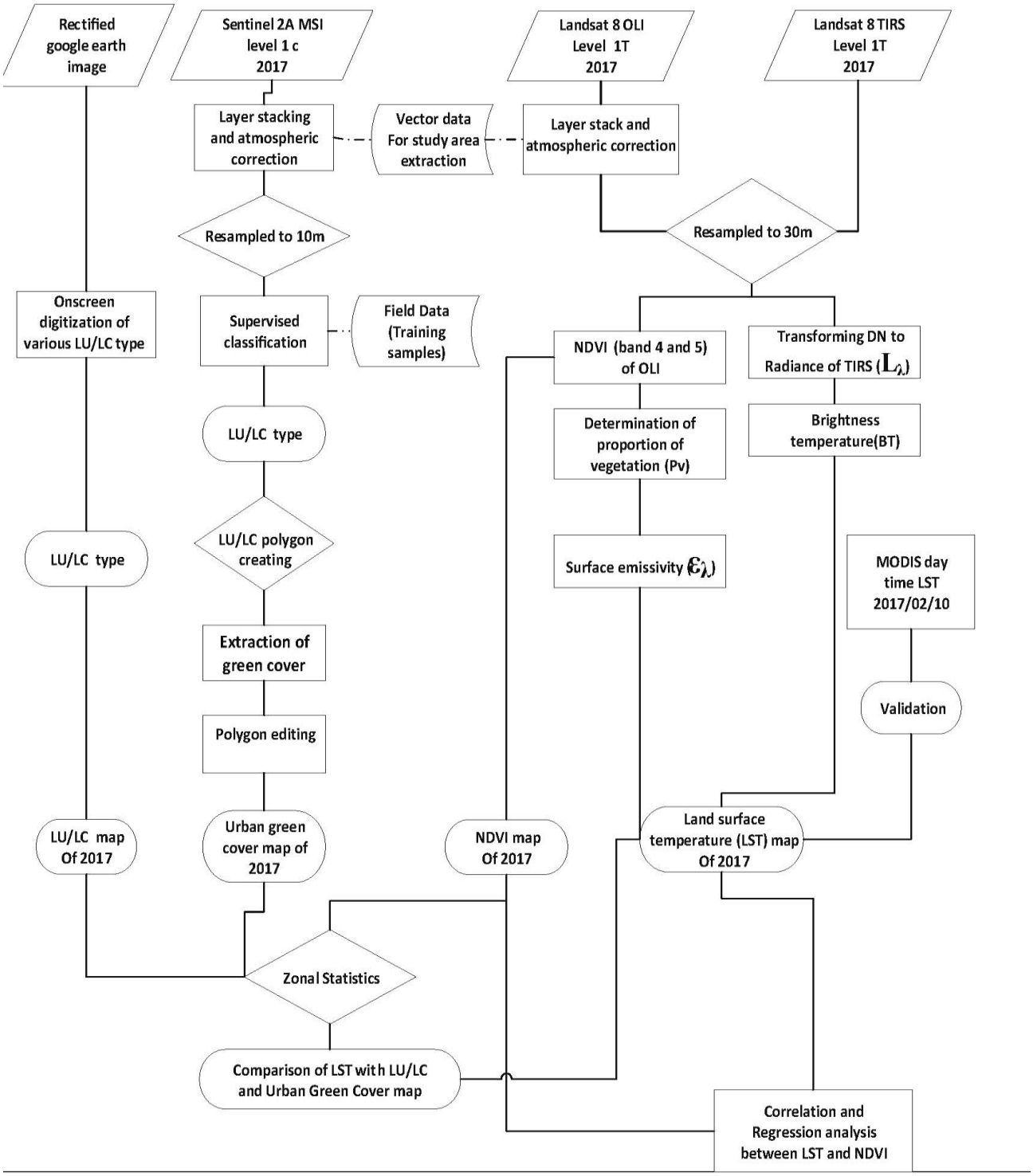

Figure 3.8: Methodological flow chart of the research activity

3.5 Image processing

3.5.1 Image preparation

As stated in the data section (Table 3.1.), four images were used for this study (sentinel-2A MSI, rectified google earth image, Landsat 8 OLI and TIRS and MODIS night time data of February 2017). The month of February is selected for the acquisition of this images, as it is a dry season for the acquisition of less cloud cover and high-quality satellite data of the area. Both satellite data (Sentinel- 2A MSI and Landsat 8 OLI and TIRS) had some atmospheric errors. Hence, they were not directly utilized for features identification and similar applications. It needs some correction. Therefore, pre-processing was undertaken before any further analysis and extraction of information from both satellite images. For the pre-processing of Sentinel-2A and Landsat 8 OLI image IMPACT Toolbox and ENVI 5.1 was used respectively. Whereas for the conversion of TIRS band data to Radiance and estimation of LST ERDAS IMAGINE 2015 was used.

For the UHI effect study of Hawassa, the analysis encompasses the surrounding areas of the city in order to have better understanding of the effect of the natural source of heat or the geological set up of the area. However, before the estimation of LST and extraction of land-use/land-cover type, all data were projected to the same coordinate system WGS_1984_UTM_Zone_37N and the sentinel-2A data was resampled to 10meter whereas the Landsat 8 OLI and TIRS were resampled to 30m x 30 meter using the nearest neighborhood resampling method.

3.5.2 Image enhancement

Before going for further analysis of the satellite images for LST retrieval and land cover classification some enhancement techniques were applied on the pixel values, to make the image more interpretable by increasing the visual discrimination between features in a scene. For example, sentinel-2A data was resampled to 10meter whereas the Landsat 8 OLI and TIRS were resampled to 30m x 30 meter using the nearest neighbor resampling method, False color composite (FCC), and computation of normalized difference vegetation indices were some of the enhancement techniques that were applied in this analysis.

3.5.3 Image classification

Mapping helps to see the spatial distribution of each land-use/land-cover type, the classification of each type has to be accurate especially for the spatial correlation of different urban phenomena's (e.g. Urban Heat Island). Therefore, to have a better LU/LC result on screen classification were applied to the rectified most current google earth image of the area. However, for the Urban Green

Cover (UGC) mapping, different methods were integrated and applied to the cloud free sentinel-2A satellite image and identified eight green cover types in the area. These are green areas in industrial units, greenery in sports facilities and open spaces, roadside greenery, ruderal vegetation, Stream bank/lake shore vegetation, urban greenery in family housing areas and public facilities, and urban park (Vatseva et al., 2016).

Relatively these data (rectified google earth and sentinel-2A) have high spatial resolution from other freely available data. For the purpose of this research the surface features were classified in to eighteen classes, such as water body, wet land, dense vegetation, high density built up, low density built up, sparse vegetation, shrubs and grass land, paved surfaces, services (schools, hospitals, different governmental offices, worship places), industries, open spaces (sport field and communal green areas), plantation (perennial vegetation), mining site, bare land (including barren and vacant land), airport, horticulture, lake side development, special function (open market and terminals). These LU/LC types were selected considering their thermal characteristics in the area. Initially the cloud free sentinel-2A image of the area was classified into six different classes using unsupervised classification technique, to examine the spectral reflectance of each type. Sample data from the field using GPS, google earth and visual interpretation the classification of selected land-use/land-cover type was prepared by applying supervised classification under maximum likelihood algorithm using ERDAS Imagine V.2015 then land cover polygons were made using ArcGIS 10.5 to extract and reclassify the urban green cover types of the area. Finally, urban green land-cover classes were identified and mapped.

3.5.4 Accuracy assessment

Looking at the spectral reflectance characteristics and considering the representative sample points from the field and google earth, a simple accuracy assessment, which is commonly used to assess the accuracy of results obtained from on screen classification was established. Therefore, similar techniques were applied to assess the accuracy of the classification results by taking systematic and random representative points from each land cover types.

Estimation of Land Surface Temperature

For the mapping or estimation of LST and characterization of urban heat island of Hawassa city, land surface temperature, which is retrieved from Landsat 8 band 10 were used considering the USGS notice not to use band 11 thermal data following the calibration uncertainty. An algorithm, which was prepared for Landsat 8 TIRS band 10 Satellite data were used to estimate LST using

ArcGIS 10.5 raster calculator. A recently developed and tested method by Avdan and Jovanovska (2016) were adopted for this single thermal data (band 10) LST retrieval using the formula stated below (eq1).

$$\mathbf{Ts} = \frac{BT}{\{1+\left[\left(\frac{\lambda BT}{\rho}\right)\ln\varepsilon\lambda\right]\}} \ldots\ldots\ldots\ldots\ldots\ldots\ldots\ldots\ldots\ldots\ldots\ldots\ldots\ldots eq1$$

Where $\mathbf{T_s}$ is the land surface temperature estimated from Landsat 8 TIRS band 10 data in Celsius (°C); BT is at-sensor brightness temperature in (°C) of band 10; λ is the wavelength of emitted radiance (for which the peak response and the average of the limiting wavelength (λ=10.895) were used) (Markham and Barker, 1985); ε_λ is emissivity calculated for band 10 data of Landsat 8 TIRS and whereas ρ was calculated using the formula (eq2)

$$\boldsymbol{\rho} = h\frac{c}{\sigma} \ldots\ldots\ldots\ldots\ldots\ldots\ldots\ldots\ldots\ldots\ldots\ldots\ldots\ldots eq2$$

Where, σ is the Boltzmann constant (1.38 × 10−23 J/K); h is Planck's constant (6.626 × 10−34 J s), and c is the velocity of light (2.998 × 10^8 m/s) (Avdan and Jovanovska (2016) and Weng *et al.* (2004).

3.5.5 Conversion of at sensor thermal spectral radiance (L_λ)

For further estimation of brightness temperature first the Landsat 8 TIRS band 10 data was changed to radiance through transformation of the DN value into thermal radiance formula stated below (eq3). This helps to transform DN for storage and transfer in a format of 16 digits, which gives the range of 0–65,535 value which make the calculation of brightness temperature easy.

$$\mathbf{L_\lambda} = M_{10}\ Q_{10} + A_{10} - O_{10} \ldots\ldots\ldots\ldots\ldots\ldots eq3$$

Where, L_λ is the spectral radiance (W·m−2·sr−1·μm−1) of band 10; M_{10} is the band-specific multiplicative rescaling factor for band 10; A_{10} is the band-specific additive rescaling factor for band 10; and Q_{10} is the DN value for the quantized and calibrated standard product pixel of band 10. Whereas O_{10} is the correction for band 10 issued by USGS for the calibration of TIRS bands of Landsat 8 TIRS before February 3, 2014, is 0.29 (W·m$_{-2}$·sr$_{-1}$·μm$_{-1}$). However, the data used for the estimation of LST was acquired after this date as a result this value has not been considered (Wang et al., 2015). The value for the coefficient M_{10} and A_{10} were obtained from the Metadata file of the image Based on the Metadata file, those constants M_{10} and A_{10} has 3.3420E-04 and 0.10000 values respectively (Table 3.2).

3.5.6 Determination of surface brightness temperature (BT)

The thermal spectral radiance (L_λ) value were converted to brightness temperature (BT) using the constants obtained from the metadata file K1 and K2 using the formula (eq4);

$$\mathbf{BT} = \frac{\mathbf{K2}}{\mathbf{ln}(\mathbf{1}+\frac{\mathbf{K1}}{\mathbf{L\lambda}})} - 273.15 \ldots\ldots\ldots\ldots\ldots\ldots\ldots\ldots\ldots\ldots\ldots\ldots \text{eq4}$$

Where, BT is brightness temperature (°C); L_λ is thermal spectral radiance; for Landsat 8 TIRS band 10 data; K1 and K2 are constants that has a value of 774.8853 and 1321.0789 respectively, in W·m−2·sr−1·µm−1 (Table 3.3).

Table 3.2: Determination of constants from the metadata file of the Landsat 8 TIRS Band 10.

Landsat8 PRODUCT_ID	M_{10}	A_{10}	K1 (W·m−2·sr−1·µm−1)	K2 (W·m−2·sr−1·µm−1)
"LC08_L1TP_168055_20170211_20170217_01_T1"	3.3420E-04	0.10000	774.8853	1321.0789

3.5.7 Derivation of Normalized Vegetation Index (NDVI)

Since the condition of vegetation is an important factor for the spatial distribution of LST and determination of ground emissivity. It was necessary to calculate NDVI of the area. Therefore, the NDVI was calculated from the multispectral satellite data of Landsat 8 OLI using the visible (red) band data (band 4) and near infrared (NIR) band (band 5) portion of the spectrum (Burgan and Hartford, 1993) using the following formula (eq5);

$$\mathbf{NDVI} = \frac{\text{NIR (band 5)} - \text{RED(band 4)}}{\text{NIR (band 5)} + \text{RED(band 4)}} \ldots\ldots\ldots\ldots\ldots\ldots \text{eq5}$$

The NDVI value range in between -1 and 1, the negative values are indicative of un healthy vegetation or the existence of other non-vegetated features or surfaces, while the positive value expresses reflective surfaces such as vegetated area or it is an indicative of high amount of healthy vegetation (Burgan and Hartford 1993). Therefore, the value of NDVI were determined as the proportion of vegetation (P_v) highly related with NDVI and ground emissivity (ε_λ), then P_v was calculated as per the following formula (eq6);

$$\mathbf{Pv} = \left(\frac{\mathrm{NDVI} - \mathrm{NDVIs}}{\mathrm{NDVIv} - \mathrm{NDVIs}}\right)^2 \ldots\ldots\ldots\ldots\ldots\ldots\ldots\ldots\ldots\ldots eq6$$

Where, P_v is the proportion of vegetation; whereas NDVIv and NDVIs is the suggested NDVI values for vegetation and soil (NDVIv = 0.5 and NDVIs =0.2) that were applied to determine the value of $P_{v,}$ respectively (Avdan and Jovanovska, 2016 and Sobrino *et al.,* 2004). However, the value may change in some cases, for higher resolution data over agricultural sites (e.g. NDVIv can reach 0.8 or 0.9 and more).

3.5.8 Determination of ground Emissivity ($\boldsymbol{\varepsilon_\lambda}$)

Emissivity is the radiant flux of an object at a given temperature over the radiant flux of a blackbody at the same temperature. The value of emissivity varies depending on surface type and wavelength, as a result, the value was calculated based on the NDVI threshold method at the same temperature and wavelength under the same viewing conditions. Because the method was not need accurate atmospheric correction since a scaled NDVI is used for the determination of vegetation fraction that is applicable for single thermal infrared data (Sobrino *et al.,* 2008). The value ranges in between 0 and 1 for a perfect reflector and emitter respectively (Flynn *et al.,* 2001; Avdan and Jovanovska, 2016; Sobrino *et al.,* 2004).

$$\boldsymbol{\varepsilon_\lambda} = \varepsilon_{v\lambda}\,\mathrm{Pv} + \varepsilon_{s\lambda}(1 - \mathrm{Pv}) + C_\lambda \ldots\ldots\ldots\ldots\ldots\ldots eq7$$

Where, ε_v and ε_s are emissivity of vegetation and soil, respectively, and the surface roughness is represented by a constant C, which is taken as a constant value of 0.005. However, for homogenous and flat surfaces the value of C = 0 (Jeevalakshmi *et al.* (2017) and Sobrino and Raissouni,2010). Emissivity is dependent on the wavelength, the values were estimated using NDVI threshold method based on the consideration of the wavelength ranges from 10-12μm (Jeevalakshmi *et al.,* 2017; Sobrino *et al.,* 2008).

$$\boldsymbol{\varepsilon_\lambda} = \begin{cases} \varepsilon_{s\lambda}, & \mathrm{NDVI} < \mathrm{NDVIs} \\ \varepsilon_{v\lambda}\,\mathrm{Pv} + \varepsilon_{s\lambda}(1 - \mathrm{Pv}) + C_\lambda, & \mathrm{NDVIs} \le \mathrm{NDVI} \le \mathrm{NDVIv} \\ \varepsilon_{s\lambda} + C_\lambda, & \mathrm{NDVI} \ge \mathrm{NDVIv} \end{cases} \quad \ldots \mathrm{eq8}$$

As per the result, NDVI values less than 0 were identified as water and the emissivity ($\boldsymbol{\varepsilon_\lambda}$) value of 0.971 is assigned; the NDVI values that ranges between 0 and 0.2 were founded as bare soil and the emissivity ($\boldsymbol{\varepsilon_\lambda}$) value of 0.986 was assigned; the NDVI value that ranges between 0.2 and 0.5 were identified as a mixture of fallow land, grass, shrubs and sparsely distributed urban vegetation

and the emissivity value was determined using the above formula (eq7), whereas the NDVI value greater than 0.5 were identified as dense woody vegetation and have the emissivity value of 0.991. Finally, the ground emissivity of the band was determined as a mean of these four land-use/land-cover types of the area.

3.6 Validation of estimated LST

Verification is important to check how well the data is for the intended activity, the validation process was done by taking random sample locations from Google Earth, and the LST value were extracted using zonal statistics from both MODIS day time and Landsat 8 TIRS LST. Finally, mean values of each polygon were compared.

3.7 Statistical analysis

3.7.1 Correlation and Regression analysis

One of the most frequently used technique to identify the quantitative relationship among different (dependent and independent) variables are statistical analysis method. From the previous studies of Urban Heat Island (UHI) that were conducted outside of the rift zones, the UHIs profile showed a significant variation in LST as one move from the center of the city to its surroundings over various land-use/land-cover types. Therefore, the correlation and regression analysis between LST and NDVI associated with urban land-use/land-cover type is discussed using different techniques such as linear regression method by integrating with zonal statistics data to identify the correlation. The impact of the geological set up of the wider area on LST was qualitatively described.

CHAPTER FOUR

4 RESULTS

4.1 Overview of LST for the years 1992-2002 in Hawassa and its surroundings:

This sub-section provides an overview of LST for the years 1992 to 2002 in Hawassa and its surrounding in order to have better understandings on the spatial/temporal variations of LST of surrounding areas of the study. As shown in figure 4.1, the areas surrounding the city and northwest of Lake Hawassa was characterized by high surface temperature as indicated in the LST map of 1992. However, the maximum temperature that was observed in 1992 was much less than that of 2002. Even though, the temperature of the surrounding areas observed in 1992 were lower as compared to that of 2002, areas that were represented as bare land (Northwest of Lake Hawassa and some parts of the city) had exceptionally recorded high surface temperature compared to settlement and vegetated areas both in 1992 and 2002. Other areas like north of Lake Hawassa around Urgi and Chebbi volcanoes and some parts of Wendo Genet hot spring areas were recognized by the high surface temperature (Fig 4.1).

As shown in figure 4.2a & b, the spatial distribution pattern of LST in the eastern part of Lake Hawassa was recognized with small variations of LST in the year 2002. However, this part had almost similar pattern of distribution to the year 1992. The South and East end of the area had almost similar spatial pattern of surface temperature in both years, and the area had also characterized by high vegetation density and complex cultivation patterns. The surface temperature of water body (Lake Hawassa) and wetland areas were almost constant in both years. Even though, the temperature of the area was high, the scattered and small hills in the city were also characterized by high surface temperature in both years.

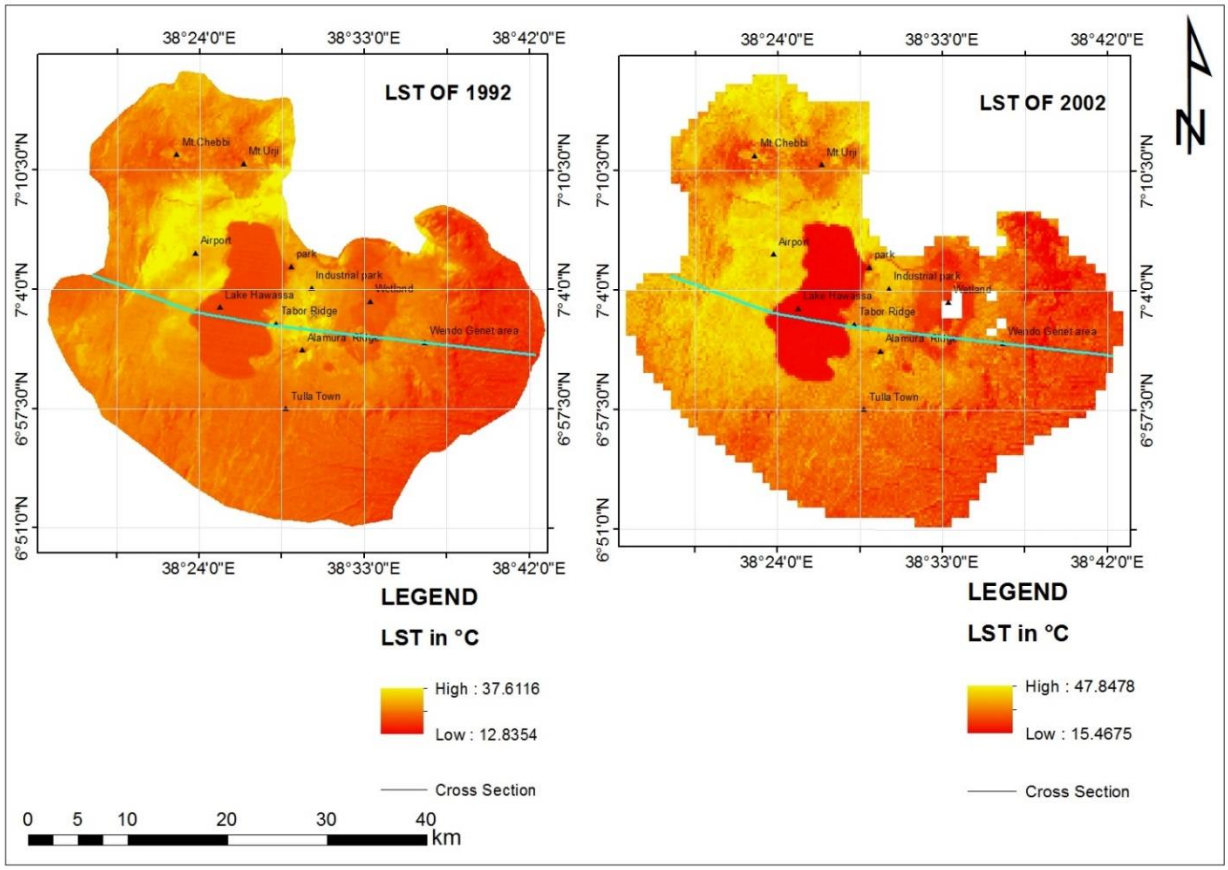

Figure 4.1: LST of surrounding areas of Hawassa for the period 1992 and 2002

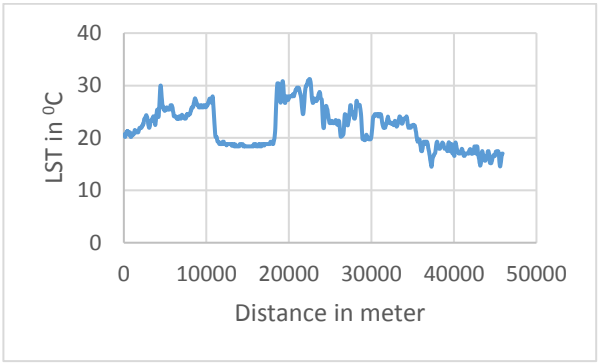

Figure 4.2a: Heat profile of Hawassa and surrounding areas from West to East end (1992)

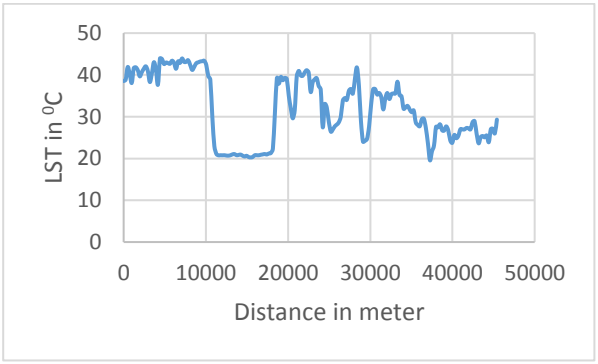

Figure 4.2b: Heat profile of Hawassa and surrounding areas from West to East end (2002)

4.2 Wider area heat variation analysis result of 2017

This sub-section provides the analysis result that are done considering the geological setting and vegetation distribution of the wider areas of Hawassa and its surroundings.

4.2.1 Spatial pattern of Normalized Difference vegetation Index (NDVI)

The vegetation distribution and condition in Hawassa and its surrounding vary from place to place. Figure 4.4 a & b show that areas to the East and South of the city have high distribution of green covers as compared to the North and west of the city, in particular, the western part of Lake Hawassa (Around the Airport) has poor vegetation, as represented by the NDVI value in the area. The area is represented as bare land since the NDVI value was less than 0.2 with relatively smooth curve in the profile. Some parts especially the northwestern end has relatively lower NDVI value whereas areas to the east of Lake Hawassa, especially the urban center is characterized as heterogeneous or coarse surface texture in terms of vegetation distribution as there was significant variation in vegetation distribution, areas like Tabor Ridge and other scattered hills are characterized by a very sparse distribution of NDVI value (Fig 4.3).

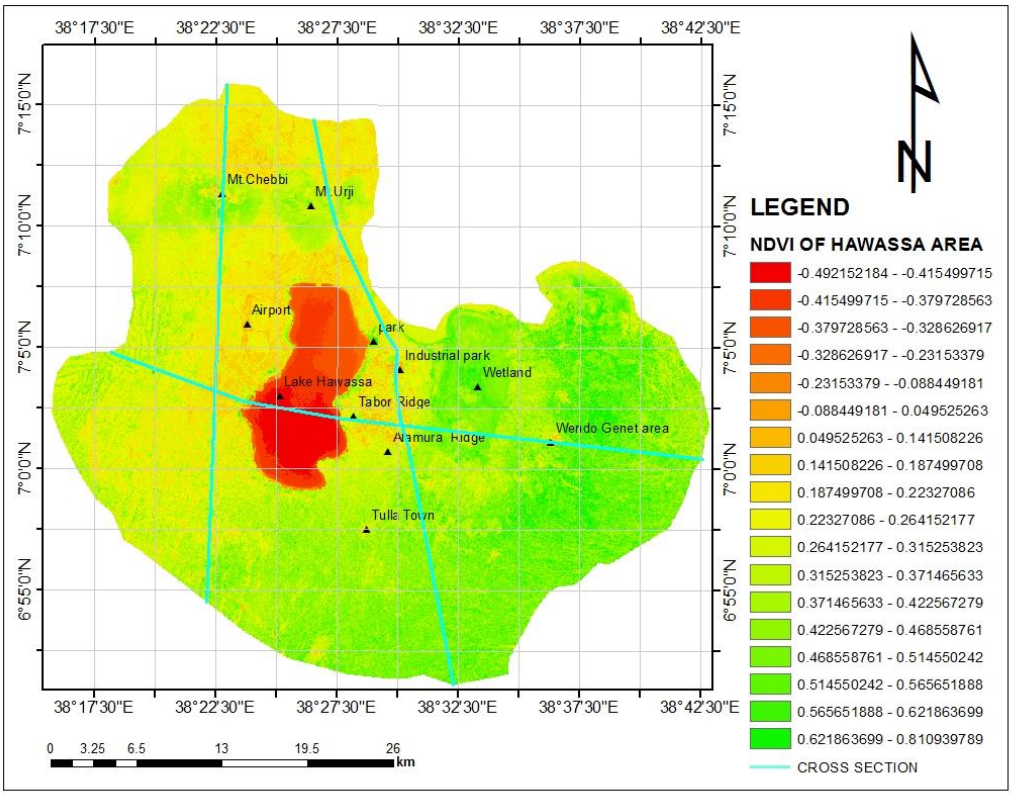

Figure 4.3: Normalized Difference Vegetation Index (NDVI) map of 2017

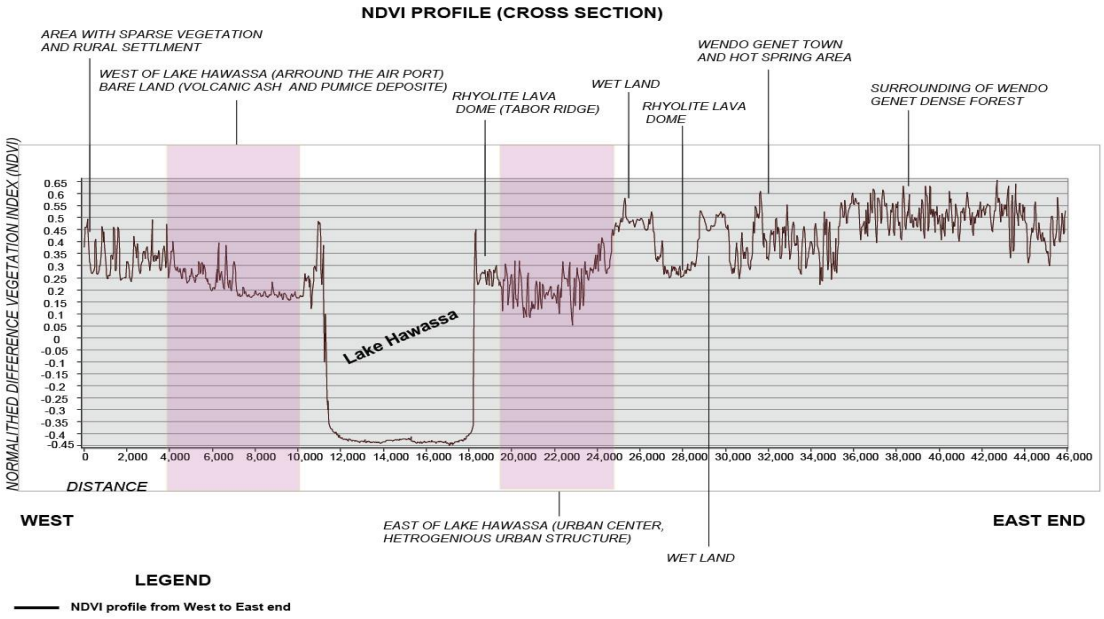

Figure 4.4a: Normalized Difference Vegetation Index (NDVI) profile of Hawassa area from West to East end

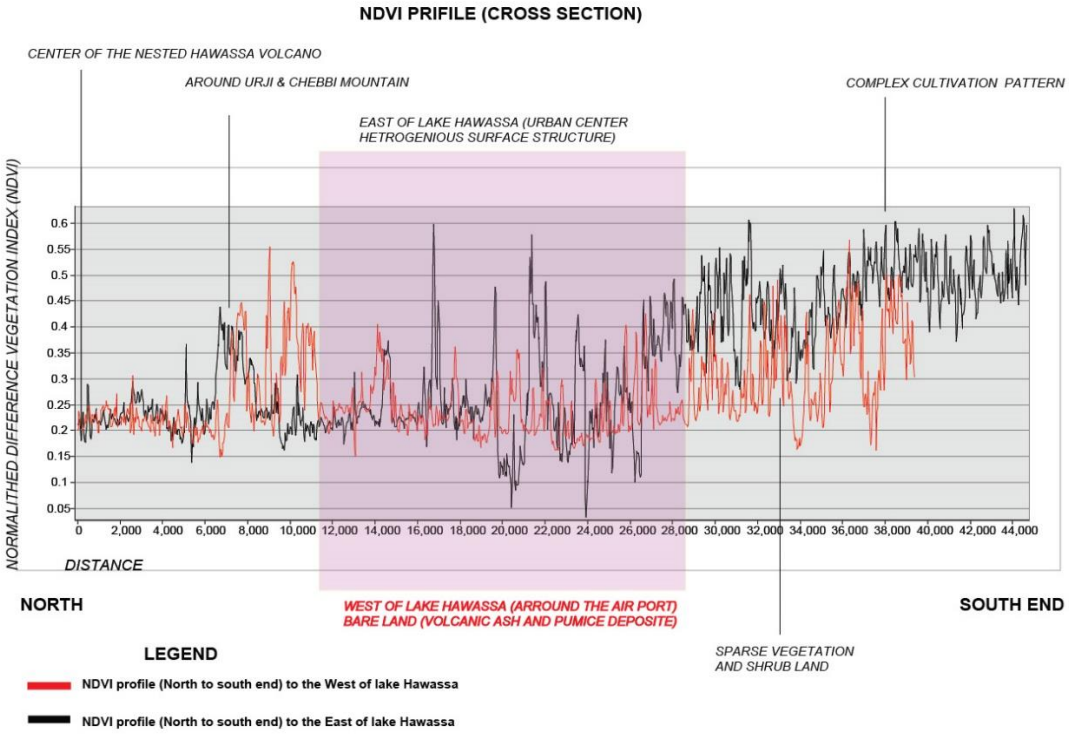

Figure 4.4 b: Normalized Difference Vegetation Index (NDVI) profile of Hawassa area from North to South end

4.2.2 Spatial distribution pattern of LST derived from Landsat 8 TIRS for Hawassa and its surroundings

As shown in figure 4.5, Hawassa and its surrounding areas experiences a temperature that ranges from 18 to 48^{0}C. From this, the maximum temperature was observed in the northern part of the area and West and eastern part, especially, around Wendo Genet area. Whereas, mount Urji and Chebbi in the northern parts of the Lake show relatively cooler surface temperature. Areas in the eastern side such as Wendo Genet forest and some parts of the south East has relatively lower surface temperature. The East and some parts of the south east direction of the study area was characterized by mixed cultivation and high-altitude rift escarpments that ranges from 2000 to 2669 m.a.s.l. As a result, the eastern and southern parts of the study area showed relatively lower surface temperature. Lowest temperature was recorded within and around Lake Hawassa (Water body). Those scattered and small hills especially those located east of Lake Hawassa experiences higher LST (Fig 4.6a & b).

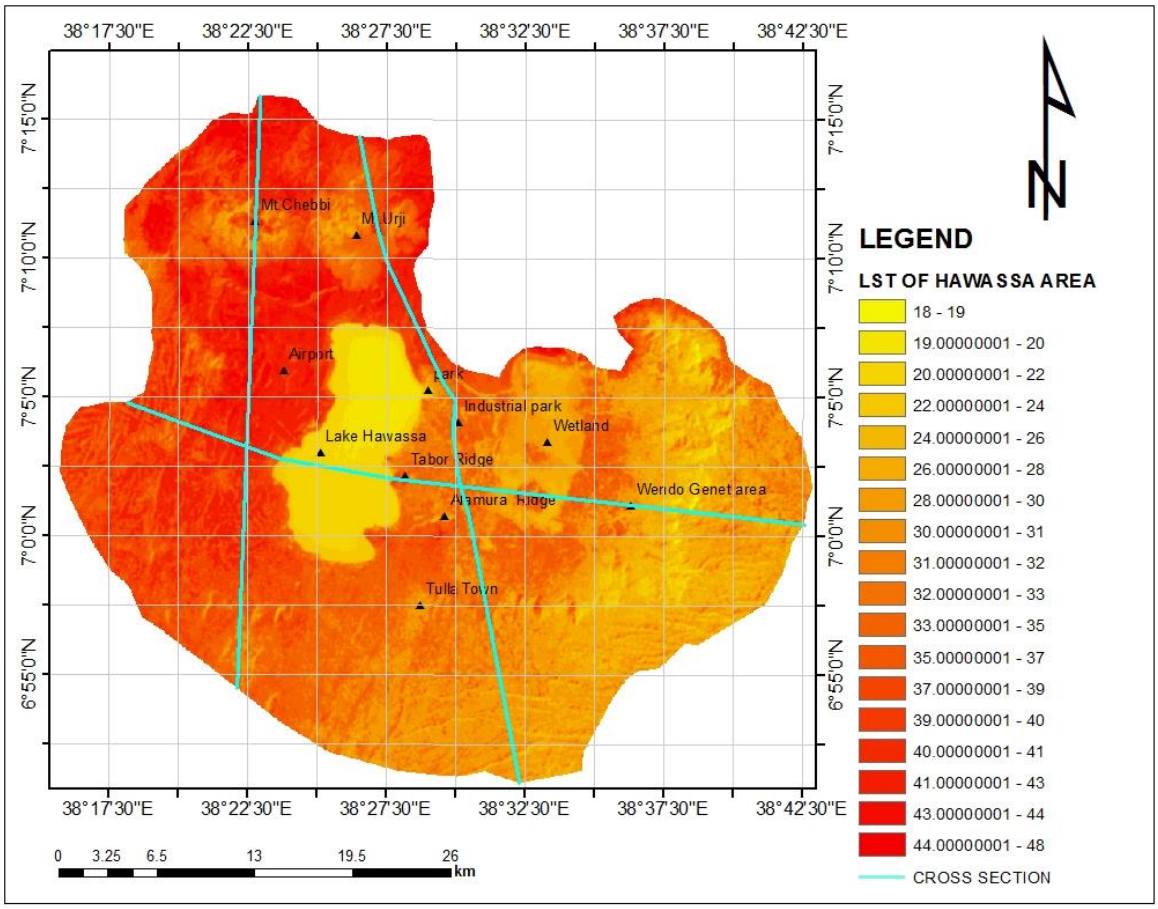

Figure 4.5: Spatial distribution pattern of Landsat 8 LST of surrounding areas of Hawassa

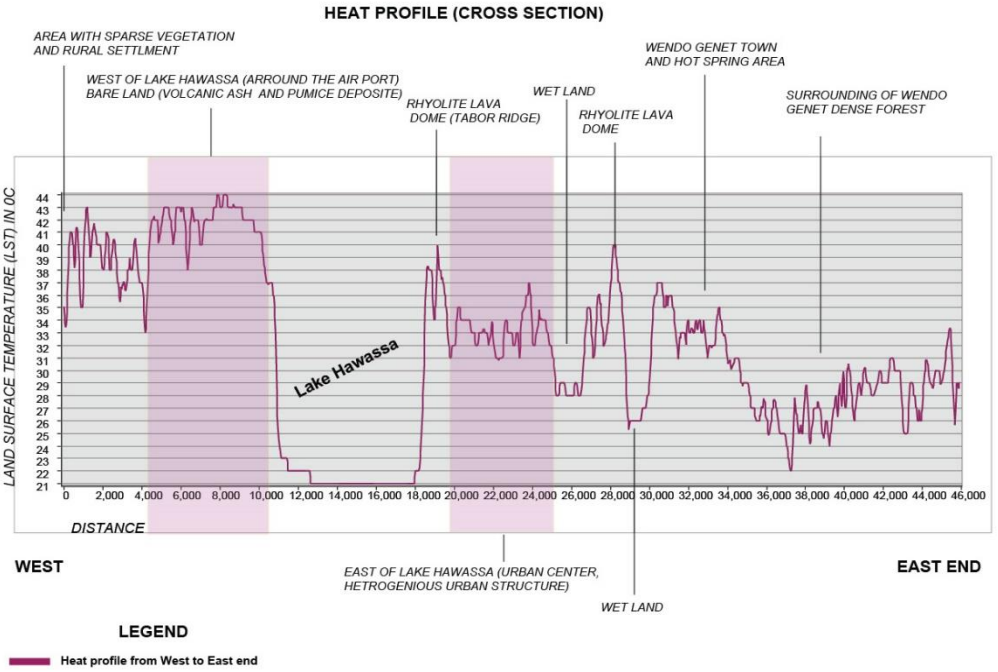

Figure 4.6a: Heat profile of Hawassa area from West to East end

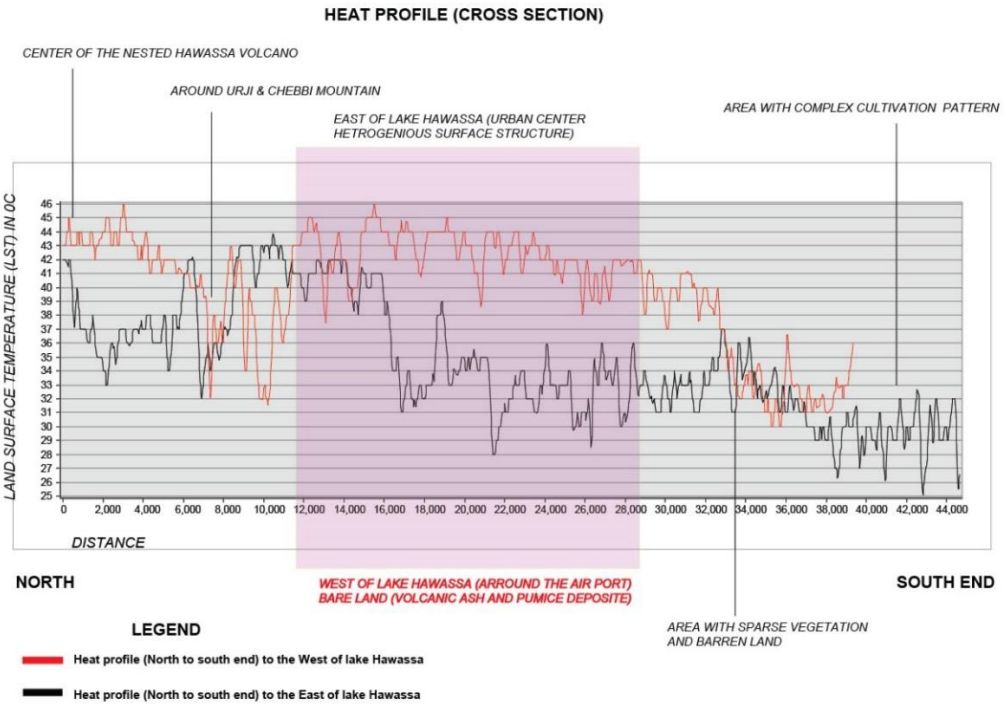

Figure 4.6b: Heat profile of Hawassa area from North to South end

As seen in figure 4.6 a & b, the area near to the center of the volcanoes (north of Lake Hawassa), composed of Rhyolite Lava flows and domes like Tabor Ridge and areas with volcanic ash and

pumice fall deposits (West of Lake Hawassa) show higher surface temperature compared to the urban area (East of Lake Hawassa). However, the settlement areas such as Hawassa city, show coarse textured surface temperature image, and this partly attributed to the variations in land cover type and vegetation density. The lower temperature in the map (Fig 4.5) close to Urji and Chebbi is due to the existence of thicker vegetation cover in the area.

4.3 Validation of estimated LST of Landsat 8 TIRS

The comparison result (appendix: 8), obtained from the extracted sample polygon shows that the variation of temperature between MODIS day time and TIRS of each polygon are all within 1.98^0C and the land surface temperature extracted from Landsat thermal band of the study area and the MODIS temperature have shown direct relationships.

4.3.1 Spatial pattern of MODIS night time Land Surface Temperature (LST)

The LST map derived from MODIS night image (Fig 4.7) shows the spatial pattern of LST in the area that ranges from 6.63 ^{o}C to 20.20^{o}C. As seen in the LST map, the eastern and southeastern parts of the area (Wendo Genet forest area) represent the coolest temperature. Whereas, southern and some parts of north west parts show relatively cooler temperature as compared to the settlement and bare land. The settlement areas in Hawassa and Wendo Genet areas (small towns such as, Wesha and Basha) exhibited relatively different LST pattern. As a result, the surrounding areas of Wendo Genet have relatively high surface temperature than Hawassa city, though, they still appear cooler during the day time as seen on LST estimated from Landsat 8 TIRS (Fig 4.5).

The northern part of the area, around Urji and Chebbi volcanoes, and volcanic domes in that area, which appear hotter in the day time LST estimated from Landsat 8 TIRS (Fig 4.5) are still hot during the night as seen on MODIS night time image (Fig 4.7). Whereas, the western part of Lake Hawassa (bare land) relatively appear colder than the Water body (Lake Hawassa) on the night time MODIS derived LST. Whereas the water body (Lake Hawassa) is hot just like what is observed around Wendo Genet and some parts of the north. However, when it's compared to the day time LST observed in Landsat 8 TIRS is nearly constant. In general, this MODIS night time LST value helps to see the inherent thermal behavior of the surface.

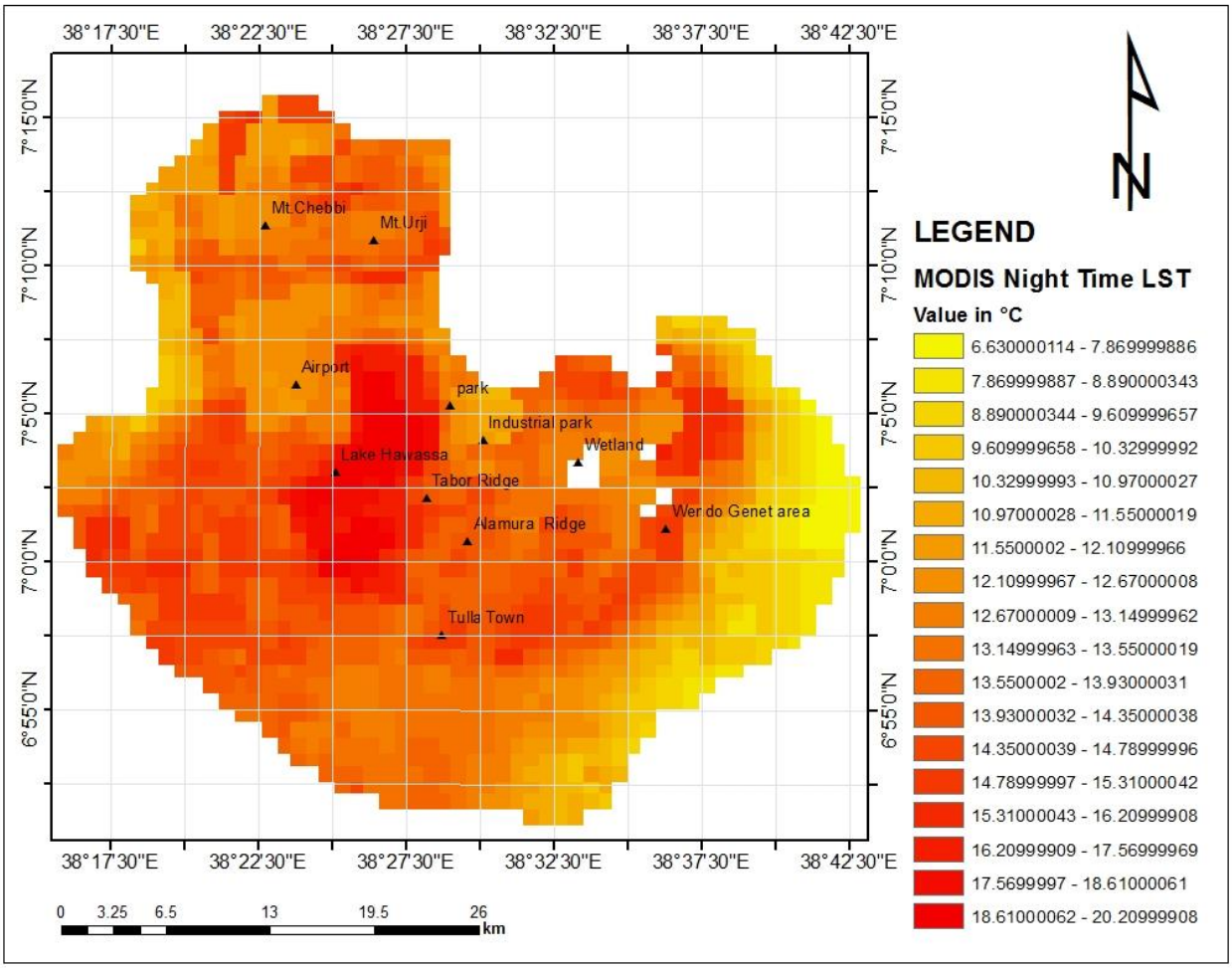

Figure 4.7: Spatial pattern of MODIS night time Land Surface Temperature (LST)

4.3.2 Correlation between LST and NDVI values

The result obtained from the study of the relationship between LST and NDVI or vegetation cover of surroundings of Hawassa area presented in this section. As depicted in the processed Landsat 8 TIRS, the area around the center of volcano (North of Lake Hawassa) experiences high surface temperature. However, mount Urji and Chebbi have relatively cold LST even though they are found around the volcano, due to the existence of vegetation cover in the area. Whereas, areas to the east end has also cold LST pattern as a result of higher vegetation cover.

Therefore, a particular relationship that exist between LST and NDVI has been identified for the area since the impact of vegetation cover is high in the spatial pattern of LST. As shown in figure 4.8, there is a very strong negative linear correlation between LST and NDVI. The correlation measure (R^2) is close to +1, which is 0.9659. As a result, those areas that have high NDVI values

have low LST and areas with low NDVI values have high LST. Negative correlation was obtained between NDVI values with LST as expected.

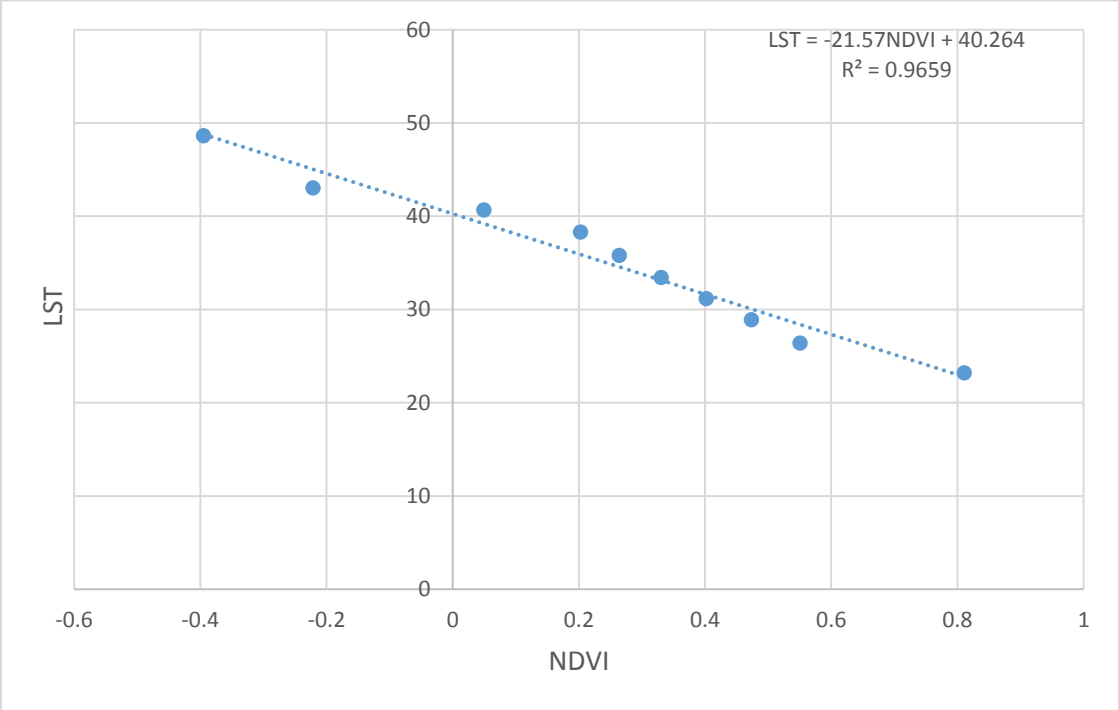

Figure 4.8: Correlation of LST with NDVI of Hawassa and its surroundings

4.4 Urban area heat variation analysis result

As described in chapter three, this sub-section provides result on the different parameters that had brought significant variations on the spatial distribution of LST in the existing settlement boundary of Hawassa city.

4.4.1 Land-use/land-cover (LU/LC) map of the period 1992, 2002 & 2017

As shown in the figure 4.9, the land-use/land-cover map of 1992 shows that most of the area of the city had bare land and low residential area that covers 19.85% and 4.2%, respectively. Whereas, sparse vegetation, wet land and shrubs and grass land together covers 6.93%. However, services, industrial areas, paved surfaces, open spaces, mining site and special function together covers 2.72%. At this period (in 1992), Lake Hawassa covers 66.28% from the total area of the study. At this period, the built-up structures (low built up areas, services and special function) were found close to the lake and they are smaller in their area coverage compared to bare land (Table 4.2).

Almost similar distribution pattern of land-use/land-cover types were observed in the year 2002 except some changes that was taken at the center of the settlement and some parts of the South

east direction of the city (Fig 4.9). As described in Table 4.2, water body covers large area of the study that is 65.04% with small changes compared to the 1992. Whereas, bare land covers 16.25%, low and high density built up area together cover 5.65% of the study area. Sparse vegetation, wet land and shrubs and grass land together covers 6.43%. However, services, industrial areas, paved surfaces, open spaces, mining site and special function areas together covers 5.12%. In this period (in 2002) new LU/LC types were added such as Airport (old airport), Lake Side development and dense vegetation that were not present in the year 1992 and covers 1.52% of the total area of study.

As shown in the figure 4.9, the present (2017) land-use/land-cover distribution of Hawassa is characterized by various land cover types that can bring a significant change on the LST variation. This includes, industrial park, high density built up areas, different service centers and extended mining activity areas and so on. As shown in the map, some sparse vegetation and low settlements are also observed within and surrounding of Tabor Ridge. From Table 4.1&4.2, Lake Hawassa have come to 59.79% from 65.04% seen in 2002. This is a decrease of around 5.25% in area. The extensive bare land that was observed in 1992 & 2002 map were reduced to only 6.18% of the area in 2017. Whereas, low and high built up area together had been increased to 15.65% from 5.65%, which is nearly 10% increase. However, sparse vegetation, wetland and shrubs and grass land together covers only 2.32% from 6.43% seen in 2002 and around 4.11% decrease. Services, industrial areas, paved surfaces, old airport open spaces, mining site and special function together covers 11.61%. Whereas, Lake Side development areas and dense vegetation covers 2.01% from 1.37% seen in 2002 around 0.64% increment. In this period (2017) new LU/LC types were added such as perennial vegetation and horticulture that were not there in the year 1992 and 2002 that covers 2.43% of the total area.

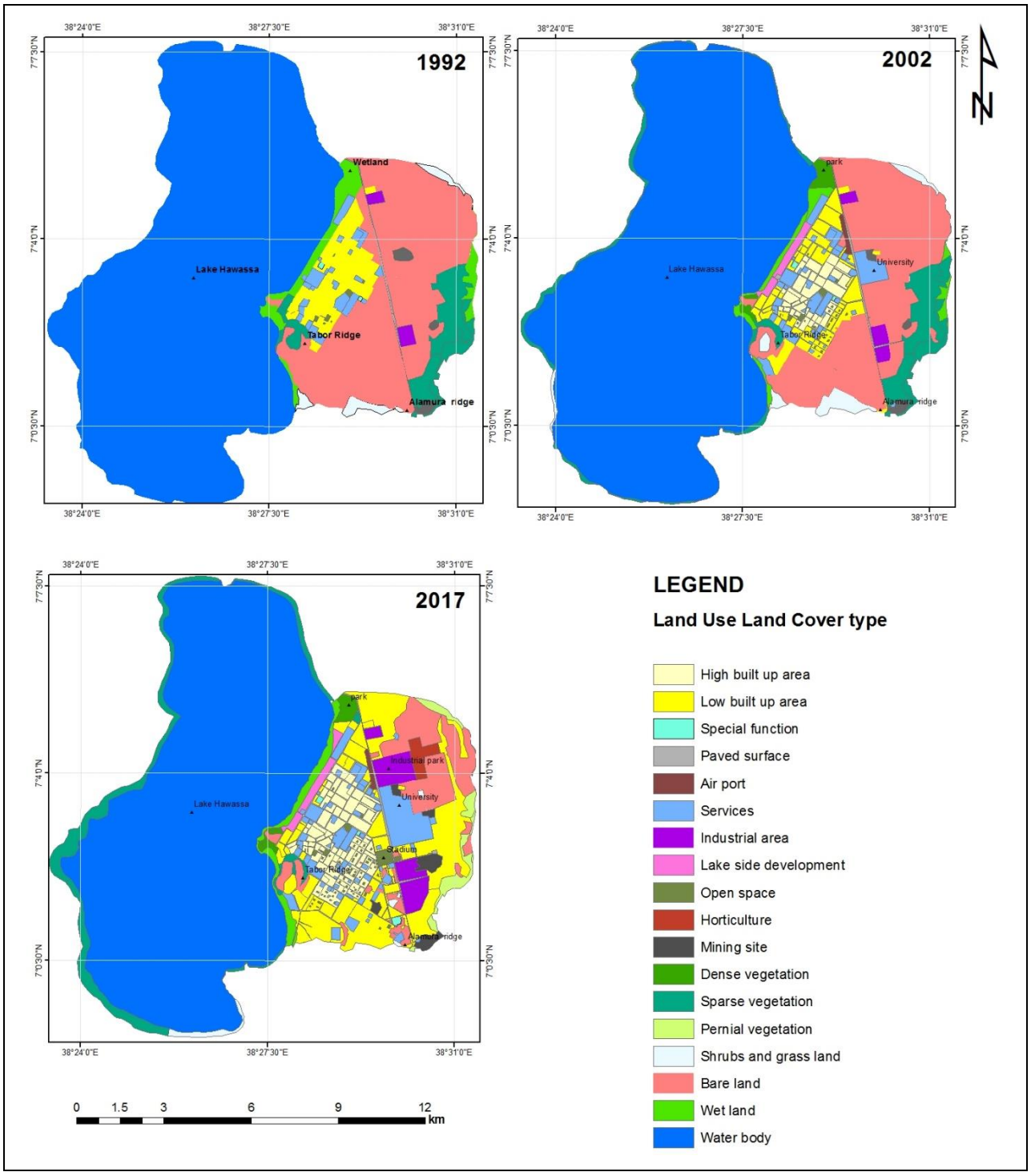

Figure 4.9: Land-use/land-cover maps of Hawassa for the year 1992, 2002 and 2017

Table 4.1: Summery of LU/LC classes with their area coverage

	1992		2002		2017	
Land cover type	Area in ha	Area in %	Area in ha	Area in %	Area in ha	Area in %
Water Body	9515.644	66.28183	9337.609	65.041717	8584.87924	59.7985294
Wet Land	319.40381	2.224828	199.61587	1.3904372	166.96408	1.162999053
Low Built up	601.73747	4.191441	608.82824	4.2408323	1303.90749	9.082451641
High Built up	0	0	202.87317	1.4131261	942.768887	6.566917415
Bare Land	2849.5372	19.84863	2330.6778	16.234486	886.664507	6.176118742
Industrial area	58.548492	0.407823	94.346328	0.6571754	358.613934	2.497948457
Service	213.51526	1.487254	360.4889	2.5110086	642.401231	4.474687157
Paved Surface	39.216766	0.273167	175.22072	1.2205112	278.581874	1.940479988
Sparse Vegetation	562.33501	3.916981	539.34568	3.7568471	97.7607426	0.680958751
Shrubs and Grass land	116.75684	0.813277	184.20891	1.283119	69.0847836	0.481214511
open Space	13.6957	0.095398	37.221631	0.2592697	135.350248	0.942790869
Minning area	59.887726	0.417152	52.615009	0.3664932	165.4975	1.152783495
Old air port	0	0	20.465033	0.1425505	20.465033	0.142550506
Special Function	6.060117	0.042212	15.646862	0.1089892	66.8007126	0.465304667
Lake side developmer	0	0	123.51534	0.860354	141.497729	0.985611544
Dense vegetation	0	0	73.659938	0.513083	146.958737	1.023650547
perennial vegetation	0	0	0	0	218.016914	1.518610857
Horticulture	0	0	0	0	130.124736	0.906392229
TOTAL	14356.338	100	14356.338	100	14356.3384	100

4.4.1.1 Spatial extent of land-use/land-cover during the period 1992-2017

The overall LU/LC mapping and spatial extent analysis is helpful to know the LU/LC dynamics of the area, which intern is important to understand the surface characteristics and the relationship with LST dynamics within the study period. In the last 25 years (1992 to 2017), the city has been under rapid land-use/land-cover change. This change not only described by the increase or decrease of the existing LU/LC but also new LU/LC types introduced in the period of 1992-2017. The most important Land cover water body that regulates the temperature of the city, has been decreasing which accounts 752.73 ha decrease from 2002 to 2017 that is much higher than the decrease observed from year 1992 to 2002, which is 178.04 ha (Table 4.3). The same is true for bare land, it has also decreased by 1,444.01ha from 2002 to 2017, which is high as compared to the decrement seen from 1992 to 2002 (518.85 ha). In general, the second phase of LU/LC change (2002-2017) same LU/LC dynamics was observed in some LU/LC types, those which were under increase are still increasing (low and high built up areas, services, Industries, paved surfaces, open space, mining areas and special function) and those which were decreasing are still decreasing (wet lands and sparse vegetation) just like what we have seen for water body and bare land (Table 4.3). However, Lake Side development, Horticulture and perennial vegetation are among the

newly introduced land use that were not there in the first phase (1992-2002) and added in the second phase (2002-2017). Whereas, old airport does not have any change in the second phase (2002-2017), however, the city has new airport, which is not under the existing settlement boundary. As seen in the change matrix (Table 4.4a & b), the transformation of most LU/LC type has been taking place as the expense of bare land. As a result, the urbanization trend of the city was taking place on bare or degraded areas of the city that does not have green vegetation cover.

Table 4.2: *Summery of Land-use/land-cover change in the period of 1992 to 2017*

	1992-2002		Rate of change	2002-2017		Rate of change	1992-2017	
Land cover type	Area in ha	Area in %	per year in ha	Area in ha	Area in %	per year in ha	Area in ha	Area in %
Water Body	-178.035	-1.2401	17.8035	-752.73	-5.24319	50.18198	-930.7648	-6.4833
Wet Land	-119.7879	-0.8344	11.97879	-32.6518	-0.22744	2.176786	-152.4397	-1.06183
Low Built up	7.0907771	0.04939	0.709078	695.0792	4.84162	46.33862	702.17	4.891011
High Built up	202.87317	1.41313	20.28732	739.8957	5.15379	49.32638	942.7689	6.566917
Bare Land	-518.8594	-3.6141	51.88594	-1444.01	-10.0584	96.26755	-1962.873	-13.6725
Industrial area	35.797836	0.24935	3.579784	264.2676	1.84077	17.61784	300.0654	2.090125
Service	146.97363	1.02375	14.69736	281.9123	1.96368	18.79416	428.886	2.987433
Paved Surface	136.00395	0.94734	13.6004	103.3612	0.71997	6.890744	239.3651	1.667313
Sparse Vegetation	-22.98932	-0.1601	2.298932	-441.585	-3.07589	29.439	-464.5743	-3.23602
Shrubs and Grass land	67.452075	0.46984	6.745208	-115.124	-0.8019	7.674942	-47.67205	-0.33206
open Space	23.525931	0.16387	2.352593	98.12862	0.68352	6.541908	121.6545	0.847393
Minning area	-7.272717	-0.0507	0.727272	112.8825	0.78629	7.525499	105.6098	0.735632
Old air port	20.465033	0.14255	2.046503	0	0	0	20.46503	0.142551
Special Function	9.5867451	0.06678	0.958675	51.15385	0.35632	3.410257	60.7406	0.423093
Lake side development	123.51534	0.86035	12.35153	17.98239	0.12526	1.198826	141.4977	0.985612
Dense vegetation	73.659938	0.51308	7.365994	73.2988	0.51057	4.886587	146.9587	1.023651
perennial vegetation	0	0	0	218.0169	1.51861	14.53446	218.0169	1.518611
Horticulture	0	0	0	130.1247	0.90639	8.674982	130.1247	0.906392

Note: The minus sign represents the negative LU/LC change

Table 4.3: Land-use/land-cover change matrix of a) 1992 to 2002 and b) 2002 to 2017

		2002																
	LULC	B	I	LO	M	OS	P	S	SL	SV	SF	W	WL	D	H	LS	OA	Grand Total
	B	2288.00	16.33	241.93		20.01	44.42	146.87	35.01	9.34	9.70		1.11		24.26		20.47	2849.54
	I		58.55															58.548492
	LO			330.19		0.93	73.53	12.95			0.08				184.06	0.01		601.737466
	M	13.80		3.13	43.03			0.02		0.01								59.887726
	OS					14.65									0.00			13.6957
	P			2.59			36.65											39.216766
	S	6.90					16.28	190.31							0.00	0.00		213.515264
	SL	1.11	20.00		9.60				96.74									116.756835
	SV	20.77		30.31	0.00		4.03	2.07	14.88	490.23			0.02	0.01				562.335005
	SF						0.20				5.86							6.060117
	W								38.30	7.04		9337.61	69.43	2.73				9515.64404
	WL	0.08								33.10			129.12	83.69		73.36		319.403812
1992	Grand Total	2330.68	94.3463	608.828	52.615	37.2216	175.221	360.489	184.209	539.346	15.6469	9337.61	199.616	73.6599	202.873	123.515	20.465	14356.34

		2017																		
	LU/LC	B	D	H	I	LS	LO	M	OA	OS	P	S	SL	SV	SF	W	WL	HO	PV	Grand Total
	B	826.665		288.136	264.197		662.607	55.8171		74.735	108.905	248.239	10.6479	0.21925	19.2021			130.125	52.6748	2330.677757
	D	1.7583	71.9016																	73.65993813
	H			198.754						4.11923										202.8731691
	I				94.3463															94.34632813
	LS		7.0926			116.423														123.5153351
	LO			455.402			268.696			13.6037	5.196217	0.10557		0.00563						743.0087971
	M	0.0027						52.9799												52.9826366
	OA								20.465											20.465033
	OS			0.47729			0.14756			36.953										37.577858
	P	0.49887									161.8615	12.7875		0.07293						175.2207181
	S						2.57475				1.573179	356.341								360.4888961
	SL	13.3709					64.1123				0.529484	0.01727	35.4686	1.30085	31.3197		1.40945		36.6804	184.2089101
	SV	9.97617	1.7583		0.07061	9.40493	280.078	56.3004		5.93934	0.516513	22.6836		27.4096	0.63212		3.3101		121.266	539.3456821
	SF														15.6469					15.64686213
	W												22.9683	23.7772		8584.88	343.717			9337.608996
	WL	34.4463	66.2062			15.6701	25.6924					2.22764		44.9753			51.1789		7.39568	247.7925117
2002	Grand Tota	886.665	146.959	942.769	358.614	141.498	1303.91	165.497	20.465	135.35	278.5819	642.401	69.0848	97.7607	66.8007	8584.88	199.616	130.125	218.017	14356.33838

B

Note: B= Bare land, D= Dense vegetation, H= High built up area, I= Industrial area, LS= Lake side development, LO= Low built up area, M= Mining site, OA= Old airport, OS= Open space, P= Paved surface, S= Service, SL= Shrubs and Grass land, SV= Sparse vegetation, SF= Special function, HO= Horticulture, PV= Perennial vegetation, W= Water body and WL= Wet land

4.4.1.2 Accuracy assessment of LU/LC map for the period 1992, 2002 & 2017

Only aerial photographs for the classification of the previous years (1992 & 2002), it was difficult to have accuracy assessment done. This is mainly due to lack of ground truth. However, the existence of similar surface features that cover large area, roof size, historical or previous documents obtained from the municipality of the city by relating with the present data (2017) of the present location, made it possible to classify and asses the accuracy reliably. As a result, the overall accuracy of these two periods result are 85.18% and 87.87% respectively. The overall accuracy of the latest year (2017) is 88.75% with a kappa of 0.87.

4.4.2 Urban green cover change of Hawassa city during the period 2002-2017

The green cover in the city has increased by 32.03%, which is around 372.845 ha. From the map (Fig: 4.10), one can see that those areas, which was bare land in the year 2002, is covered by green surfaces that has a little bit fair distribution in the city center. In the year 2002, the urban green cover was 791.28ha, but in the year 2017, it occupies 1,164.125ha. Most of the green covers in the year 2017 are the result of urbanization, because, most of these green covers are found within individual housing and service areas. In terms of distribution those green covers that are found along the lake shore and in service areas are dense as compared to vegetation that are found in housing areas.

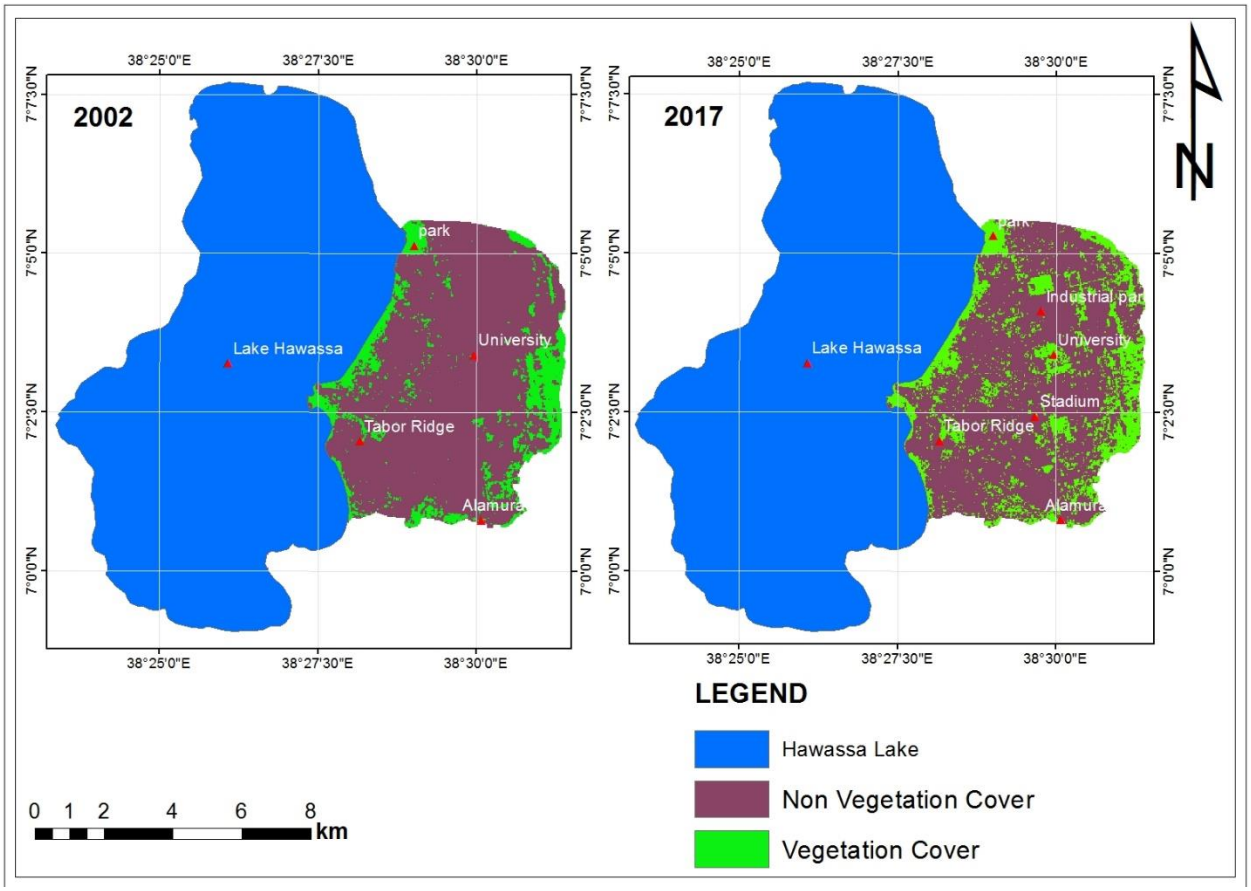

Figure 4.100: Urban green cover change of 2002 and 2017 of Hawassa

4.4.3 Urban Green Cover (UGC) type of Hawassa

The result of green cover classification (Fig: 4.11) shows, the eight main urban green cover types that are identified and mapped. These are, greeneries in industrial units, greeneries in sport facilities and open space, ruderal vegetation, Stream bank/lake shore vegetation, urban greenery in family housing areas, urban greenery in public facilities, urban park and road side greenery. Greeneries that are found surrounding the water bodies or wetlands (Stream bank/lake shore vegetation) have high density and it includes herbaceous plants and other broad leaf vegetation that cover large areas of the city. Whereas, greeneries that are found in family residential areas are characterized by sparse distribution and limited in settlement areas. Greeneries that are found in public facilities (service areas) have somehow regular shape and located in the main part (center) of the city like that of greeneries in sport fields and open spaces. Whereas, sparse vegetation are found at the periphery and some parts of mountainous area (Tabor and Alamura) and surrounding of horticulture and they are categorized under ruderal vegetation. Two urban parks are found in the city with dense vegetation cover close to Lake Hawassa (Tikur Wuha and Amora Gedel Park)

and few street segments have street trees in both sides of the street segment including median around Piazza. However, in the city few industries are found with few vegetation covers such as Hawassa textile and flour mill factory, the rest including industrial park are characterized by poor vegetation cover.

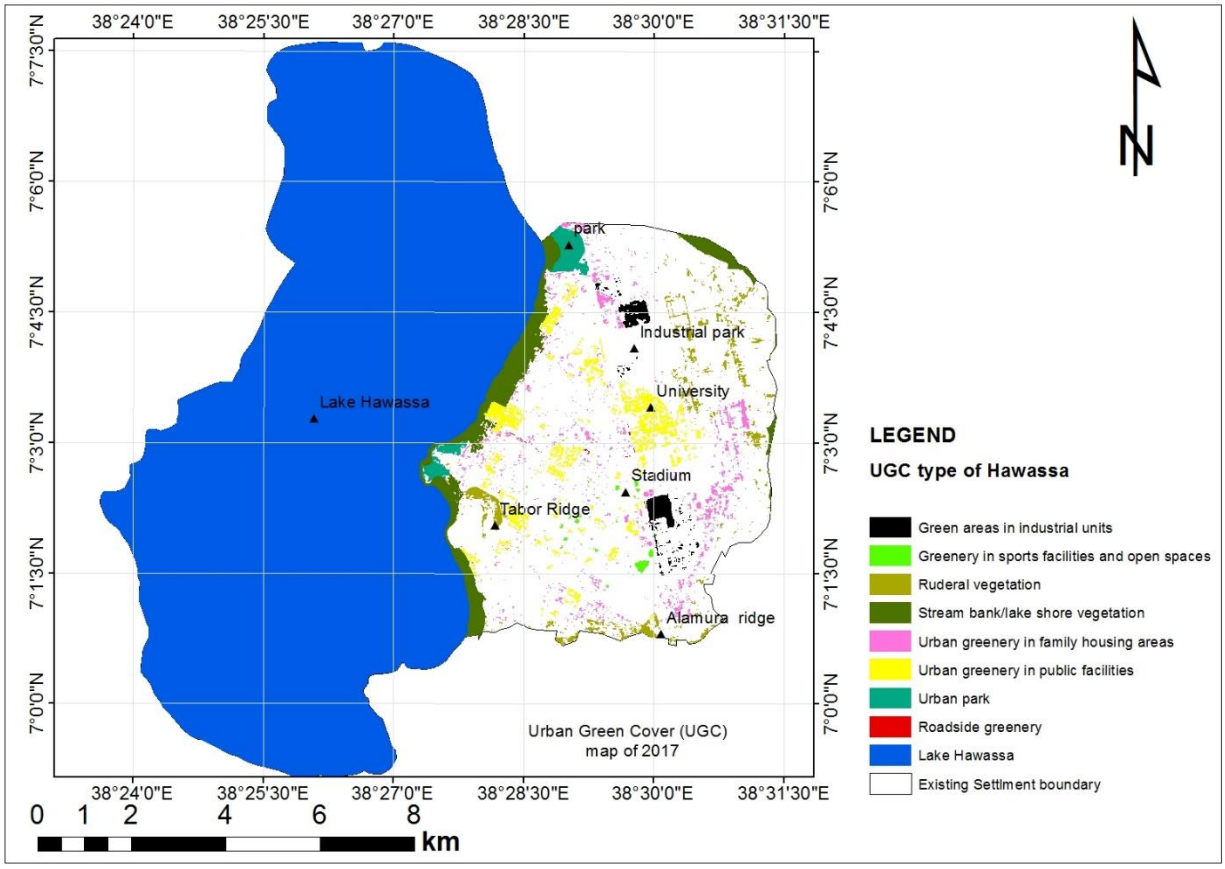

Figure 4.111: urban green land cover type of 2017 of Hawassa

As shown in figure 4.12 stream bank/lake shore vegetation, greeneries in public facilities and family (individual) housing areas has high distribution with an area of 335.58, 203.90 and 148.27 ha, respectively. Others like road side greenery, greenery in sport facilities and open spaces and green areas in industrial unit has lower vegetation distribution with an area of 7.40, 14.79 and 66.28 ha, respectively. Whereas, ruderal vegetation and urban park covers an area of 134.24 and 91.43 ha, respectively.

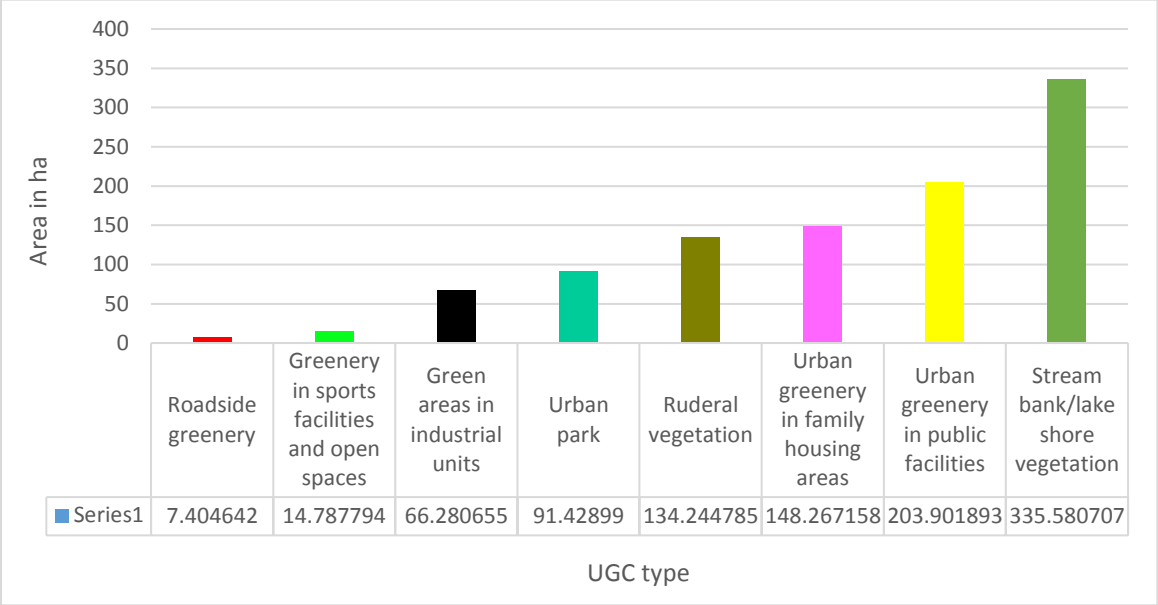

Figure 4.122: urban green land cover distribution of 2017 for Hawassa

4.4.3.1 Accuracy assessment of UGC map of 2017

The classification result in figure 4.11 shows, eight main urban green cover types that are identified and mapped with the accuracy of 86.25% with a kappa of 0.82 using 80 systematic and random samples (Table 4.5). The mapping process of Hawassa green cover consider dominant vegetation that are detected with in the spatial resolution of 20 meter. However, small polygons within this map class present difficulties in both the mapping and accuracy assessment phases.

Table 4.4: Accuracy assessment error matrix for UGC classification of 2017

Ground truth

On screen classification result										
LU/LC type	GI	GS	RG	RV	LV	GF	GP	P	**Total**	**User accuracy**
GI	3	0	0	0	0	1	0	0	4	75
GS	0	6	0	0	0	1	1	0	8	75
RG	0	0	2	0	0	1	0	0	3	66.67
RV	0	1	0	10	0	1	0	0	12	83.33
LV	0	0	0	0	5	0	0	0	5	100
GF	0	0	1	1	0	29	0	0	31	93.55
GP	0	0	1	0	0	1	12	0	14	85.71
P	0	0	0	0	0	1	0	2	3	66.67
Total	3	6	4	11	5	36	13	2	80	
Producer accuracy	100	85.71	50	90.91	100	82.86	92.31	100		
Overall accuracy = 86.25% Kappa coefficient =0.82										

Note: GI= Green areas in industrial units, GS= Greenery in sports facilities and open spaces, RG= roadside greenery, RV= Ruderal vegetation, LV= Stream bank/lake shore vegetation, GF= Urban greenery in family housing areas, GP= Urban greenery in public facilities, and P= Urban park

4.4.4 Mean NDVI by land-use/land-cover type

As shown in Figure 4.13, the highest mean NDVI value is found in densely vegetated areas, Wet land, Lake Side development and Horticulture and perennial (plantation) areas. Whereas, the minimum value of mean NDVI are found in bare land, paved surface, old airport and Mining areas of the city respectively. The shrubs and grass land, open spaces, services and low density built up areas of the city have almost closely associated mean NDVI value with sparsely vegetated areas. However, the mean NDVI value of Water is always low (negative).

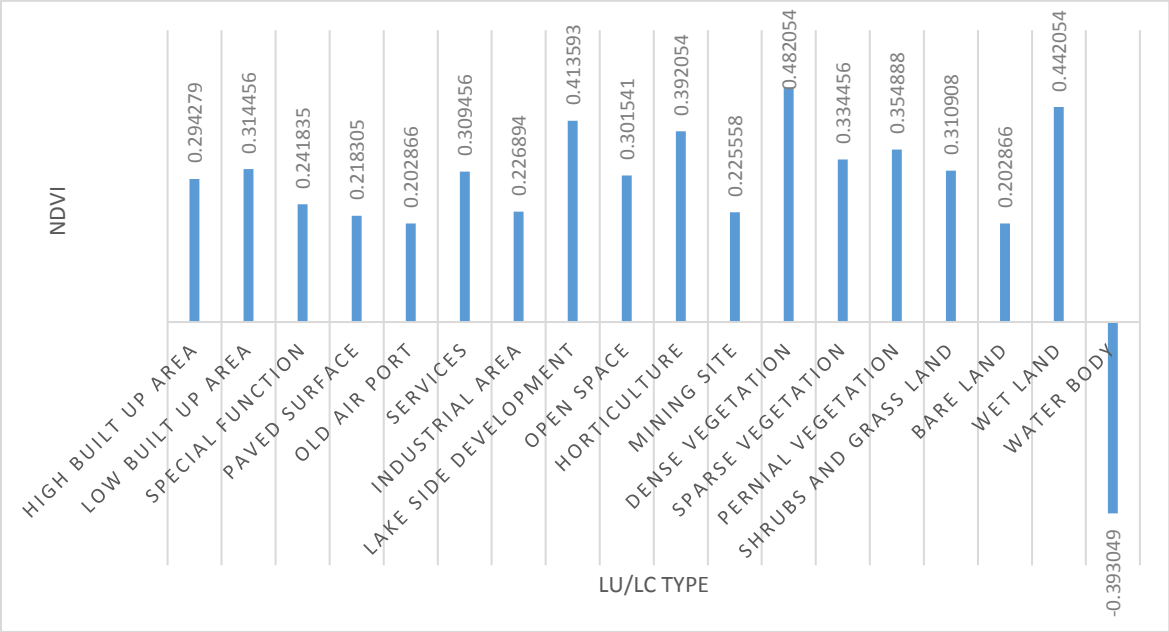

Figure 4.133: Mean NDVI of LU/LC type of Hawassa city for 2017

4.4.5 Spatial variation of LST in the urban area with respect the various LU/LC types

The LST of the city was extracted for the larger surrounding areas of the city in order to analyze the spatial variations at appropriate scale. Therefore, as shown in the map (Fig 4.14), the surface temperature of the city ranges from 20.6 to 41.3^{0}C and the minimum temperature was recorded in the lake and the surrounding areas of wetlands. On the other hand, the maximum temperature was registered in mountainous areas (Tabor Ridge) and areas that are being used for quarry and some parts of bare lands including industrial park of the city.

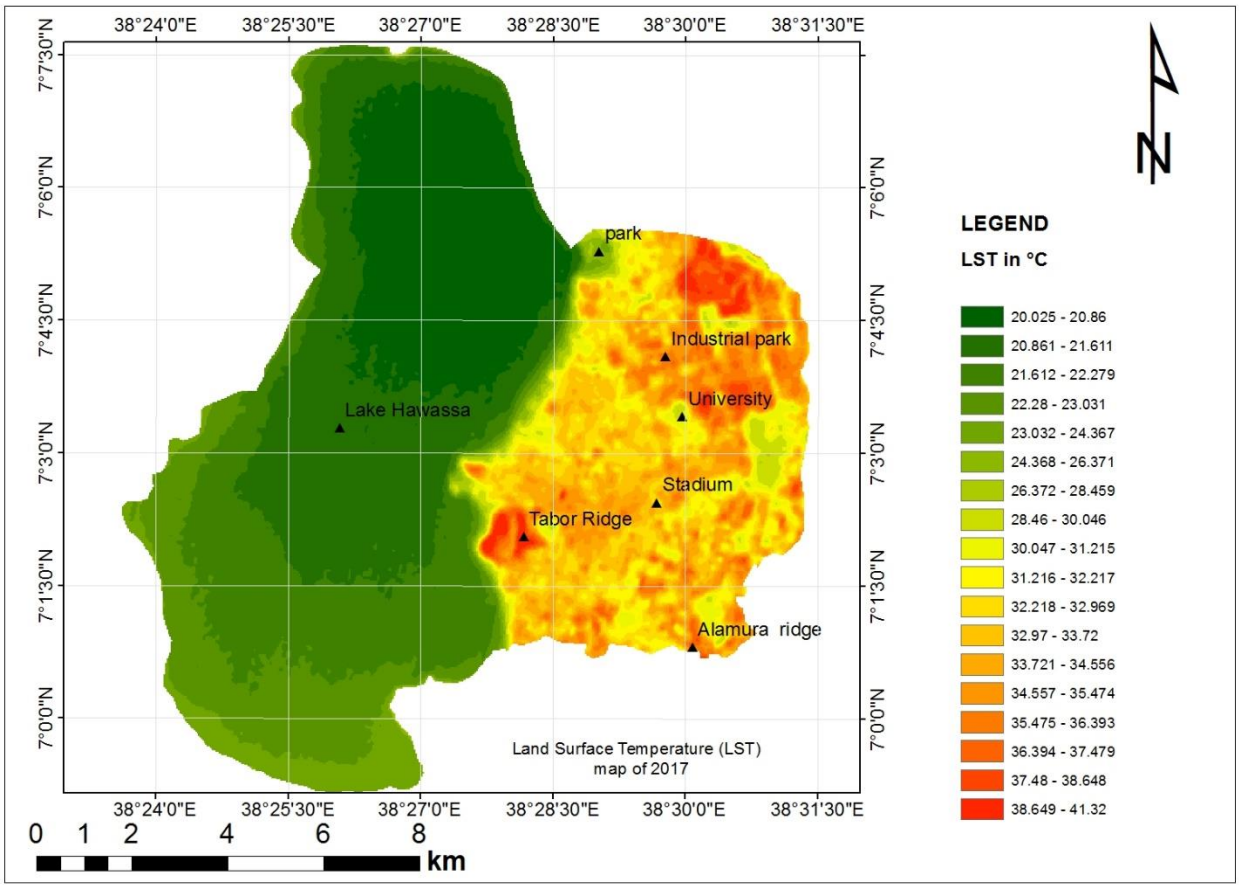

Figure 4.144: Spatial pattern of LST of Hawassa city in 2017

4.4.6 Mean LST by land-use/land-cover (LU/LC) type

The mean LST value associated with various LU/LC type in figure 4.15 shows that quarry site (areas that are used for excavation of scoria and building stone) shows the highest mean LST in the city, because these areas are highly sensitive to natural sources of heat since these areas were created by volcanic lava domes. Similarly bare land shows higher mean surface temperature because these areas does not have green cover and the surface is covered with basaltic ash deposit with high surface reflectance. As a result, the mean LST observed in these area does not represent the thermal property of the surface, because, the measured LST is the aggregate of radiance and reflectance of the surface due to the nature of the surface (Fig 4.7). Other areas, such as large open market and bus terminals, industries, paved surfaces, old airport and high built up area shows high mean LST value because of heat generated by human activities, warehouses with large roof size, shortage of green cover and closeness to the city center for urban heat island effect. Whereas, lake side development, sparse vegetation, shrubs and grass land, services and low built up areas shows lower mean LST because of scattered and broad leaf ever green trees in the urban center that

contributes for the reduction of the UHI effect. Others like, dense vegetation, wetland and perennial vegetation shows the lowest mean LST values because of dense and ever green trees that has high rate of evapotranspiration due to greater vegetation cover and extensive water they had.

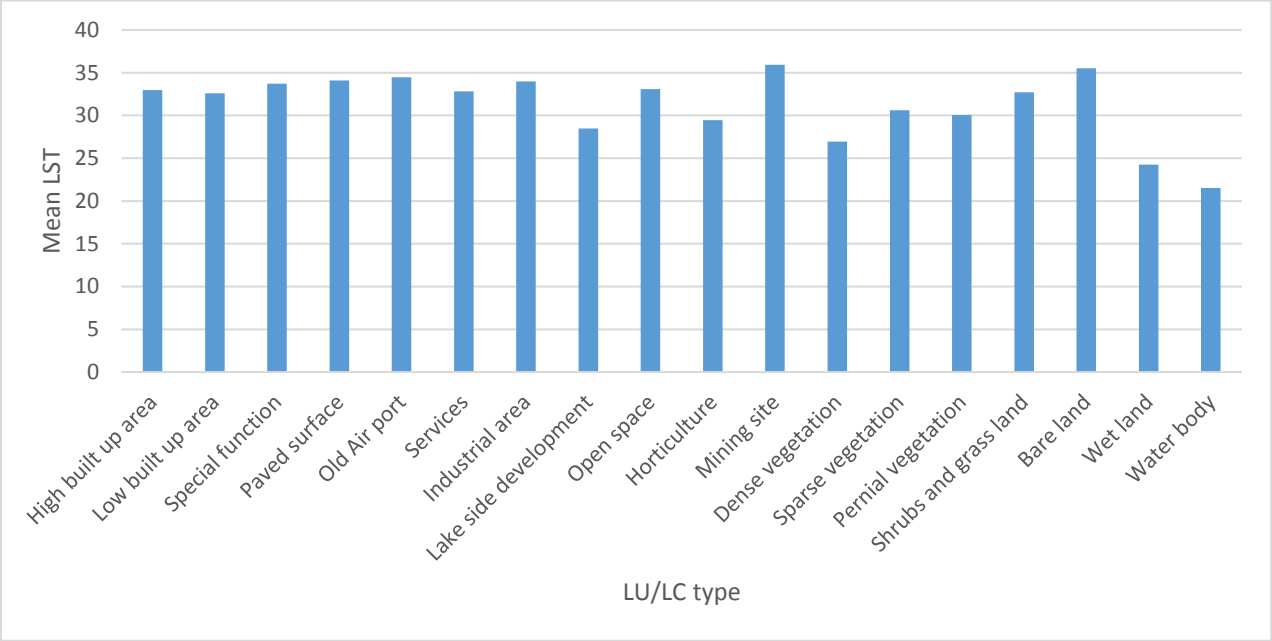

Figure 4.155: Mean LST of LU/LC type of Hawassa city for 2017

4.4.7 Multiple comparison of mean LST per LU/LC type

As described in the summery (Table 4.6), active mining sites have high mean LST variation compared to the other LU/LC type, and it is identified as the hottest surface in the city. The mean LST value associated with water body is significantly different from other land-use/land-cover types depending up on the nature of the surface for absorption and release of heat during the day and night time. Whereas, bare land shows high mean LST variation like that of mining areas. However, the mean LST variation of wetlands observed in the Table 4.6 is relatively small due to the existence of vegetation cover and water body (Lake Hawassa). In general, the observed variation in mean LST can be explained depending up on the density of vegetation cover and the nature of surface material they have. This means that the variation becomes higher when the LU/LC type has few or no vegetation cover and construction material that has high reflectance or absorbance. Besides the natural sources of heat caused by volcanic activities and thermal properties of bare land, the variation of LST in different LU/LC types are also associated to the mixture of different plant species.

Table 4.5: Multiple comparison of mean LST variation of each LU/LC type

Mean LST VARIATION	High built up area	Low built up area	Special function	Paved surface	Old Air port	Services	Industrial area	Lake side development	Open space	Horticulture	Mining site	Dense vegetation	Sparse vegetation	Pernial vegetation	Shrubs and grass land	Bare land	Wet land
Low built up area	-0.3507																
Special function	0.76202	1.11276															
Paved surface	1.15677	1.50751	0.39475														
Old Air port	1.51258	1.86332	0.75056	0.35581													
Services	-0.1382	0.21257	-0.9002	-1.2949	-1.6508												
Industrial area	1.03249	1.38323	0.27047	-0.1243	-0.4801	1.17066											
Lake side development	-4.4764	-4.1256	-5.2384	-5.6331	-5.989	-4.3382	-5.5089										
Open space	0.14312	0.49386	-0.6189	-1.0137	-1.3695	0.28129	-0.8894	4.61949									
Horticulture	-3.5124	-3.1617	-4.2745	-4.6692	-5.025	-3.3743	-4.5449	0.96393	-3.6556								
Mining site	2.96828	3.31902	2.20626	1.81151	1.4557	3.10645	1.93579	7.44465	2.82516	6.48072							
Dense vegetation	-5.9974	-5.6467	-6.7594	-7.1542	-7.51	-5.8592	-7.0299	-1.521	-6.1405	-2.485	-8.9657						
Sparse vegetation	-2.343	-1.9922	-3.105	-3.4997	-3.8556	-2.2048	-3.3755	2.1334	-2.4861	1.16947	-5.3113	3.65442					
Pernial vegetation	-2.9124	-2.5617	-3.6745	-4.0692	-4.425	-2.7743	-3.9449	1.56393	-3.0556	0.6	-5.8807	3.08495	-0.5695				
Shrubs and grass land	-0.2412	0.1095	-1.0033	-1.398	-1.7538	-0.1031	-1.2737	4.23513	-0.3844	3.2712	-3.2095	5.75615	2.10173	2.6712			
Bare land	2.55428	2.90502	1.79226	1.39751	1.0417	2.69245	1.52179	7.03065	2.41116	6.06672	-0.414	8.55167	4.89725	5.46672	2.79552		
Wet land	-8.6917	-8.3409	-9.4537	-9.8485	-10.204	-8.5535	-9.7242	-4.2153	-8.8348	-5.1792	-11.66	-2.6943	-6.3487	-5.7792	-8.4504	-11.246	
Water body	-11.416	-11.066	-12.178	-12.573	-12.929	-11.278	-12.449	-6.94	-11.559	-7.9039	-14.385	-5.419	-9.0734	-8.5039	-11.175	-13.971	-2.7247

In the Table 4.6, the negative sign shows that the LU/LC type listed in the left side column of the table relatively Cooler than the respective LU/LC type listed in the first row of the table with the specified LST in ^{0}C and Vis versa.

4.4.8 Mean LST per Urban green Cover type

As shown in Figure 4.16, the lowest mean LST were observed in stream bank/lake shore vegetation and urban park due to high density and broad leaf ever green trees and complex cultivation pattern. Whereas, the maximum mean LST were registered on ruderal vegetation as these vegetation covers are found within and surrounding of volcanic domes with low density and poor distribution pattern. However greeneries in the individual housing area has high impact on the LST distribution even if it has scattered distribution pattern because these greeneries are purposely planted for shading and different plant species are also found even in a single plot of land, as a result, these greeneries have relatively low mean LST as compared to greeneries that are found along the road and industrial unit. Greeneries that are found in public facilities still have high impact on LST variation because they are relatively dense, shading and complex species type, decorative plants including large space grass lands. In general, the observed variation can be drawn that the differences in mean LSTs associated with all urban green cover types are directly related to the complexity of species and density of vegetation cover and distribution patterns.

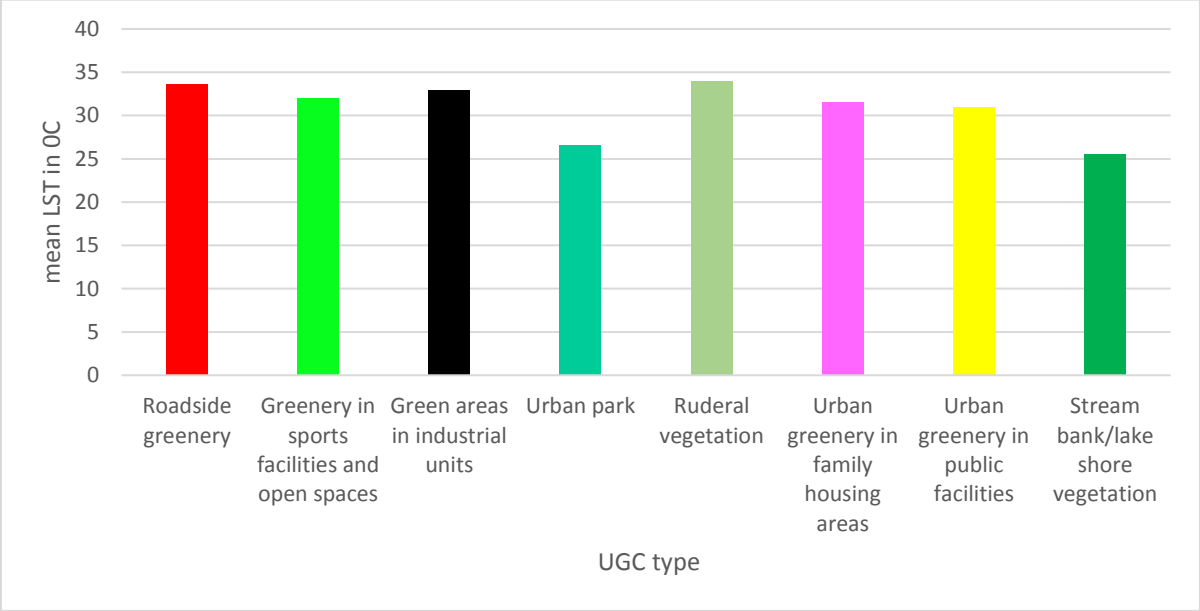

Figure 4.166: Mean LST of UGC type of Hawassa city for 2017

4.5 Descriptive analysis result

Due to different factors in the city both cold and hot islands were observed in different parts of the city. As seen in Figure 4.14 areas close to Lake Hawassa, like wet lands, park and lake side developments shows a temperature gradient that ranges from 22.01^0C up to 30.14^0C and rising towards high built up and industrial areas depending on the density and complexity of species distribution, and reach its maximum temperature on scattered and small hills like Tabor Ridge and areas that are used for red ash extraction and other quarry sites (for example mining site that is located in between Hawassa industrial park and Hawassa university main campus). Open market that is located at the back of Hawassa University agricultural college, also has high temperature that are caused by human induced activities. There are several areas where this pattern of temperature differences dissolves into areas that has more homogenized surfaces such as exhibition center, Large playing ground in front of "Logita hotel", degraded areas to the North east direction of the city and some under construction areas in front of Haile resort has this kind of elevated temperature pattern.

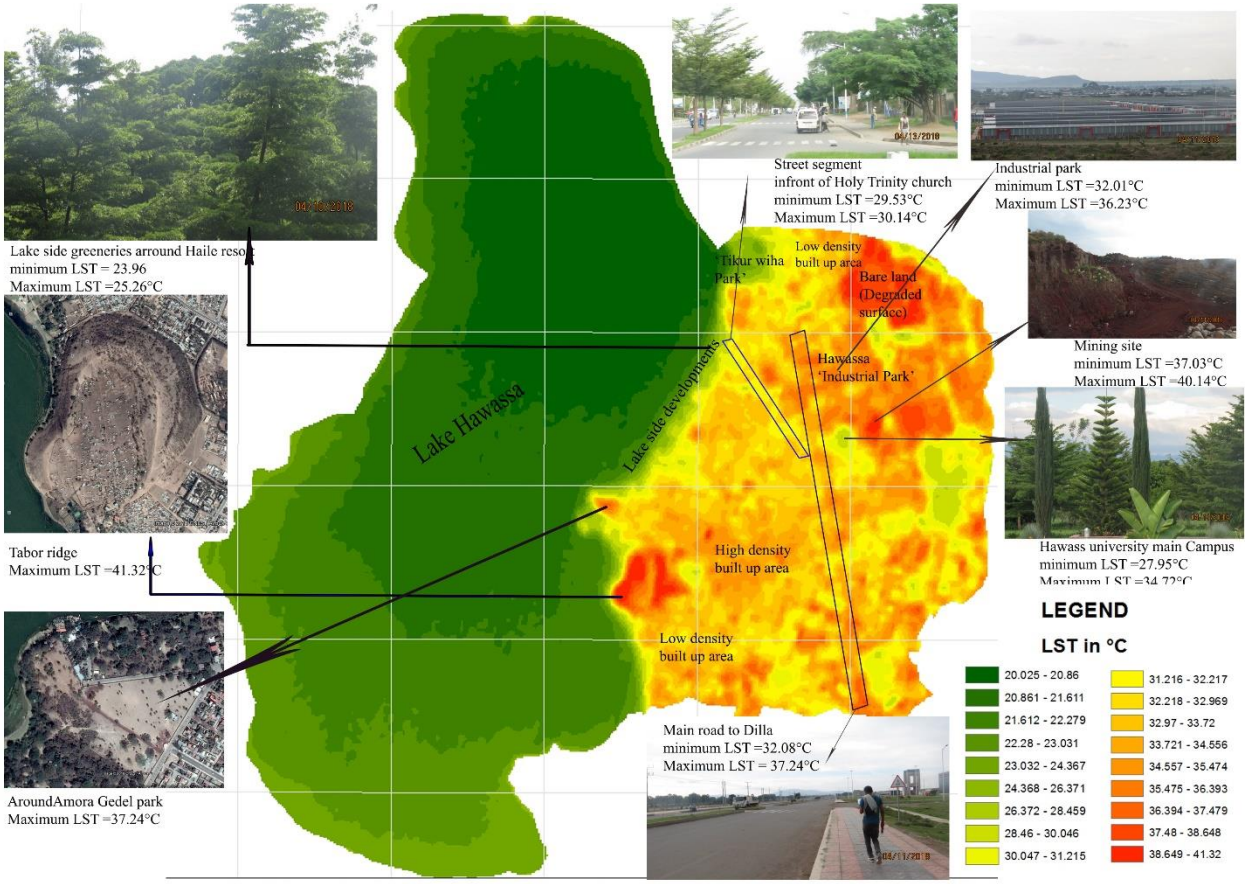

Figure 4.177: Descriptive map of the spatial variation of LST of Hawassa city for 2017

CHAPTER FIVE

5 DISCUSSION

5.1 Land-use/land-cover status of Hawassa

Unlike most urban centers of the country, especially since the last 15 years (2002_2017), the city has been undergoing through a rapid development and urbanization (horizontal expansion) due to its very rapid population growth. The significant population increase in Hawassa, has facilitated dramatic urbanization processes in terms of change in land-use/land-cover types and urban sprawl, especially over the past few decades (Ministry of works and urban development, 2006). From the results of land-use/land-cover change of 1992, 2002 and 2017 (Fig 4.9 and Table 4.2), statistical and visual examination of the classification result suggests a drastic change in the LU/LC patterns. However, these changes are not only in terms of additional growth in built-up space as in the other urban centers of the country. Instead, a very different urban pattern change has emerged in the urban green land-cover. As shown in the 2002 and 2017 urban green land cover change (Fig 4.10) and UGC type of 2017 (Fig 4.11) classification result, a prominent increase of green urban sites, both in the form of larger, newly created green patches in residential and service areas and in the form of increased greening alongside of selected street segments were observed. Even though, the present green cover of the city is relatively high, as per the norms and standards, the urban green space should cover 30 to 40 % from the total area of the city (Office for the revision of Addis Ababa master plan, 2002). However, the green cover is still less than the specified standard including those small green patches that are found in residential areas. As examined from the summery of LU/LC change matrix of the city (Table 4.3 a & b), bare (fallow) land is the most dominant LU/LC that was transformed in to different land use type, such as, low and high built up areas, service, industries, paved surfaces and other LU/LC type. Whereas, the water body (Lake Hawassa) is still decreasing and transformed into wetland and vegetation cover. The classification result of 2017 (LU/LC and UGC) of the area have a kappa coefficient greater than 0.8. As of Rahman *et al.* (2006), those classification that has a kappa coefficient greater than 0.8 represent strong agreement. As a result, all classification results in the period were done with strong agreement and taken as reliable data for other analysis purpose.

5.2 Spatial pattern of Land Surface Temperature (LST)

As the study area is located within the central zone of the Main Ethiopian Rift, it is expected to have an impact from its geological setting. The derived LST of Landsat 8 TIRS was found suitable to examine the relationship between Land surface temperature and LU/LC type. Because, according to Srivastava *et al.,* (2009) the derived LST is consistent with MODIS day time LST. As a result, it provides important information to monitor human activities and spatial variation. In some cases the day time LST alone may not be sufficient in detecting the real thermal properties of surfaces. However, it reveals that Landsat images are useful in quantifying and mapping of NDVI and LST. The integration of interpreted result of both Landsat 8 TIRS and MODIS night time data was found very useful for the present study area, since it provides better understanding of the real thermal properties of surfaces.

As per the integration of the interpreted results of Landsat 8 TIRS and MODIS night time (Fig 4.5 & 4.7), the spatial variation of day time LST derived from Landsat 8 is associated with different factors among which the geological setting of the area and reflectance of surfaces are the major one. The geological setting of the area was found to be one of the major causes for the spatial variation of LST. Because, those scattered and small volcanic domes (hills) and mining sites in the area have high surface temperature, both in the day and night. Hellman and Ramsey (2004) had proved that the existing phenomena of the present study area is the result of geological processes caused by the presence of young igneous bodies or hot rocks located deeper in the crust. Based on his study, heat can be transferred to the Earth's surface often via conduction of rocks, water and any other associated minerals. Other surface expressions such as hot springs and heated ground following the natural process that takes place inside the earth can change the surface temperature of the area (Buongiorno *et al.,* 2013; Hellman and Ramsey, 2004).

Whereas, the LU/LC type especially, bare lands of the area were found the second major factor for the spatial variation of LST. Because the second highest surface temperature were registered on bare lands (fallow lands). As December to February is the dry season (harvesting time) in the area, bare land has high surface reflectance during the season. MODIS night time of the area proves that the day time LST observed on bare land is not the inherent behavior of the area. Rather, it is the nature of the lithology (volcanic ash), associated with the immediate response as a result of absorbance of incident energy from the sun and lack of vegetation cover. A research conducted in other towns located within the Ethiopian Rift Valley such as Adama Zuriya Woreda by Belete Tafese (2017), proves that the LST result observed on bare land is the effect of the reflectance of

the surface. This study identified that those surfaces that have low NDVI values during the harvesting time (Fallow land) showed high surface reflectance. Similarly, surfaces like farmland and bare lands in the area have high surface temperature. In general, the observed high day time LST derived from Landsat 8 (Fig 4.5) is the aggregate of radiance and reflectance of the surface.

Even though, different contributing factors are found in the city such as, large roof structures of industries and different mining sites and paved surfaces, the settlement areas have exceptionally lower LST with heterogeneous spatial characteristics as compared to surrounding areas such as the bare lands. Because, the rapidly growing urban agglomeration represents heterogeneous landscape structures that brought higher vegetation cover that were not present in the area. As a result, a significant spatial variation of LST was observed in all LU/LC type of the city depending on the density and complexity of species distribution of vegetation they have besides natural factors.

As according to Rajendran and Mani, (2015), the spatial variation of LST values derived through the analysis are highly dependent on LU/LC distribution and are negatively correlated with vegetation abundance. Because, the statistical relationship between NDVI and LST suggest that they are predictive factors in the UHI pattern. The higher mean LST values of LU/LC typical of the urban environment and lower mean values of natural vegetated surfaces further confirm of an association. As a result, the variations of land surface temperature are also indicators of the spatial patterns of urban heat island effects and vegetation cover (NDVI).

However, different studies that were conducted outside of rift zones, proves that as urbanization increases the surface temperature of the area also increases. Because, the urbanization process mostly accompanied by the process of replacing natural vegetation with man-made non-transpiring and non-evaporating impervious structures or surfaces (Odindi *et al.,* 2015). Whereas, the urbanization process in the present study area has taken place by converting bare lands (degraded area) that did not have evergreen tree covers. Most of the urban green covers were introduced as a result of the urbanization process. Consequently, the settlement areas have lower LST value as compared to bare lands (Fig 4.15 & Table 4.5). According to Yue *et al.* (2007), dense and evergreen (non-seasonal) trees have high rate of evapotranspiration due to greater vegetation cover that can lower the surrounding surface temperature. Besides the city has preserved parks and wetlands, that are used for recreation. As stated by Spronken *et al.* (2000), urban parks have 300% higher evaporation rate as compared to the developed (settlement) areas and it is highly recommended to control the LST of the urban environment. In general, settlement of the study

area has relatively low LST as compared to bare lands due to the existence of evergreen trees. Besides, the time series LST result of 1992 and 2002 in (Fig 4.2 a and b) shows that areas that were bare in all years had high LST value due to the reflectance and absence of vegetation cover of the surface and the settlement areas had relatively lower LST values and those scattered and small hills and mining sites had the highest LST result in both years. In general, the over view of the previous LST result proves that as urbanization increases using bare land as expansion, the spatial distribution of surface temperature registered on bare land decreases, because it is converted to heterogeneous landscape structures that has relatively higher vegetation cover with different species type. As a result, the city has relatively lower LST as compared to the surrounding bare lands.

5.3 Mitigation strategy

The main purpose of this study was to examine the urban heat island effect and it's causing factors in order to establish relatively good urban climate. Because, the impact of heat island is not only limited to the environmental conditions, but also to the economic and societal status of the area. Therefore, potential mitigation strategies are required in order to mitigate the cumulative heat island effect of the area. Since the geological set up of Hawassa and its surrounding shows that the city is located within the central zone of the main Ethiopian rift that has considerable contribution to the surface temperature change like hot spring from the lower parts of Wendo Genet (Wesha and Wendo hot spring) and volcanic activities following the two post-caldera volcanos (Chebbi and Urji). Even though, it is difficult to prevent heat island that emanate from the natural sources, it is still possible to mitigate the cumulative effect. Because, the analysis result of the surrounding areas shows that due to the change in land-use/land-cover the intensity of temperature varies. For example the observed surface temperature of mount Chebbi and Urji is relatively low due to the existence of vegetation cover.

Whereas, in the urban center the heat island effect is the aggregate of different factors. However the most significant method to mitigate urban heat island effect still lies on planning and management practices. Because urban land cover is a main factor in controlling LST and the formation of the UHI. Therefore, systematic conversion of the land-cover to those that can keep the LST lower is one of the possible mitigation. Further mitigation strategies are described below considering the analysis result: -

Increasing of green land cover

As per the results observed, the study area has good experience in increasing the urban green land cover, due to the urbanization and conservation practice taken during the past few years. As a result, a significant surface temperature change is observed in areas that have complex trees like Zembaba (Borassus aethiopum Mart), Grevillea, Diredawa zaf (Hook), Wanza (Cordial africana), Jacaranda mimosifolia, Araucaria heterophylla, Enset (Enseteventricosum), Terminalia mantaly, Shola (Ficus sycamores), Grar (Acacia), warka (Ficus vasta) and other broad-leaved trees. Therefore, identifying areas such as street segments and non-vegetated open spaces and other hilly areas like Alamura and Tabor, and cover them with the above stated vegetation (tree) types provide high cooling effect to Hawassa city.

Rehabilitation of Mining areas

As the city is located within the center of the Main Ethiopian Rift, it has scattered small hills. Some of these hills are currently used for quarry for building stones and others for red ash extraction. The analysis result obtained from multiple comparison of mean LST by LU/LC type, showed that the quarry sites have the highest surface temperature as compared to other LU/LC type in the city. Even though these areas have low vegetation cover, the spatial pattern of LST obtained from MODIS night time shows that those areas are inherently hot due to heat convection caused by volcanic activities in the ground. Therefore, protecting these area from mining activity by itself cannot be a solution for heat mitigation. It is highly recommended to rehabilitate or afforest these areas with dense and evergreen trees and to use them as urban parks. Ca *et al.* (1998) reported that a 600 m^2 park can decrease temperatures by 1.5°C in urbanized area.

Support future expansion and other development areas to have sufficient green cover

As seen from the urban green land cover change analysis, those green cover change had come following the urbanization or expansion process of the city. However, this does not mean that urbanization process can have positive impact on heat mitigation for all cities. Therefore, new rules and regulation and other incentives are required that can invite dwellers to have green cover in their compound, because the previous expansion areas of the city were taken in bare land that is why the previous urbanization trend played great role for heat mitigation. In general, increasing urbanization in rift zones taking place on the bare land (West of Lake Hawassa) as expansion target can be taken as a useful tool to maintain or improve the climate of the city, if aided by effective planning philosophies. Because, large parks by itself do not provide cooling benefits far beyond

their boundaries, tree planting to cool buildings and mitigate the UHI effects should be approached at the individual plot or neighborhood level.

Development of green roof

Large roof structures have high LST. Therefore, in order to reduce the impact of large roofs observed in industrial area, it is highly promoted to have green roof structures. Because integrating this type development in this area provides lots of advantages such as lowering temperature profile, insulating properties (painting), possibility of increasing evapotranspiration to roof tops, reduction of storm water runoff, and greater capacity to filter the air (Coffyn ,2011).

Enhancing of Lake Side vegetation

Lake Hawassa and surrounding development plays significant role in urban heat mitigation. Because, covering the lake shores and the surrounding by green vegetation can create a lower temperature gradient, which gradually climbs as land cover transitions to residential areas with more intensive green surfaces that would help to regulate local climate (Coffyn ,2011).

Promoting of permeable and cool pavements

Having large asphalt concrete pavement structures in cities has high absorption of sun radiation. Therefore, having such extensive pavement materials has high heat island effect in cities. So best materials like cool asphalt shingles (like cobble stone), tile and other soft green landscaping materials are highly recommended to lower surface temperature of the area (Parker *et al.*, 2000).

CHAPTER SIX

6 CONCLUSION AND RECOMMENDATIONS

6.1 Conclusion

Remote sensing and GIS technology are found to be appropriate for mapping and estimation of urban phenomenon such as Urban Heat Island, due to their fair representation of the spatial distribution of land surface temperature. For the purpose of this study, integrated Landsat 8 TIRS band 10 and MODIS night time data were used to better understand the inherent thermal properties of surfaces and identify the major factors responsible for the spatial variation of surface temperature of the area. Even though the spatial resolution of MODIS data is low, the integration result was found to be good for the observation of the thermal behavior of different surfaces. Spatial variation of LST in the study area is directly associated with factors such as human induced activities following the existence different pavement material and distribution of vegetation cover under the urbanization process. As Hawassa is located within the central zone of the main Ethiopian rift, the geological setting of the area was found to be the major cause for the spatial variation of LST.

Following the rapid growth of population in the city for the past few years, the LU/LC of the city have been changing dramatically. As a result, expansion and conversion of different LU/LC types were observed and these change in LU/LC type were found to be the main causes for the spatial variation of LST. As shown from the spatial pattern of LST obtained in the year 2002 and 2017 (Fig 4.1and 4.5), the dynamics of surface temperature of the city decreased, following the increasing of vegetation cover in settlement areas. Even though, there are industries that can bring a change on the spatial pattern of LST, the urbanization trend of the city had played a significant role for the increase of vegetation cover and decrement of LST.

The day time LST value obtained from Landsat 8 TIRS of bare lands in the study area especially West of Lake Hawassa is not the inherent behavior of the surface. Because, the observed day time high temperature in the area is attributed to the nature of the rock (Volcanic ash and Pumice fall deposits) and absence of land-use/land-cover. Therefore, it doesn't represent the actual land surface temperature of the area. Instead it represents immediate response as a result of absorbance of incident energy from the sun.

The mapping of UGC of the area using Sentinel-2A optical data were found to be good, even though the mapping and validation of small and scattered tree cover is difficult. Most of the green cover change observed in the map of 2017 were found to be greeneries that are located in individual housing areas and in different public facilities. As a result, the urbanization trend in the city played significant role for the increase of vegetation cover in the study area. Besides, areas that have complex species type and dense vegetation in the city has recorded low LST value.

In general, the finding of this reserch shows that the spatial variation of LST in the study area is highly associated with LU/LC variation, vegetation density and distribution pattern, human induced activities, geological setting and volcanic ash deposit of the area.Whereas, the NDVI values of the area were found to be as a good indicator of the spatial variation and status of LST. The extracted mean LST value of sample polygones using zonal statistics confirmed that the estimated LST using Landsat 8 TIRS band 10 are highly correlated to the MODIS day time LST.

6.2 Recommendation

The main purpose of this study was to examine the urban heat island effect and its causing factors in order to establish relatively conducive urban climate. The analysis result showed that the heat island effect in the urban center is the aggregate of different factors among these, LU/LC type, geological setting and quarry sites are the major one. Therefore, it is recommended ed to integrate different techniques that can lower the UHIs effect in the city. However, the most significant one lies in planning and management practices of LU/LC types. As urban land cover is a main factor in controlling LST and the formation of the UHI. Therefore, based on the finding of the research, the following recommendations have drawn:-

- Study of the UHI using remote sensing is effective. However, in order to filter out the diurnal effect and analyze the impact of small urban structures, the resolution (spatial and temporal) of the data should be high.
- The future land-use plan of the area should be supported by a research that considers the geological setting and its heat island effect.
- Rehabilitate existing quarry sites and protect and enhance urban green cover.
- The estimation of LST and mapping of UGC to examine UHI effect using only satellite data has certain drawbacks. Therefore, further study is required by combining and correlating different sensors and satellites with the conventional meteolrological station data. However, the subject of this study can serve as basis for related studies in the area.

REFERENCES

Abutaleb, K., Adeline, Ngie, F. Ahmed, M. H. Ahmed, S.B. Elkafrawys, S. M. Arafat, A. Darwish (2014). Investigation of urban heat island using Landsat data. **In**: Proceedings of the 10th Int. Cong, pp9, AARSE, University of Johannesburg, Wits University South Africa and National Authority for Remote Sensing and Space Sciences, Egypt.

Avdan, U. and Jovanovska, G. (2016). Algorithm for Automated Mapping of Land Surface Temperature Using Landsat 8 Satellite Data. *Journal of Sensors*. **2016**:1-8. Article ID 1480307. http://dx.doi.org/10.1155/2016/1480307.

Basalfew Zenebe, Mathios Agonafir, Meskerem Teshome, Mekdes Taye, Mekonen Bekele, Mohamed Edris, Getachew Burusa and Ezra Yehualashet (2012). BASIC geoscience mapping directorate geology geochemistry and gravity survey of the Hosaena area. Unpublished report; 68pp.

Becker, F. and Li, Z. L. (1990). Towards a local split window method over land surfaces. *Int. J. Remote Sens*. **11**: 369–393.

Belete Tafesse (2017). Impact of land-use/land-cover changes on land surface temperature in Adama Zuria Woreda, Ethiopia, using geospatial tools. Unpublished MSc thesis, Addis Ababa University, Addis Ababa, Ethiopia, 91 pp.

Buongiorno, M. F., David, P. and Malvina, S. (2013). Thermal Analysis of Volcanoes Based on 10 Years of ASTER Data on Mt. Etna. *Remote Sensing and Digital Image Processing*. **17**:409-428.

Burgan, R.E. and Hartford, R. A. (1993). Monitoring vegetation greenness with satellite data. Gen. Tech. Rep. INT-297. Ogden, UT: U.S. Department of Agriculture, Forest Service, Intermountain Research Station. 13pp.

Ca, V. T., Asaeda, T. and Abu, E. M. (1998). Reductions in air-conditioning energy caused by a nearby park. Energy and Buildings. **29**: 83-92.

Claudia, K. and Stefan, D. (2013). *Thermal Infrared Remote Sensing: Sensors, Methods, Applications*. 546 pp.

Coffyn, B. M. (2011). Urbanization and Land Surface Temperature in Pinellas County, Florida. Unpublished MA thesis, University of South Florida, USA, 155pp.

CSA. (1998).The 1994 population and housing census of Ethiopia: results for SNNPR Amhara region, Volume II analytical report (Census report). Federal Democratic Republic of Ethiopia,

Office of population and housing census commission, Central Statistical Agency, Addis Ababa, Ethiopia.

CSA. (2008). The 2007 population and housing census of Ethiopia: statistical reports for SNNPR (Census report). Federal Democratic Republic of Ethiopia, Office of population and housing census commission, Central Statistical Agency, Addis Ababa, Ethiopia.

CSA. (2013). Population Projection of Ethiopia for All Regions at Wereda Level from 2014 – 2017 (Population projection). Federal Democratic Republic of Ethiopia Central Statistical Agency, Addis Ababa, Ethiopia.

Czajkowski, K.P., S.N., Goward, J.S. Stadler, and A. Walz (2000). Thermal remote sensing of near surface environmental variables: application over the Oklahoma Mesonet. *Prof. Geogr*. **52**: 345–5.

Denis, M., Scotty, S. and Thomas, A. (2015). Land Surface Temperature and Surface Air Temperature in Complex Terrain. *IEEE Journal of Selected Topics in Applied Earth Observations and Remote Sensing*. **8**(10): 4762-4774.

Dewan, A. and Corner, R. (2012). The impact of land use and land cover changes on land surface temperature in a rapidly urbanizing megacity. **In**: Proceedings of the IEEE International Geoscience and Remote Sensing Symposium, pp 100 .IGARSS, Munich, Germany.

Di Gregorio, A. and Jansen, L.J. (2000). Land-cover classification: classification concepts and user manual, Food and Agriculture Organization (FAO) of the United Nations, Rome.92pp.

DiPippio, R. (2005). *Geothermal power plants: principles, applications and case studies and environmental impact*. 3rd edition, Elsevier, Kidlington, Oxford, UK. 624 pp.

Dousset, B. and Gourmelon, F. (2003). Satellite multi-sensor data analysis of urban surface temperatures and land cover. *ISPRS J. Photogram. Remote Sens*. ***58*** *(2):43–54.*

Falahatkar, S., Seyed Mohsen Hosseini and Ali Reza Soffianian (2011). The relationship between land cover changes and spatial-temporal dynamics of land surface temperature, Isfahan, Iran, *Indian Journal of Science and Technology*. **4** (2):76-81.

Flynn Luke, P., Andrew, J.L., Harris Robert and Wright (2001). Improved identification of volcanic features using Landsat 7 ETM+, *Remote Sensing of Environment.* **78**:180–193.

Fu, P. and Qihao Weng (2016). A time series analysis of urbanization induced land use and land cover change and its impact on land surface temperature with Landsat imagery. *Remote Sensing of Environment*.**175** :205–214.

Hellman, M. J. and Ramsey M. S. (2004). Analysis of hot springs and associated deposits in Yellowstone National Park using ASTER and AVIRIS remote sensing. *Journal of Volcanology and Geothermal Research.* **135**(2): 195-219.

http://landsat.usgs.gov/documents/Landsat8DataUsersHandbook.pdf accessed on 21.05. 2018.

Icaza-Echevarria, L., Van der Hoeven, F. and Van den Dobbelsteen, A. (2016). Surface thermal analysis of North Brabant cities and neighborhoods during heat waves. Tema. *Journal of Land Use, Mobility and Environment*. **9** (1): 63-87. Doi: http://10.6092/1970-9870/3741.

Jackson, K.T. (1985). The Suburbanization of the United States. Crabgrass Frontier, Oxford Univ. Press, New York, 396 pp.

Jeevalakshmi, D., S. Narayana Reddy and B. Manikiam (2017). Land Surface Temperature Retrieval from Landsat data using Emissivity Estimation. *International Journal of Applied Engineering Research*. **12** (20): 9679-9687.

Jim, CY. and Chen, S.S. (2003). Comprehensive greenspace planning based on landscape ecology principles in compact Nanjing city, China. *Landscape and Urban Planning*. **65** (3):95-116.

Kayet, N., Pathak, K., Chakrabarty, A., and Sahoo, S. (2016). Spatial impact of land-use/land-cover change on surface temperature distribution in Saranda Forest, Jharkhand. *Modeling Earth Systems and Environment*. **2**(3): 1–10.

Kuang, W.H., Liu, Y., Dou, Y.Y., Chi, W.F., Chen, G.S., Gao, C.F., Yang, T.R., Liu, J.Y. and Zhang, R.H. (2015). What are hot and what are not in an urban landscape: quantifying and explaining the land surface temperature pattern in Beijing, China. *Landsc. Ecol*. **30**: 357–373.

Lamson-Hall, Patrick, David Degroot, Richard Martin, Tsigereda Tafesse, and Shlomo Angel (2015). A New Plan for African Cities: The Ethiopia Urban Expansion Initiative. NYU Stern Urbanization Project. 216pp.

Lillesand, TM. and Kiefer, RW. (1994). Remote sensing and image interpretation, 3rd edn. John Wiley, New York, 748pp.

Lisa Gartland (2008). *Heat islands understanding and mitigating heat in urban areas*. First edition, Earth scan, UK and USA, 225 pp.

Liu, L. and Zhang Yuanzhi (2011). Urban Heat Island Analysis Using the Landsat TM Data and ASTER Data: A Case Study in Hong Kong, *remote sensing*.1535-1552.

Lo, C.P., Quattrochi, D.A. and Luvall, J.C. (1997). Application of high-resolution thermal infrared remote sensing and GIS to assess the urban island effect. Int. J. Remote sensing. **18**(2): 287-304.

Markham, B. L. and Barker, J. L. (1985). Spectral characterization of the Landsat thematic Mapper sensors, *International Journal of Remote Sensing.* **6 (**5): 697–716.

Meyer, W. B., and Turner, B. L. (1992). Human population growth and global land-use/cover change. Annual review of ecology and systematics. **23**(1): 39-61.

Ministry of Works and Urban Development (2006). Federal Urban Planning Institute, Report on Hawassa Integrated Development Plan, Addis Ababa, Ethiopia. 52pp.

Norman, J. M., and Becker, F. (1995). Terminology in thermal infrared remote sensing of natural surfaces. Remote Sensing Reviews. **12**:159–173.

Odindi, J.O., Bangamwabo, V. and Mutanga, O. (2015). Assessing the value of urban green spaces in Mitigating Multi-Seasonal urban heat using MODIS land surface temperature (LST) and Landsat 8 data. *Int. J. Environ. Res*. **9**: 9–18.

Office for the revision of Addis Ababa master plan (2002). Norms and standards of the Addis Ababa structure plan components, unpublished report, Addis Ababa, Ethiopia, 30pp.

Oke, T.R. (1982). The Energetic Basis of the Urban Heat Island. *Quarterly Journal of the Royal Meteorological Society.* **108**: 1-24.

Oke, T.R. (1988). The urban energy balance. *Progress Phys. Geogr*. **12**:471–508.

Oliveira, S., Henrique, A. and Teresa, V. (2011). The cooling effect of green spaces as a contribution to the mitigation of urban heat: A case study in Lisbon. *Building and Environment*. **46**(2011): 2186-2194.

Osman Orhan, Semih Ekercin and Filiz Dadaser-Celik (2014). Use of Landsat Land Surface Temperature and Vegetation Indices for Monitoring Drought in the Salt Lake Basin Area, Turkey. *Journal of sensor*. **2014**(2014): 1-11. http://dx.doi.org/10.1155/2014/142939.

Parker, D S, J E R McIlvaine, S F Barkaszi, D J Beal and M T Anello (2000). Laboratory Testing of the Reflectance Properties of Roofing Material. FSEC-CR670-00.Florida Solar Energy Center, Cocoa, FL.11pp. http://www.fsec.ucf.edu/en/publications/html/FSEC-CR-670-00/. Accessed on 21 May 2018 20:34:14 GMT.

Price, J.C. (1984). Land surface temperature measurements from the split window channels of the NOAA 7 advanced very high resolution radiometer, *J. Geophys. Res.* **89**: 7231–7237.

Qin, Q., Ning Zhang, Peng Nan and Leilei Chai (2011). Geothermal area detection using Landsat ETM+ thermal infrared data and its mechanistic analysis: A case study in Tengchong, China. *International Journal of Applied Earth Observation and Geoinformation.* **13**: 552–559.

Rahman, M.M., Csaolovics, E., Koch, B., & Kohl, M. (2006). Interpretation of Tropical Vegetation Using Landsat ETM+ Imagery, South-eastern Bangladesh.

Rajendran, P. and Mani, K. (2015). Estimation of Spatial Variability of Land Surface Temperature using Landsat 8 Imagery, *The International Journal of Engineering and Science (IJES).* **4 (**11): 19-23.

Rizwan, A.M., Dennis, Y.C. and Liu, C. (2008). A review on the generation, determination and mitigation of urban heat island. *J. Environ. Sci*., **20**: 120–128.

Roza Assaye, Suryabhagavan, K. V., Balakrishnan, M. and Hameed, S. (2017). Geo-Spatial Approach for Urban Green Space and Environmental Quality Assessment: A Case Study in Addis Ababa City. *Journal of Geographic Information System*. **9**: 191-206.

Schmidt, M., King, EA. and Mcvicar TR (2006). A user-customized Web-based delivery system of hyper temporal remote sensing datasets for Australasia. *Photogramm Eng. Remote Sensing*.**72**:1073–1080.

Sentinel-2 User Handbook 2015.

Shahmohamadi, P., A. I. Che-Ani, K. N. A. Maulud, N. M. Tawil, and N. A. G. Abdullah (2011). The Impact of Anthropogenic Heat on Formation of Urban Heat Island and Energy Consumption Balance. *Journal of Sensors*. **2011**(2015):1-9. Article ID 497524. doi:10.1155/2011/497524

Sobrino, J. A. and Raissouni, N. (2010). Toward Remote Sensing Methods for Land Cover Dynamic Monitoring: Application to Morocco, *International Journal of Remote Sensing*. **21**(2): 353 – 366.

Sobrino, J. A., Jiménez-Muñoz and Leonardo, J. C. P. (2004). Land surface temperature retrieval from LANDAT TM5. *Remote Sensing of Environment*. **90** (4): 434-440.

Sobrino, J. A., Juan, C., Jimenez-Munoz, Guillem Sòria, Mireia Romaguera, Luis Guanter, Antonio Plaza & Pablo Martínez (2008). Land Surface Emissivity Retrieval from Different VNIR and TIR Sensors, *IEEE Transactions on Geoscience and Remote Sensing*. **46** (2):316 – 327.

Sobrino, J. A., Li, Z. L., Stoll, M. P. and Becker, F. (1994). Improvements in the split window technique for land surface temperature determination. *IEEE Transactions on Geoscience and Remote Sensing*. **32**: 243-253.

Spronken, S., R. A., T. R. Oke, and W. P. Lowry (2000). Advection and the surface energy balance across an irrigated urban park. *International Journal of Climatology*. **20**: 1033-1047.

Srivastava, P.K., Majumdar, T.J. and Bhattacharya, A.K. (2009). Surface temperature estimation in Singhbhum Shear Zone of India using Landsat-7 ETM+ thermal infrared data. Advances in Space Research. **43** (10): 1563–1574.

Sundara, K., Udayabhaskar, P. and Padmakumari, K. (2012). Estimation of land surface temperature to study urban heat island effect using Landsat ETM+ image, Vijayawada, city of Andhra Pradesh, India. *International Journal of Engineering Science and Technology (IJEST).***4**(2):771-778

Tadesse and Zenaw (2003). Hydrogeology and Engineering Geology of Hawassa Lake Catchment. Geological survey of Ethiopia, Addis Ababa.46pp.

Teshale Refera (2015). Land-use/land-cover Dynamics in Hawassa Tabor and Alemura Ridge and its Surroundings in the case of SNNPR, Ethiopia. Unpublished M.A thesis, Haramaya University, Haramya, Ethiopia. 84 pp.

Tongliga, B., Xueming Li, Jing Zhang, Yingjia Zhang and Shenzhen Tian (2015). Assessing the Distribution of Urban Green Spaces and its Anisotropic Cooling Distance on Urban Heat Island Pattern in Baotou, China. *ISPRS Int.J.Geo-inf*. **5**(12):1-13.

Tsegaye Tegenu (2010). Urbanization in Ethiopia: Study on Growth, Patterns, Functions and Alternative Policy Strategy. Unpublished paper, Department of Human Geography, Stockholm University, Stockholm.48pp.

Vatseva, R., Monika Kopecka, Jan Otahel, Konstantin Rosina, Atanas Kitev, Stefan Genchev (2016). Mapping urban green spaces based on remote sensing data: case studies in Bulgaria and Slovakia. **In**: Proceedings, 6th International Conference on Cartography and GIS, pp10. Albena, Bulgaria.

Voogt, J.A. and Oke, T.R. (2003).Thermal remote sensing of urban climates, *remote sensing of Environment*. **86**(3):370-384.

Wang, F., Zhihao Qin, Caiying Song, Lili Tu, Arnon Karnieli and Shuhe Zhao (2015). An Improved Mono-Window Algorithm for Land Surface Temperature Retrieval from Landsat 8 Thermal Infrared Sensor Data, *Remote Sens*. **7**:4268-4289.

Weng, Q. (2001). A remote sensing–GIS evaluation of urban expansion and its impact on surface temperature in the Zhujiang Delta, China, *Int. J. Remote sensing*. **22**: 1999-2014.

Weng, Q. (2003). Fractal analysis of satellite detected urban heat island effect. *Photogrammetric Engg. Remote Sensing*. **69**:555-566.

Weng, Q., H.D, S. Lu, and J. Schubring (2004). Estimation of land surface temperature-vegetation abundance relationship for urban heat island studies, *Remote Sensing of Environment.* **89**(4): 467–483.

Wu, R. (1999). The classification for green space system. Chinese Horticulture. **15**(6):26-32.

Yu, X., Xulin Guo and Zhaocong, Wu. (2014). Land Surface Temperature Retrieval from Landsat 8 TIRS—Comparison between Radiative Transfer Equation-Based Method, Split Window Algorithm and Single Channel Method, *Remote Sens.* **6**:9829-9852.

Yue, W., Xu, J., Tan, W. and Xu, L. (2007), the relationship between Land surface temperature and NDVI with remote sensing: application to Shanghai Landsat 7 ETM+ data, *International Journal of remote sensing*. **28**(15), 3205-3226.

Zacek, V., Vladislav Rapprich, Jiri Sima, Radek Skoda, Frantisek Laufek, and Firdawok Legesa (2015). Kogarkoite, Na3 (SO4) F, from the Shalo hot spring, Main Ethiopian Rift: implications for F-enrichment of thermal groundwater related to alkaline silicic volcanic rocks, *Journal of Geosciences.* **60**: 171–179.

APPENDICES

APPENDIX: 1 Sample pictures of the site that brought significant change in LST

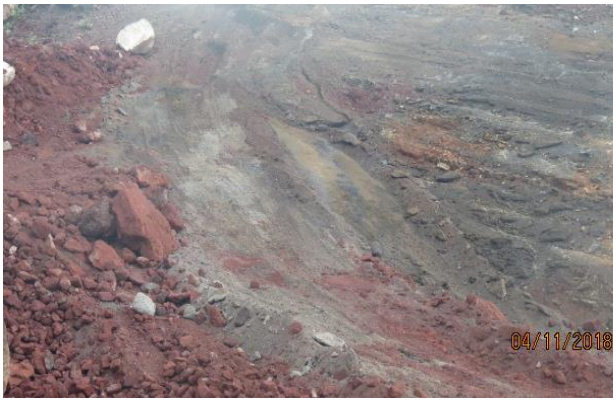

Red ash extraction site

Quarry site

Tabor Ridge

Hawassa Industrial Park

Large roof size (Hawassa Textile Factory)

Paved surface (Street with out street tree)

Street side greeneries

service area greenery (Hawassa university)

service area greenery (St.Gebriel church)

Terminale

Shola (Ficus sycamores)

APPENDIX: 2 Sample data map for accuracy assessment of LU/LC of 2017

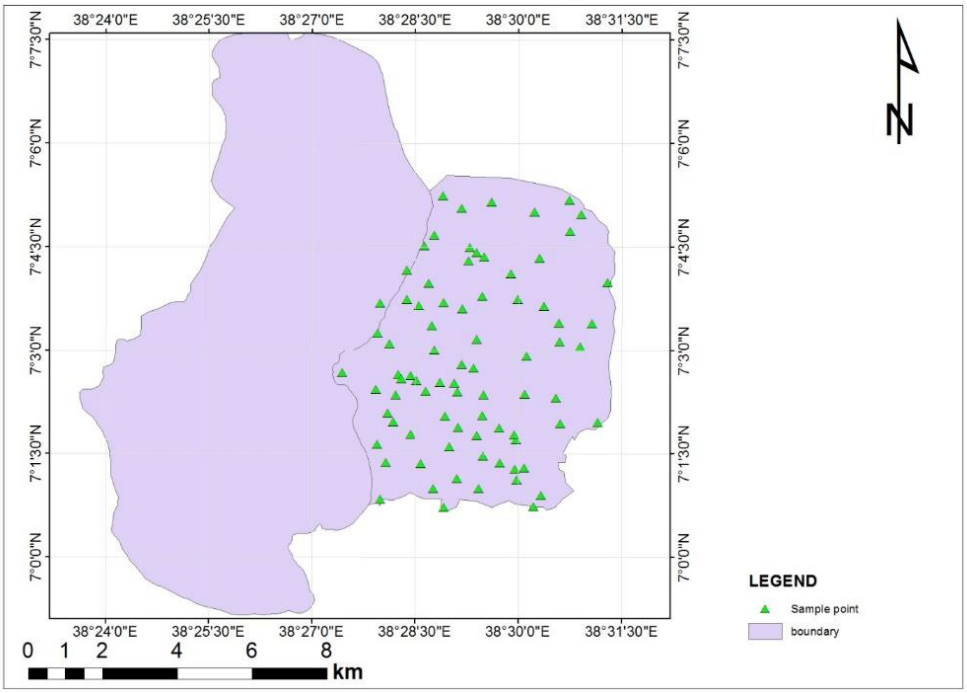

APPENDIX: 3 Sample data map for accuracy assessment of UGC of 2017

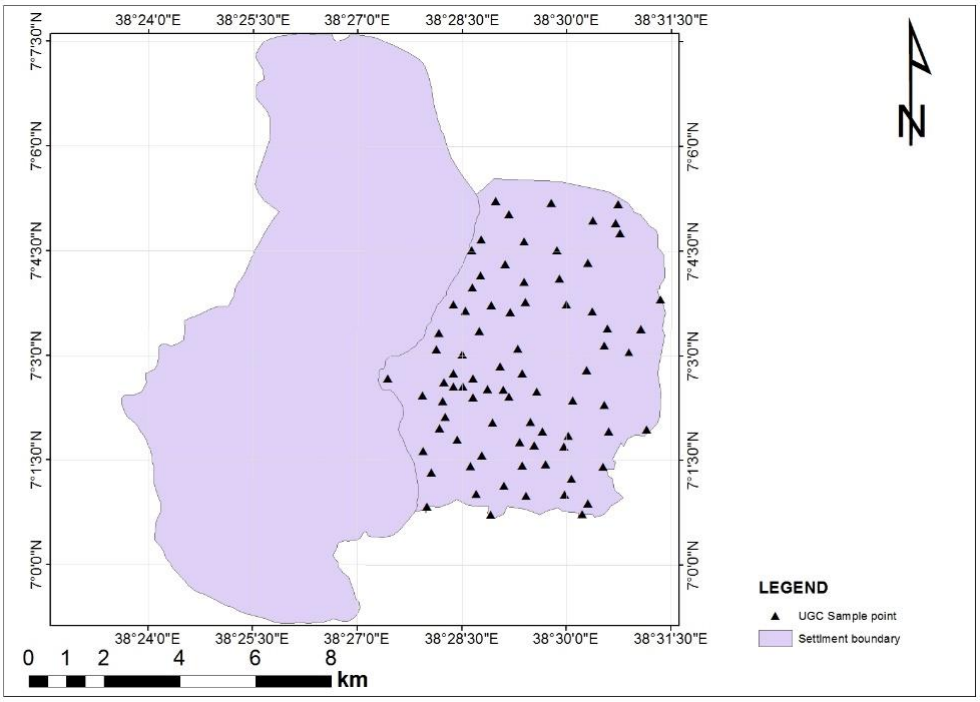

APPENDIX: 4 Sample data map for validation of Landsat8 LST of 2017

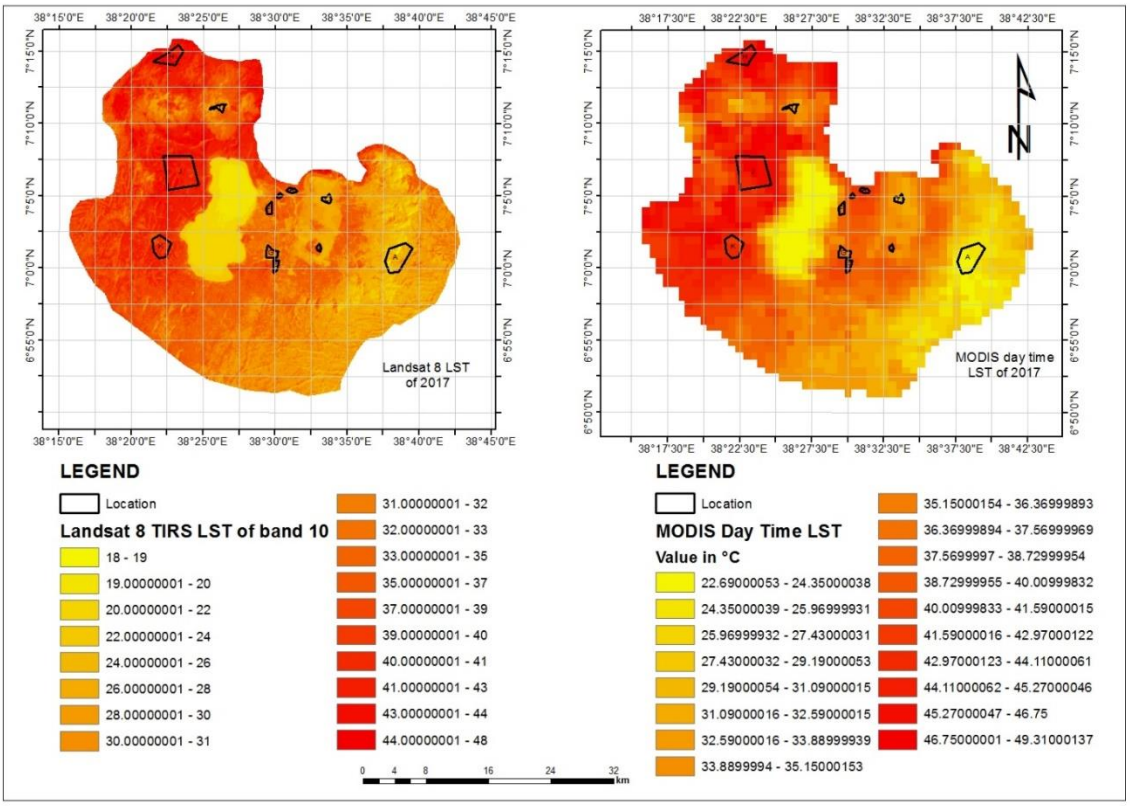

APPENDIX: 5 Summery report for NDVI distribution per LU/LC map of 2017

TYPE	ZONE-CODE	COUNT	AREA	MIN	MAX	RANGE	MEAN	STD	SUM
High built up area	1	3151	2835900	0.001187	0.522087	0.523273	0.294279	0.060569	624.3325
Low built up area	2	20402	18361800	0.044054	0.616257	0.660312	0.314456	0.071684	4919.076
Special function	3	154	138600	0.025745	0.476529	0.450784	0.241835	0.058446	29.02159
Paved surface	4	2450	2205000	0.201328	0.614745	0.816074	0.218305	0.079725	555.891
Old Air port	5	228	205200	0.126767	0.434801	0.308034	0.202866	0.051529	53.09353
Services	6	6419	5777100	0.015185	0.612839	0.628025	0.309456	0.082844	1785.958
Industrial area	7	3391	3051900	0.02481	0.502008	0.526818	0.226894	0.089579	672.6064
Lake side development	8	926	833400	0.091851	0.672023	0.580172	0.413593	0.12212	382.9867
Open space	9	756	680400	0.042802	0.571352	0.52855	0.301541	0.082565	161.6509
Horticulture	10	846	761400	0.093341	0.524921	0.431581	0.392054	0.082594	229.007
Mining site	11	1238	1114200	0.033514	0.520412	0.486899	0.225558	0.0789	279.2414
Dense vegetation	12	982	883800	0.247859	0.696583	0.944442	0.482054	0.117406	473.3769
Sparse vegetation	13	500	450000	0.11361	0.630875	0.517265	0.334456	0.089158	157.2279
Pernial vegetation	14	1806	1625400	0.028154	0.606804	0.57865	0.354888	0.07412	640.9286
Shrubs and grass land	15	176	158400	0.068228	0.4613	0.393072	0.310908	0.0764	56.47986
Bare land	16	9234	8310600	0.041383	0.563318	0.521934	0.202866	0.052865	2440.356
Wet land	17	2111	1899900	0.379654	0.643932	1.023586	0.442054	0.232152	338.282
Water body	18	94811	85329900	-0.49215	0.02481	1.060976	-0.39305	0.047889	-37265.3

APPENDIX: 6 Summery report for LST distribution per LU/LC map of 2017

Rowid	TYPE	ZONE-COI	COUNT	AREA	MIN	MAX	RANGE	MEAN	STD	SUM
1	High built up ar	1	3151	2835900	30.7638	35.78387	5.020063	32.94838	0.88327	105090
2	Low built up ar	2	20408	18367200	25.61036	39.54254	13.93218	32.59764	1.464568	669538.3
3	Special functio	3	154	138600	32.10183	36.10014	3.998318	33.7104	0.920687	5273.63
4	Paved surface	4	2450	2205000	25.51823	37.24105	11.72282	34.10515	1.342189	81083.11
5	Old Air port	5	228	205200	32.13537	36.29593	4.160561	34.46096	1.175555	7823.356
6	Services	6	6402	5761800	27.63421	38.20284	10.56863	32.81021	1.528667	212787.4
7	Industrial area	7	3391	3051900	29.23211	37.28227	8.050159	33.980868	1.439218	115229.1
8	Lake side devel	8	926	833400	24.46215	34.18836	9.726208	28.472009	2.012087	26365.08
9	Open space	9	756	680400	32.03854	39.14289	7.104343	33.0915	1.056244	25636.26
10	Horticulture	10	846	761400	28.21103	36.86699	8.655956	29.43594	2.007304	27440.8
11	Mining site	11	1249	1124100	28.80119	37.34245	8.54126	35.91666	1.448231	43051.91
12	Dense vegetati	12	982	883800	23.3268	34.00697	10.68017	26.950989	2.152006	26465.87
13	Sparse vegetati	13	500	450000	26.13791	39.70586	13.56796	30.60541	3.744503	16474.19
14	Pernial vegetat	14	1806	1625400	28.85627	37.8593	9.003025	30.03594	1.58767	59445.42
15	Shrubs and gras	15	176	158400	31.24673	35.55636	4.309631	32.70714	0.903301	5847.183
16	Bare land	16	9234	8310600	28.95572	41.32008	12.36436	35.50266	1.847073	331654.5
17	Wet land	17	2111	1899900	20.89931	33.15814	12.25883	24.256699	2.366039	51205.89
18	Water body	18	94811	85329900	20.02452	30.78225	10.75774	21.532028	0.878042	2041473

APPENDIX: 7 Summery report for LST distribution per UGC map of 2017

Rowid	TYPE	ZONE-CODE	COUNT	AREA	MIN	MAX	RANGE	MEAN	STD	SUM
1	Urban greenery in family housing areas	1	1556	1400400	24.53897	38.70146	14.16249	31.52632	1.747029	50190.83
2	Ruderal vegetation	2	1481	1332900	23.13603	39.97902	16.84299	33.79428	2.073576	50049.32
3	Urban park	3	1032	928800	22.62874	34.73555	12.10681	26.59715	2.145162	27448.26
4	Green areas in industrial units	4	749	674100	29.32861	35.42072	6.092104	32.87454	0.926581	24623.03
5	Urban greenery in public facilities	5	2250	2025000	24.718	37.12006	12.40207	30.93013	1.849002	72677.92
6	roadside greenery	6	38	34200	29.75768	34.63427	4.876585	31.99032	1.326719	1215.632
7	lake shore vegetation	7	1057	951300	23.59746	33.44107	9.843609	28.04236	1.913477	29640.78
8	Greenery in sports facilities and open spaces	8	158	142200	32.05645	35.55636	3.499908	33.68806	0.839241	5322.714
9	Stream bank/lake shore vegetation	9	2222	1999800	20.89931	37.46756	16.56825	25.49107	3.826065	56641.15
10	Water body	10	94807	85326300	20.02452	30.78225	10.75774	21.53184	0.877551	2041369

APPENDIX: 8 Comparison of validation LST results of 2017

Loaction	Sensor	Spatial resolution	Minimum	Maximum	Average	Average change
	TIR	100m	18	33	25.5	
A	MODIS	1km	22.75	25.75	24.25	1.25
	TIR	100m	41	42	41.5	
B	MODIS	1km	42.87	43.45	43.16	1.66
	TIR	100m	36	39	37.5	
C	MODIS	1km	38.91	39.99	39.45	1.95
	TIR	100m	33	40	36.5	
D	MODIS	1km	34.91	38.45	36.68	0.18
	TIR	100m	33	39	36	
E	MODIS	1km	37.02	38.31	37.665	1.665
	TIR	100m	32	37	34.5	
F	MODIS	1km	36.01	36.05	36.03	1.53
	TIR	100m	34	37	35.5	
G	MODIS	1km	37.13	37.49	37.31	1.81
	TIR	100m	42	47	44.5	
H	MODIS	1km	43.79	49.17	46.48	1.98
	TIR	100m	32	35	33.5	
I	MODIS	1km	33.67	35.99	34.83	1.33
	TIR	100m	38	47	42.5	
J	MODIS	1km	40.77	47.89	44.33	1.83
	TIR	100m	40	43	41.5	
K	MODIS	1km	42.59	43.99	43.29	1.79
	TIR	100m	29	30	29.5	
L	MODIS	1km	31.81	30.63	31.22	1.72

Addis Ababa University

School of Earth Sciences

APPENDIX: 8 FORMAT FOR THESIS ORIGINALITY TEST REPORT

Name of student	DAGNACHEW SISAY CHAKA
ID No	GSR/3422/09
Stream	Remote sensing and Geo-informatics
Thesis title	Remote sensing and GIS approach for estimation of land surface temperature to examine Urban Heat Island effect on a city scale; the case of Hawassa city, Ethiopia.
Online site used for originally test	http://www.paperrater.com/plagiarisim_checker

No	particulars	Test I		Test II		Test II		Test IV		Test V		Average	Remark
		Originality (%)	Plagiarism (%)	Originality (%)	Plagiarism (%)	Originality (%)	Plagiarism (%)	Originality (%)	Plagiarism (%)	Originality (%)	Plagiarism (%)		
1	Abstract	100	-	-	-	-	-	-	-	-	-	100	
2	Introduction	100	-	100	-	100	-	-	-	-	-	100	
3	Literature review	100	-	100	-	100	-	100	-	100	-	100	
4	Methodology	100	-	100	-	100	-	100	-	100	-	100	
5	Results	100	-	99	1	100	-	100	-	100	-	99.8	NDVI
6	Discussion	100	-	-	-	-	-	-	-	-	-	100	
7	Conclusion	100	-	-	-	-	-	-	-	-	-	100	
	Overall Thesis											99.97	

	Name	Signature
Student	Dagnachew Sisay Chaka	
Advisor (1)	Dr. Tesfaye Korme	
Advisor (2)	-	